Volume 7 SEPTEMBER, 1936 Number 9

PHYSICS

A Journal of General and Applied Physics

# Some Special Solutions for the Motion of the Powder Gas*

R. H. KENT, *Aberdeen Proving Ground, Maryland*

(Received June 4, 1936)

An important error in Pidduck's special solution is pointed out. Special solutions for a perfect and an imperfect gas are obtained. Modifications to take account of projectile friction and the burning of the powder are given.

PIDDUCK[1] has published a special solution of the equation of motion of the powder gas in a gun. Apparently without being aware of it, he has assumed that the initial density does not vary as a function of the distance from the breech. The solution he obtains however, is inconsistent with this assumption. He finds, for example, that the ratio of the pressure on the projectile to that on the breech is independent of the time and less than unity. On the assumption of initial constant density and his pressure volume relation, the ratio should be unity. We propose in the following to modify Pidduck's solution and get one which is consistent with the initial conditions.

Pidduck's solution assumes an adiabatic pressure-volume relation of the form $p(v-b)^\gamma = \text{Const.}$ Because of the greater simplicity of the analysis, we shall first obtain a special solution for a perfect gas and then later a solution for the case where the co-volume, $b$, is not negligible. For brevity, we call the case where $b$ is not negligible, the imperfect gas case.

In obtaining the solutions, the methods used by Pidduck have been of great help. We use his terminology also.

The symbols are defined as follows:

| Symbol | Meaning | Symbol | Meaning |
|---|---|---|---|
| $x$ | the initial coordinate of any element of the gas in the gun. | $M$ | the mass of the projectile. |
| $y$ | the coordinate of this element at time $t$. (We assume that this element always contains the same molecules of gas that it originally contained.) | $C$ | the weight of the charge. |
| | | $\epsilon$ | $C/M$. |
| | | $S$ | the cross-sectional area of the bore. |
| $\rho_0$ | the initial density.* | $b$ | the length of the chamber. |
| $\rho$ | the density of the gas at any time, $t$. | $\gamma$ | ratio of the specific heats. |
| $p_0$ | the initial pressure.* | $R$ | ratio of pressure on base of projectile to that on breech. |
| $p$ | the pressure at any time, $t$. | | |

* $\rho_0$ and $p_0$ are in general functions of $x$; $\rho$ and $p$ are functions of $x$ and $t$.

## A Special Solution for a Perfect Gas

We assume that the powder is all burnt and that the motion is one dimensional.

The equation of motion of the gas is

$$\rho\partial^2 y/\partial t^2 = -\partial p/\partial y. \tag{1}$$

The equation of continuity is

$$\rho = \rho_0/(\partial y/\partial x).$$

The gas is assumed to be perfect and its expansion adiabatic, hence

$$p\rho^{-\gamma} = p_0\rho_0^{-\gamma}.$$

* Published by permission of the Chief of Ordnance, U. S. A.

[1] Love and Pidduck, Phil. Trans. Roy. Soc. **222**, 222 (1922). Pidduck assumes the responsibility for the special solution.

It is furthermore assumed that the original pressure and density distribution follows adiabatically from an antecedent regime of uniform pressure and density.

Thus, $p\rho^{-\gamma}=p_0\rho_0^{-\gamma}=K$ (a constant).

By virtue of these relations (1) may be reduced to

$$\frac{\partial^2 y}{\partial t^2}=\gamma K\rho_0^{\gamma-1}\left(\frac{\partial y}{\partial x}\right)^{-(\gamma+1)}\left[\frac{\partial^2 y}{\partial x^2}-\frac{1}{\rho_0}\frac{\partial\rho_0}{\partial x}\frac{\partial y}{\partial x}\right]. \quad (1a)$$

We consider a special solution of the following type:

$$y=f(x)\varphi(t).$$

However, when $t=0$, $y=x$ by definition and

$$x=f(x)\varphi(0).$$

It is evident that the most general form for $f(x)$ consistent with this is $f(x)=a_1x$. It is also clear that $a_1$ and $\varphi(0)$ are related by

$$a_1\varphi(0)=1.$$

Hence we may take $a_1$ arbitrarily provided that we take $\varphi(0)=1/a_1$. For simplicity, we take $a_1=1$. Thus our solution is restricted to the following,

$$y=x\varphi(t).$$

By substitution in (1a) and dividing both sides by $x\varphi(t)^{-\gamma}$, one obtains

$$\varphi''(t)[\varphi(t)]^{\gamma}=(-\gamma K\rho_0^{\gamma-2}/x)\cdot(\partial\rho_0/\partial x).$$

It is clear that both sides are equal to the same constant, $B$; that is

$$\varphi''(t)=B/[\varphi(t)]^{\gamma} \quad (2)$$

and

$$Bx=-\gamma K\rho_0^{\gamma-2}\partial\rho_0/\partial x. \quad (3)$$

Our proposed solution is therefore consistent with the differential equation provided (2) and (3) are satisfied.

Upon integrating (3) and taking $b=1$ ($b$ is the chamber length), we find

$$\rho_0^{\gamma-1}=-[(\gamma-1)B/2\gamma K]x^2 \quad [\rho_0(0)]^{\gamma-1};$$

or, if

$$a=(\gamma-1)B/2\gamma K[\rho_0(0)]^{\gamma-1}, \quad (4)$$

$$\rho_0=\rho_0(0)[1-ax^2]^{1/(\gamma-1)}, \quad (5)$$

where $\rho_0(0)$ is the value of $\rho_0$ at $x=0$, i.e., at the breech.

The constant "$a$" may be determined as follows:

The equation of motion of the projectile is, if $S=1$ and $b=1$,

$$K[\rho_0(1)]^{\gamma}\cdot[\varphi(t)]^{-\gamma}=M\varphi''(t)=MB[\varphi(t)]^{-\gamma}.$$

From this it follows that

$$B=(K/M)[\rho_0(0)]^{\gamma}(1-a)^{\gamma/(\gamma-1)}.$$

From this relation and (4),

$$a=[(\gamma-1)/\gamma]\cdot(\rho_0(0)/2M)(1-a)^{\gamma/(\gamma-1)}.$$

The weight of charge,

$$C=\int_0^1\rho_0dx=\rho_0(0)\int_0^1(1-ax^2)^{1/(\gamma-1)}dx.$$

If the pressure on the base of the projectile is real and positive, $a<1$. Hence, expanding

$$(1-ax^2)^{1/(\gamma-1)}$$

and integrating, we obtain

$$\rho_0(0)\approx\frac{C}{1-a/3(\gamma-1)+(2-\gamma)a^2/10(\gamma-1)^2}$$

$$=C\left[1+\frac{a}{3(\gamma-1)}+\frac{(9\gamma-8)a^2}{90(\gamma-1)^2}\cdots\right].$$

From this and (4), we find, if $\epsilon$, $C/M$, is small,

$$a=\frac{\gamma-1}{\gamma}\cdot\frac{\epsilon}{2}\left(1-\frac{\epsilon}{2}+\frac{\epsilon}{6\gamma}\right)+\cdots \quad (6)$$

From the equation of motion of the center of gravity of the charge and projectile, we show that $R$, the ratio of the pressure on the projectile to that on the breech is given by,

$$\frac{1}{R}=1+\frac{\int_0^1\rho_0xdx}{M}=1+\frac{\epsilon}{2}-\frac{\epsilon^2}{24\gamma}$$

$$+\frac{1}{10\gamma}\left(\frac{1}{8}+\frac{1}{36\gamma}\right)\epsilon^3+\cdots,$$

or

$$R=1-\frac{\epsilon}{2}+\left(\frac{1}{4}+\frac{1}{24\gamma}\right)\epsilon^2$$

$$-\left[\frac{1}{8}+\frac{1}{24\gamma}+\frac{1}{10\gamma}\left(\frac{1}{8}+\frac{1}{36\gamma}\right)\right]\epsilon^3+\cdots. \quad (7)$$

Pidduck, for the case of an imperfect gas, apparently was unable to obtain an explicit expansion for $R$ in terms of $\gamma$ and $\epsilon$. However, for

$$\gamma=11/9,$$

he gives,

$$R=1-\epsilon/2+75\epsilon^2/264-14{,}913\epsilon^3/87{,}120+\cdots,$$

which agrees up to and including the $\epsilon^3$ term with the result obtained by the use of (7) for this value of $\gamma$. In view of the fact that his solution is inconsistent with his assumption of uniform initial density, this is surprising.

On the customary assumption of uniform density of the gas,

$$1/R=1+\epsilon/2.$$

Thus the error in the value of $1/R$ resulting from this assumption is

$$-\epsilon^2/24\gamma+(\epsilon^3/10\gamma)(1/8+1/36\gamma)\cdots.$$

When $\epsilon<\frac{1}{2}$, as is usually the case, this would amount to less than one percent.

It is easy to show that the kinetic energy of the gas, $E$, is given by:

$$E=\frac{CV^2}{6}\left[1-\frac{2\epsilon}{15\gamma}+\frac{(24\gamma+8)}{630\gamma^2}\epsilon^2+\cdots\right],^{2}$$

where $V$ is the velocity of the projectile at any time.

## A Special Solution for an Imperfect Gas

We assume the following pressure-density relation, taking the co-volume as approximately unity;

$$p(1/\rho-1)^\gamma=p_0(1/\rho_0-1)^\gamma=K.$$

We now set

$$z=y-\int_0^x \rho_0 dx. \tag{8}$$

By these relations, we obtain in place of (1)

$$\frac{\partial^2 z}{\partial t^2}=\frac{\gamma K}{\rho_0[(1/\rho_0)(\partial z/\partial x)]^{\gamma+1}}\left[\frac{1}{\rho_0}\frac{\partial^2 z}{\partial x^2}-\frac{1}{\rho_0^2}\frac{\partial \rho_0}{\partial x}\cdot\frac{\partial z}{\partial x}\right]. \tag{9}$$

We assume that the equation has a solution of the form,

$$z=f(x)\varphi(t).$$

Upon inserting this in (9) and multiplying both sides by

$$[\varphi(t)]^\gamma/f(x),$$

we get,

$$\varphi''(t)[\varphi(t)]^\gamma=\gamma K\rho_0{}^{(\gamma-1)}[f(x)]^{-1}[f'(x)]^{-\gamma-1}[f''(x)-(1/\rho_0)\cdot(\partial\rho_0/\partial x)f'(x)].$$

The left-hand side of the equation is a function of $t$ only and the right-hand a function of $x$ only. Hence both sides may be equated to a constant, $B$. We obtain:

$$\varphi''(t)[\varphi(t)]^\gamma=B;$$

$$\gamma K\rho_0{}^{(\gamma-1)}[f(x)]^{-1}[f'(x)]^{-\gamma-1}[f''(x)-(1/\rho_0)(\partial\rho_0/\partial x)f'(x)]=B. \tag{10}$$

When $t=0, \quad z=z_0=f(x)\varphi(0).$

When $t=0, \quad y=y_0=x.$

Hence, $\rho_0=1-f'(x)\varphi(0).$

By virtue of these relations, (10) may be written,

$$f''(x)=(B/\gamma K)\rho_0{}^{2-\gamma}[f'(x)]^{\gamma+1}f(x). \tag{10a}$$

[2] Pidduck gives $E=(CV^2/6)[1-6\epsilon/55\cdots]$ for $\gamma=11/9$, which is consistent with the above.

We attempt to integrate (10a) by a series:

$$f(x)=\sum_{k=0}^{k=\infty} a_k x^k.$$

By virtue of the definition, (8),

$$f(x)\varphi(0)=x-\int \rho_0 dx.$$

and $$a_0=0.$$

We note that

$$k!a_k=f^k(0).^3$$

Since $f(0)=0$, $f''(0)=2!a_2=0$.

By differentiating (10a), we get

$$f'''(x)=\frac{B}{\gamma K}\rho_0{}^{2-\gamma}[f'(x)]^{\gamma+1}f(x)\left\{\frac{(2-\gamma)\rho_0{}^{1-\gamma}}{\rho_0{}^{2-\gamma}}\frac{\partial\rho_0}{\partial x}+\frac{(\gamma+1)[f'(x)]^{\gamma}}{[f'(x)]^{\gamma+1}}f''(x)+\frac{f'(x)}{f(x)}\right\}.$$

Now $\partial\rho_0/\partial x_{x=0}=0$; hence

$$a_3=f'''(0)/3!=(B/3!\gamma K)[\rho_0(0)]^{2-\gamma}[a_1]^{\gamma+2}. \tag{11}$$

Differentiating again, we find for $\gamma K f^{iv}(x)/B$ the following expression:

$$\begin{aligned}&(2-\gamma)(1-\gamma)\rho_0{}^{-\gamma}(\partial\rho_0/\partial x)^2[f'(x)]^{\gamma+1}f(x)+(2-\gamma)(\gamma+1)\rho_0{}^{1-\gamma}[f'(x)]f''(x)(\partial\rho_0/\partial x)f(x)\\&\quad+(2-\gamma)\rho_0{}^{1-\gamma}[f'(x)]^{\gamma+2}\partial\rho_0/\partial x+(2-\gamma)\rho_0{}^{1-\gamma}[f'(x)]^{\gamma+1}f(x)\cdot(\partial^2\rho_0/\partial x^2)\\&\quad+(\gamma+1)\gamma\cdot\rho_0{}^{2-\gamma}[f'(x)]^{\gamma-1}f(x)[f'(x)]^2+(\gamma+1)\rho_0{}^{2-\gamma}[f'(x)]^{\gamma+1}f''(x)\\&\quad+(\gamma+1)\rho_0{}^{2-\gamma}[f'(x)]^{\gamma}f(x)f'''(x)+(\gamma+1)(2-\gamma)\rho_0{}^{1-\gamma}[f'(x)]^{\gamma}f(x)f'(x)\cdot(\partial\rho_0/\partial x)\\&\qquad+(2-\gamma)\rho_0{}^{1-\gamma}[f'(x)]^{\gamma+2}(\partial\rho_0/\partial x)+(\gamma+2)\rho_0{}^{2-\gamma}[f'(x)]^{\gamma+1}f''(x).\end{aligned}$$

In view of the fact that $\varphi(0)\,f''(0)=-(\partial\rho_0/\partial x)_{x=0}=0$, it follows that;

$$a_4=f^{iv}(0)/24=0.$$

By virtue of these relations, it readily also follows that

$$f^v(0)=(B/\gamma K)\{3(2-\gamma)[\rho_0(0)]^{1-\gamma}[f'(0)]^{\gamma+2}(\partial^2\rho_0/\partial x^2)+[3(\gamma+1)+1][\rho_0(0)]^{2-\gamma}[f'(0)]^{\gamma+1}f'''(0)\}.$$

Now $$\partial^2\rho_0/\partial x^2{}_{x=0}=-\varphi(0)f'''(0)$$

and $$\varphi(0)=[1-\rho_0(0)]/f'(0).$$

Hence, $$a_5=(B/5\cdot4\gamma K)\{-3(2-\gamma)[\rho_0(0)]^{1-\gamma}f'(0)+10[\rho_0(0)]^{2-\gamma}[f'(0)]^{\gamma+1}\}a_3. \tag{12}$$

$B$ is determined by the equation of motion of the projectile. We find;

$$B=K[\rho_0(b)]^{\gamma}/Mf(b)[f'(b)]^{\gamma}.$$

$R$ may be expressed by

$$R=[\rho_0(b)]^{\gamma}[f'(0)]^{\gamma}/[\rho_0(0)]^{\gamma}[f'(b)]^{\gamma}.$$

It should be noted that $R$ is independent of $t$. We may now express $B$ by

$$B=K[\rho_0(b)]^{\gamma}/Mf(b)[f'(b)]^{\gamma}=KR[\rho_0(0)]^{\gamma}/Mf(b)\cdot[(f'(0)]^{\gamma}.$$

By virtue of this relation, we obtain

$$a_3=R[\rho_0(0)]^2a_1{}^2/6\gamma Mf(b) \tag{11a}$$

and $$a_5=(R/20\gamma Mf(b))\{-3(2-\gamma)\rho_0(0)+10[\rho_0(0)]^2\}a_3f'(0). \tag{12a}$$

---

[3] $f^k(x)$ denotes the $k$th derivative of $f(x)$.

To determine $a_1$, we note that we have the liberty of choice as in the perfect gas case, provided that $\varphi(0)$ is chosen so that the relation

$$f(b)\varphi(0)=b-\int\rho_0 dx=b-C$$

is satisfied. We take $a_1=1$.

To make further progress we evaluate approximately

$$\rho_0(0)=1-\varphi(0)f'(0)=[f(b)+f'(0)(C-b)]/f(b),$$

neglecting $a_3$, $a_5$ etc.

We insert this expression for $\rho_0(0)$ in (11a) and (12a) and thus obtain approximate values of $a_3$ and $a_5$. We then repeat the process obtaining a more accurate value of $\rho_0(0)$ in terms of $a_3$ and $a_5$ and then of $a_3$ and $a_5$ etc.

The result of this procedure is that, if $\epsilon^3$ is neglected in comparison with unity,

$$a_3=\frac{R\epsilon C}{6\gamma b^3}\left\{1+\left(2-\frac{3C}{b}\right)\frac{R\epsilon}{6\gamma}\left[1+\frac{R\epsilon}{60\gamma}(2+9\gamma)\right]+\frac{R^2\epsilon^2}{36\gamma^2}\left[1-6\frac{C}{b}+6\frac{C^2}{b^2}\right]+\cdots\right\},$$

$$a_5=\frac{R^2\epsilon^2 C}{120\gamma^2 b^5}\left\{-3(2-\gamma)\left[1+\frac{R\epsilon}{6\gamma}\left(3-5\frac{C}{b}\right)\right]+10\frac{C}{b}\left[1+\frac{R\epsilon}{\gamma}\left(\frac{2}{3}-\frac{C}{b}\right)\right]\right\}.$$

We have not yet evaluated $R$ for the imperfect gas case.

From the equation of motion of the center of gravity of the projectile and charge, we show that

$$\frac{1}{R}=1+\frac{\int_0^b\rho_0 f(x)dx}{Mf(b)}.$$

From this it follows that

$$\frac{1}{R}=1+\frac{b}{2M}-\frac{a_3b^3}{4M}+\frac{a_3^2b^5}{4M}-\frac{1}{3}\frac{a_5b^5}{M}+\frac{C}{2M}-\frac{b}{2M};\quad \frac{1}{R}=1+\frac{\epsilon}{2}-\frac{a_3b^3}{4M}+\frac{a_3^2b^5}{4M}-\frac{1}{3}\frac{a_5b^5}{M}.$$

If we substitute for $a_3$ and $a_5$ their values and express $R$ on the right-hand side by

$$R=1-\epsilon/2,$$

we obtain, neglecting terms in $\epsilon^4$,

$$\frac{1}{R}=1+\frac{\epsilon}{2}-\frac{\epsilon^2}{24\gamma}+\frac{\epsilon^3}{10\gamma}\left(\frac{1}{8}+\frac{1}{36\gamma}\right)+\cdots;\quad R=1-\frac{\epsilon}{2}+\left(\frac{1}{4}+\frac{1}{24\gamma}\right)\epsilon^2-\left[\frac{1}{8}+\frac{1}{24\gamma}+\frac{1}{10\gamma}\left(\frac{1}{8}+\frac{1}{36\gamma}\right)\right]\epsilon^3+\cdots.$$

As the projectile moves down the bore, the gas expands and approaches more and more closely the condition of a perfect gas. $R$ is unchanged during the expansion. Thus one might expect the value of $R$ obtained for the imperfect gas to hold also for the perfect gas. Eq. (7) on page 320 shows that this is the case, at least if terms in $\epsilon^4$ are neglected.

### Effect of Forcing Resistance and Burning of the Powder

The solution may readily be modified to take approximate account of the forcing resistance by substituting for $M$, the mass of the projectile, $M'$, given by

$$M'=M(1+p_f/p(b)).$$

where $p_f$ is the pressure required to overcome the friction (forcing resistance) of the projectile. It is assumed that

$$p_f/p(b) \text{ is a constant.}$$

To allow approximately for the burning of the powder, we assume (1) that the co-volume is equal to the volume of the unburnt powder and

(2) that the pressure is given by

$$p(1/\rho-1)^{\gamma}=p_0(1/\rho_0-1)^{\gamma}\psi(t)=K\psi(t). \quad (13)$$

We find that this leaves the differential equation for $f(x)$ unchanged.

For (13) to hold it is necessary, (1) that the rate of burning of the powder shall be proportional to the pressure, (2) that the burning surface per unit volume shall initially and afterwards be independent of $x$.

This latter condition (2) must hold even though the density varies with $x$. Thus a special design of charge would be required.

LaGrange's ballistic problem is the problem of the motion of the gas, when the pressure and density are initially uniform and the projectile is then suddenly released. Pidduck points out that the ratio, $R$, obtained by Love[4] in his solution of LaGrange's ballistic problem oscillates about its mean value. This suggests the idea of treating the variations from the special solution pressures as waves instead of treating the variations from the initial uniform pressure as waves, as Love does, following Riemann.

It appears that by this new method, simple approximate solutions of LaGrange's and other wave problems may be obtained. It is proposed to elaborate this method of attack in a subsequent paper.

I am indebted to Mr. J. R. Lane for checking the calculations.

[4] Reference 1, pp. 167–216.

# The Flow of Gas-Liquid Mixtures Through Unconsolidated Sands

R. D. WYCKOFF AND H. G. BOTSET, *Gulf Research & Development Company, Pittsburgh, Pennsylvania*

(Received July 22, 1936)

A method is described for studying the flow of gas-liquid mixtures through unconsolidated sands. Results are given for experiments on four sands of widely different permeabilities using carbon dioxide and water as the fluids. A relation between permeability and liquid-saturation of the sand is found which permits the correlation of saturation and the steady state flow of the gas and liquid components. Generalization of these results for all unconsolidated sands seems permissible. The phenomena of equilibrium permeability and equilibrium liquid-saturation are described and their significance discussed. It is believed that the experimental attack and type of analysis is applicable to the general problem of the flow of gas-liquid mixtures through porous media.

## I. INTRODUCTION

THE validity of d'Arcy's law which states that the viscous flow of homogeneous fluids through porous media is proportional to the pressure gradient and to the permeability of the medium and inversely proportional to the viscosity of the fluid, is now firmly established. With the dynamic behavior of the fluids thus defined it is possible to carry out complete analyses of specific problems involving the flow of either gases or liquids through porous media. However, the practical problems confronting the petroleum technologist very frequently involve not homogeneous fluids, but mixtures of immiscible fluids such as water-oil or gas-oil mixtures. A few simple experiments suffice to show that for such nonhomogeneous fluids the simple statement of d'Arcy's law is inadequate to describe the dynamical behavior of the system and that further extensions of this basic law are required if analytical studies of such systems are to be made possible. Apparently the principal difficulty arises from the fact that in the case of the flow of mixtures the apparent permeability of the medium to either component is a variable and is dependent in a complex manner upon the relative concentration of the two fluid components present within the porous medium.

The cause of this variation in permeability is apparent upon recalling the existence of the Jamin effect.[1] Thus if a bubble of gas is caused to flow through a liquid-filled capillary, the presence of a constriction or an abrupt change in diameter of the capillary acts as an obstruction to the gas bubble and it will not flow through the nonuniform section unless a certain critical force is exerted on the bubble. In a capillary of uniform bore a stationary bubble of gas will have a symmetrical contour such that the surface tension forces on all sides are in equilibrium and a pressure gradient, however small, applied across the bubble will induce flow. However, in a nonuniform capillary such as one having a constriction, a bubble advancing into the constricted portion must suffer distortion which involves an increase in surface energy at the interface between the gas and liquid at the small radius end of the bubble. Thus the surface tension forces of such a bubble are no longer in equilibrium, the net stress being such as to drive the bubble back and out of the constriction. Clearly then the application of a slight external pressure will only serve to drive the bubble partially into the constriction where it will remain stationary, maintaining such a position that the distortional surface tension forces are in equilibrium with the externally applied force. Evidently the system will behave as if the capillary contains a positive obstruction and no flow is possible until a critical pressure gradient, sufficient to overcome the distortional forces, is applied across the bubble. This critical force will depend upon the amount of distortion fixed by the change in diameter of the capillary and upon the value of the interfacial tension at the surface of the bubble. Obviously a similar effect obtains in the case of a bubble of liquid in another immiscible liquid traversing a constricted capillary field.

Now the pore structure of a medium such as a

[1] J. C. Jamin, Comptes rendus **50**, 172 (1860).

sand pack corresponds to a network of capillaries having an extremely large variation in diameter and a pronounced Jamin effect is to be expected if a mixture of immiscible fluids is forced through it. One then visualizes the flow of a gas-liquid mixture as constituting a continuous moving-liquid phase with interposed masses of gas also moving through the pores. Statistically, however, in view of the Jamin effect, a certain percentage of the gas masses or bubbles is stationary or locked in the pores and does not contribute to the flow. Rather they form obstructions to the flow of both the gas and liquid components.

In view of the above very qualitative considerations it is evident that the effective permeability of a porous medium cannot be constant when the flow of fluid-mixtures is involved. Furthermore, unless the variation in permeability is governed by laws which may be properly generalized, any analytical development of the subject is impossible. We are, therefore, faced with the necessity of investigating the problem experimentally in the hope of obtaining empirical relations between the various factors involved such that, for given conditions at any point in a flow-system, the dynamical behavior may be uniquely described.

In the discussion which follows, it is to be understood that we are dealing only with the flow of nonhomogeneous fluids, specifically with gas-liquid mixtures, through porous media comprising unconsolidated sands.

## II. Experimental Technique

It might be supposed that a study of the behavior of gas-liquid mixtures in individual pores would provide the key to the solution of the problem. Indeed, we have already seen qualitative implications derived from cursory consideration of such details. But it will be found quite impossible by this method to carry the analysis beyond the point of constructing a crude and qualitative picture of the performance of the system. In the case of homogeneous fluids it is impossible to describe the macroscopic performance of the system from a study of the microscopic details. Even more remote is the possibility of determining the overall dynamical behavior of nonhomogeneous fluids from a study of microscopic details. In fact, as already suggested, the problem should be attacked essentially from a statistical angle which involves the study of large aggregates of pores.

It is evident, therefore, that to carry our concepts further we must be able experimentally to determine at any instant the exact conditions existent at any point within the flow system, such conditions involving:

1. The liquid content or saturation of the sand which, of course, determines the free-gas content.
2. The rate of flow of liquid.
3. The rate of flow of gas.
4. The pressure gradient.

Since these data define the dynamic conditions completely it should be possible to derive therefrom the overall or macroscopic behavior of the system.

The determination of the pressure gradients within the flow system involves no great difficulty. Likewise the rate of flow of liquid through any given cross section of the column is determined simply by measurement of the rate of efflux. The rate of flow of gas may also be measured at the outlet and when dealing with a gas-saturated liquid, the flow across any other section may be inferred from a knowledge of the gas-saturation characteristics and the pressures existent at the point in question, assuming no supersaturation.

The determination of the volume of free gas present in the system or the liquid saturation of the sand at any instant is a more difficult problem. The method which we have used and which appeared to be the most practical was to make the liquid slightly conducting and then, by means of an alternating current bridge, to measure the increase in resistance of a section of the column due to the formation of free gas bubbles within the sand body. A brief description of the details of the method is warranted.

In all cases the flow system used is a column of sand packed in a tube several inches in diameter and of suitable length. This simple geometry, providing a linear or one dimensional flow, is used because of the simplification it provides in final interpretation. In order to provide for the necessary electrical resistance measurements it is a simple matter to arrange cylindrical electrodes at suitable intervals along the length of the tubular container. Thus the main portion of the

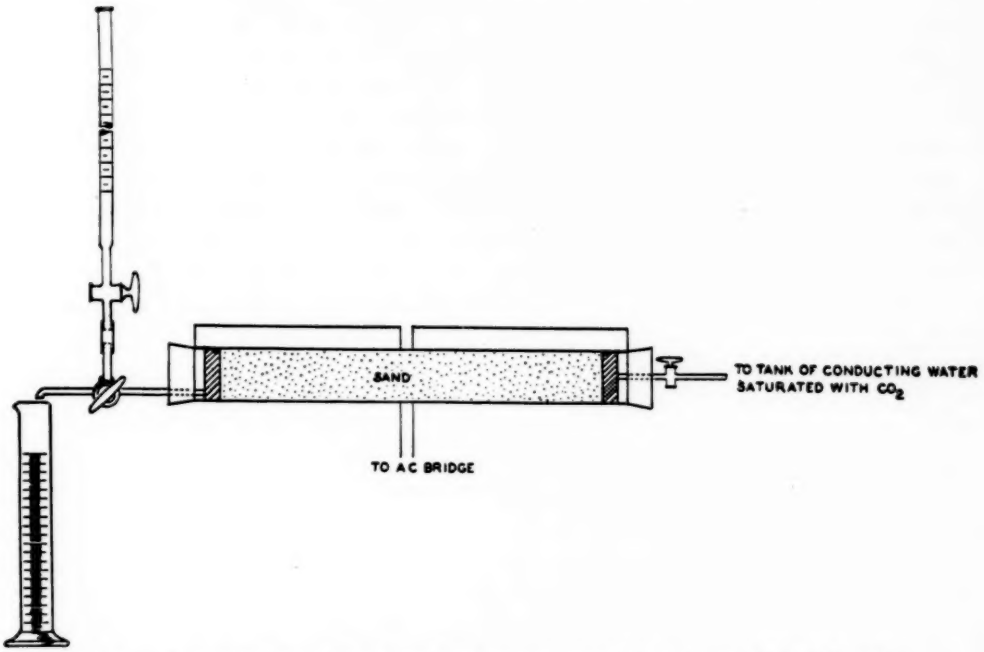


FIG. 1. Apparatus for calibration of resistance-saturation characteristics of sand.

tube comprises several sections of Bakelite tubing which are joined together by short brass couplings whose inner diameter is the same as the Bakelite sections. These couplings form the electrodes whereby the variations in electrical resistance of the intervening column of liquid may be measured. Other types of electrode have been tried but found unsatisfactory.

It is necessary that the relation between the electrical resistance of the fluid column and the liquid-saturation of the sand (or percentage of gass-filled pores) be known accurately. Fricke[2] has found a relation between the conductivity and porosity of a somewhat similar system given by the empirical equation:

$$p=1-(2\sigma-2)/(2\sigma+1)$$

where $p$=porosity and $\sigma=R_2/R_1$, $R_2$ being the resistivity of the fluid-filled sand column and $R_1$ the resistivity of the fluid column without sand. Our experiments showed this equation to hold very well for various sands and gas-free liquids but considerable discrepancy appeared when the sand contained gas bubbles. An empirical determination of the relation between resistivity and volume of gas bubbles in a sand was necessary and is described in some detail because of its importance in the work which follows.

The experimental setup for this determination is shown in Fig. 1. The sand was contained in a glass tube, the ends of which were sealed with rubber stoppers containing inlet and outlet tubes as shown. The tube was filled with a known weight of sand of known grain density, the stoppers sealed in with De Khotinsky cement, and the tube was connected to a Hyvac pump. The tube, after evacuation, was filled with distilled water. The distilled water was then displaced by boiled conducting water (flowed by gravity) until the resistance became constant. The dead liquid was next displaced by $CO_2$-saturated liquid of the same conductivity, care being taken that during the displacement no increase in resistance occurred, as this would indicate the formation of free gas in the sand. When the dead liquid had all been displaced, the stopcock leading to the supply tank was closed. The liquid in the tube was then allowed to expand very slowly, by small increments, into a burette, the resistance and volume displaced being determined for each increment. When the expansion had reached its limit the supply tank was re-

[2] Fricke, Phys. Rev. **24**, 575 (1924).

placed by a $CO_2$ tank and gas forced through the sand, the displaced liquid being measured in the graduated cylinder. The resistance was determined for additional small increments of displaced liquid until only a small percentage of the pore space contained liquid. The experiment was repeated on three different mesh sands; heterogeneous sand, porosity 27.76 percent; 50–60 mesh sand, porosity 42.96 percent; Ottawa (20–30 mesh) sand, porosity 35.4 percent; and finally on consolidated Berea sandstone of porosity 19.65 percent. In Fig. 2 are plotted the data for all these sands and the resulting curve relating the percent of the original conductivity and the percent of the original liquid saturation. This curve was used in all subsequent experiments in determining the total volume of gas or liquid in the sand from the electrical resistance measurements.

## III. Permeability *vs.* Saturation Relations

Having facilities available for the measurement of the liquid saturation of the sand body, the rate of flow of liquid and gas, and the pressure distribution and gradients within the system we are equipped to determine all of the physical features characterizing the flow system.

Experience with the flow of homogeneous fluids through porous media shows that d'Arcy's law together with a knowledge of the permeability constant of the medium permits a complete analytical solution of all problems whose geometrical complexity is within the scope of the powerful methods of potential theory. It will be judicious to proceed in a similar manner with the problem involving nonhomogeneous fluids, bearing in mind, as revealed in the introduction, that we must expect the permeability of the medium to enter as a variable. However, we have no reason whatever to doubt the validity of d'Arcy's law itself, provided the fluid velocities do not exceed the range involving only viscous flow. For whatever the complexity of the system may be, the velocity of any fluid actually partaking in the general motion at any point may quite reasonably be expected to be proportional to the pressure gradient at the point in question. We will, therefore, assume without further question that d'Arcy's law is applicable and that the permeability of the medium, which was a constant characterizing the medium in the case of homogeneous fluids, in the case of mixtures, becomes a variable and is dependent upon the relative volumes of gas and liquid present in the pores of the medium. In other words, we must attempt to obtain an empirical relation between the *effective* permeability and the liquid or gas saturation of the porous medium.

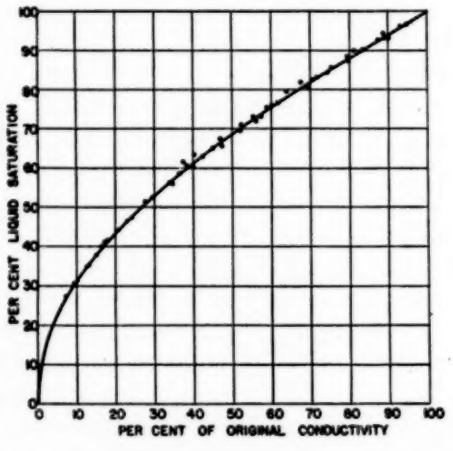


Fig. 2. Calibration curve relating sand conductivity and saturation.

### 1. Experimental equipment

The apparatus used in the final experiments and which is typical of the equipment involved in much of the extensive preliminary work,[3] is shown in Fig. 3. Each section of the Bakelite flow-tube was one foot long, the entire length being ten feet with an inside diameter of two inches. The brass couplings which served both as piezometer rings and electrodes for the resistance measurements already described, were carefully constructed so that the assembled tube presented a perfectly smooth and uniform bore with no gaps in the walls at the junctions. A detail of considerable importance is the use of piezometer rings rather than a single opening into the tube for pressure measurements. Preliminary experiments showed the latter to be wholly unreliable, the presence of gas masses within the sand body

[3] The results presented here, in particular as represented in Figs. 5–10, were obtained essentially in the preliminary work as early as 1933. The apparatus and experiments described briefly in this paper were made primarily to amplify and confirm certain details of the broad general picture which resulted from these earlier experiments.

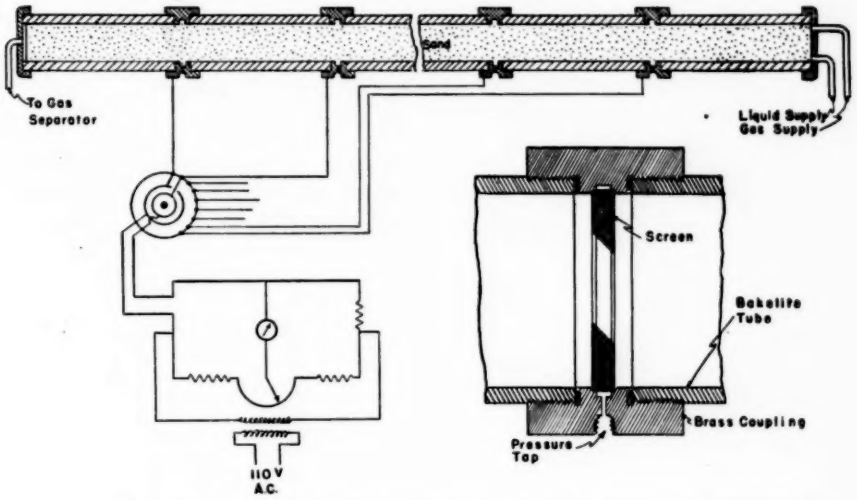


FIG. 3. Electrical circuit for sand column, with detail of piezometer ring coupling.

frequently giving rise to erratic pressure measurements which were eliminated when the piezometer rings were used. The details of their construction are shown in Fig. 3 and it is clear that the observed pressure represents the average over the entire circumference of the sand column. The completely assembled tube was tested at 125 lb. pressure, and at this pressure the 1/4″ wall thickness of the Bakelite tubes was adequate to preclude any appreciable expansion of the tubes which might seriously disturb the packing of the sand.

The tube was carefully filled with a known weight of sand of the desired grain size by standing it vertically, filling it with distilled water and progressively adding small quantities of clean sand thoroughly wet in a beaker of distilled water. Each additional quantity of sand was thoroughly tamped in place by a small rod, carefully avoiding the nonuniform packing which is almost certain to occur if a large quantity of sand is poured into the tube and then tamped with a piston of large diameter. Finally the homogeneity of the completed sand column was tested by measuring the permeability of individual sections before proceeding with the regular experiments. The porosity of the sand body was determined from the known volume of the tube, the weight of the sand introduced and its grain density.

The pressure gradients along the tube were measured by mercury manometers connected across individual sections of the tube, each being capable of measuring a pressure difference of two atmospheres. In view of the necessity for measuring the electrical resistance of the liquid in the sand column it is evident that suitable insulation must be provided to eliminate conduction through the water and mercury columns in the U-tube manometers. This was accomplished by interposing a 5-cm column of dibutylphthalate (density 1.06) between the mercury and water in each arm of the manometers. Pressure differences were measured across eight of the ten sections of the tube, the inflow and outflow sections being neglected because of possible irregularities of flow which might occur there. A mercury manometer capable of reading to about 45 lb. gauge was used to determine accurately the pressure drop between the last measured section and the atmosphere.

The input end of the flow-tube was supplied with gas-saturated liquid from a corrosion proof tank having a capacity of 30 gallons. Constancy of pressure in the supply tank and thereby constancy of flow into the sand column was obtained by displacing liquid from the tank by gas fed from a high pressure source through a two-stage regulator. There was also a special gas inlet at the input end of the tube to permit mixing excess gas with the saturated liquid in order that very high gas/liquid ratios might be attained.

Since the experiments require measurement of the electrical resistance of the liquid, only con-

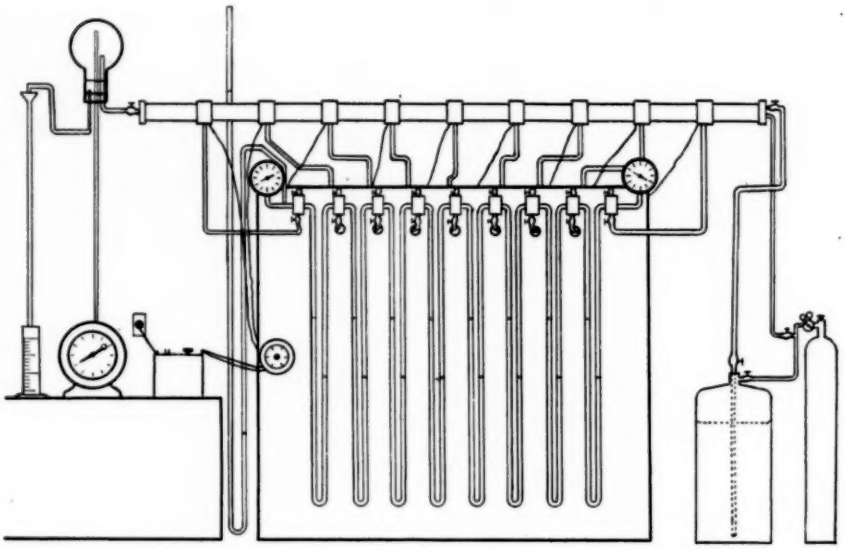

FIG. 4. Complete assembly for studying permeability-saturation relations.

ducting liquids could be used. Therefore, with the exception of some special tests, the liquid used was distilled water to which was added a sufficient quantity of NaCl to make it slightly conducting. Because of its high solubility $CO_2$ was used as the gas. The gas-liquid mixture after flowing from the tube passed through a gas separator, the gas volume being measured by a sensitive wet-test meter and the liquid collected in graduated cylinders.

The resistance measurements were made by means of a Leeds and Northrup 60-cycle a.c. bridge which could be connected to the electrodes of any section by means of a quick throw multiple-contact switch. It was essential that the bridge be of a type permitting very rapid balancing since eight measurements were required to be as nearly simultaneous as possible. In the instrument used the balance is obtained on a single dial covering the entire range and its sensitivity was found to be adequate. Previously a 500-cycle precision bridge was used but it was not practical to operate it at the required speed nor was the available precision required in view of the accuracy demanded in the final results.

The entire assembly ready for operation is shown in Fig. 4 from which a better idea of some of the details may be obtained. It should be mentioned, however, that the necessity for taking simultaneous readings requires two men to observe the manometers, one for the resistance measurements and one for the gas and liquid output measurements.

## 2. Experimental procedure

In order that the interpretation of the experimental results may be properly understood it will be necessary briefly to outline the procedure followed in a typical series of observations.

Assuming the liquid in the supply tank to be saturated with $CO_2$ at 45 lb. pressure and with the outflow end of the flow tube closed off, the auxiliary gas pressure on the supply tank was raised for example, to 60 lb. The outflow needle valve was then opened a sufficient amount to permit a steady flow through the sand column, care being taken, however, that the pressure at any point along the tube was well above the saturation pressure of the liquid. This assured that no free gas was released within the sand body, a condition which was readily checked by the electrical resistance measurements. When a sufficient volume of liquid had been flushed through the tube to insure the elimination of any water or free-gas originally present, the flow was carefully regulated for a constant rate and simultaneous measurements made of the rate, pressure drop and electrical resistance across each section of the tube.

The auxiliary pressure on the supply tank was

then reduced to a value just slightly above the saturation pressure of the liquid and the inflow and outflow needle valves on the sand column adjusted so that the pressure within the flow tube was slightly below saturation pressure. A small amount of gas was thus released continuously within the sand body and flowed through the system along with the liquid. When *steady state* conditions were reached, the rate of flow of gas and liquid, the resistances and pressures were measured simultaneously. This process of gradually decreasing the absolute pressure within the flow system, so as progressively to increase the volume of free gas released within the sand, was continued until the outflow section of the system reached atmospheric pressure. At this point, in order that the ratio of free gas to liquid might be increased far beyond the solution ratio, an auxiliary gas inlet at the inflow end of the column was brought into action. Additional $CO_2$ from the supply tank was fed to the system through a two-stage pressure regulator. In this manner the gas/liquid ratio flowing through the system was varied from zero during the initial stage to very high values at the completion of a series of observations. It should be mentioned that such a complete series might require an entire week's work since, especially at high gas/liquid ratios, steady state conditions are not attained until several hours after a readjustment has been made. However, it is significant that except for a certain region of low gas/liquid ratios to be considered in detail later, the steady state condition at any given ratio *may be approached from either direction*. Thus the flow may be stopped and the work continued at a later time without starting from the initial pure liquid stage. Or if inadvertently an improper adjustment of flow conditions has been made, it can be remedied without interfering with the results. This fact should be especially noted as it bears directly upon the final interpretation.

### 3. Experimental results

As previously outlined, the information desired from these experiments is: the liquid saturation of the sand, and the effective permeability of the system to the gas and liquid components separately.

The electrical resistance measurements, from which may be obtained the ratio of the conductivity during any observation to the gas-free conductivity, together with the calibration curve shown in Fig. 2 give the percentage of pore space filled with liquid or the liquid saturation of the sand within the section of the tube involved.

From the pressure data on the same section taken simultaneously with the resistance measurement and the measured rate of flow of liquid, the liquid-permeability of the sand within the section may be computed.

The volume of free gas flowing through any section is not so easily determined. It is necessary to determine the amount of free gas at the outflow face of the sand, from which, knowing the pressure conditions along the tube and the solubility of the gas, it is possible to calculate the volume flowing at the mean pressure of any section of the tube, and hence the permeability of that section to gas. In calculating the gas permeability in the various sections along the tube the following equation was used:

$$k_g = \frac{\mu L}{A} \frac{q_0 p_0 - Q(ds/dp)(\bar{p} - p_0)}{\bar{p}\Delta p},$$

in which $k_g$ is the permeability to gas, in darcys; $\mu$, the gas viscosity in centipoises; $L$, the sand length in centimeters; $A$, the total cross-sectional area of the sand column. $Q$ is the liquid rate in cc per sec.; $q_0$, the gas rate in cc per sec. at atmospheric pressure; $ds/dp$ is the pressure coefficient of gas solubility; $p_0$ is atmospheric pressure; $\bar{p}$, the mean pressure in the sand section being measured; and $\Delta p$ is the pressure drop across the section being measured. All pressures are expressed in atmospheres. This equation takes into consideration both the change in gas volume due to expansion and the change in volume due to evolution from solution under decreasing pressure.

Experiments were made at various rates of flow and saturation pressures. In each experiment the flow was continued at a constant rate until the resistances and pressure gradient along the sand column became constant, at which time a series of readings was taken and averaged to obtain the final values used in plotting the curves. Each point on the curves thus represents a steady-state condition. They have been plotted

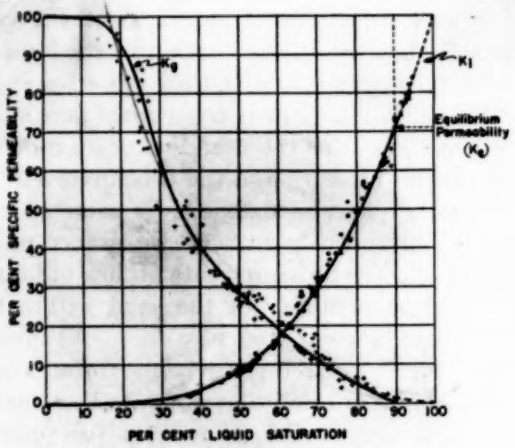


FIG. 5. Permeability-saturation relation for unconsolidated (70–120 mesh) sand with specific permeability of 17.8 darcys.

using percent liquid saturation of the sand and the percent of the initial or specific permeability (percent $k_0$) as the two coordinates in order to show the variation in effective permeability as a function of the liquid saturation of the sand. Such curves for each of the four sands are shown in Figs. 5–8. In addition to the effective liquid permeability ($k_e$), similar curves are plotted showing the variation in permeability to the gas component of the mixture ($k_g$) as a function of the liquid saturation of the sand. Thus the sum of the ordinates of the $k_g$ and $k_l$ curves at any liquid saturation represents the *total* effective permeability[4] of the sand under steady state conditions.

The spread of the observed data is due to experimental difficulties such as the impossibility of making exactly simultaneous readings of all the pressures and saturations as well as small inherent transient fluctuations in the system. It is felt, however, that considering the problem as a whole, the experimental error is satisfactorily small.

[4] To avoid the possibility of misinterpretation we wish to emphasize that unless otherwise stated, permeabilities given represent specific permeability expressed in darcys. For example, the maximum permeability (100 percent on the ordinate) of the sand represented in Fig. 5 is 17.8 darcys for either gas or liquid, which means that for a pressure gradient of 1 atmosphere per centimeter, 17.8 cc of water of viscosity 1 centipoise will flow through each $cm^2$ cross section of sand per second. On the other hand if $CO_2$ gas having a viscosity of 0.015 centipoise is the fluid, its volume rate of flow at the mean pressure in the sand with a pressure gradient of 1 atmosphere per cm will be $17.8/0.015 = 1186$ cc per sec.

An outstanding feature of the curves, Figs. 5–8 is their striking similarity, considering that the specific permeabilities of the sands comprising the separate experiments ranged from 17.8 to 262 darcys (1400 percent variation). In fact for our present purposes, and in view of the normal spread of the experimental data, it is not unreasonable to represent them as the average curves shown in Fig. 9.

At this point it will be convenient to discuss briefly certain features of these curves which provide some qualitative insight into the mechanism of the flow of mixtures briefly touched upon in the introduction. Moreover certain experiments will be presented which, while very incomplete and seemingly a digression from the principal features of the study, may serve to clarify to some extent this qualitative picture.

Attention is called to a detail of the curves shown particularly strikingly in Fig. 5. The portion of the gas permeability curve below about 40 percent saturation represents very high gas/liquid ratios; for example, the ratio of the gas/liquid volume flowing at 30 percent liquid saturation of the sand being about 4100 (23,000 cu. ft. per bbl.).[5] When the liquid saturation of the sand is still about 10 percent the gas permeability has, within observational accuracy, reached 100 percent: the flow is entirely gas. This indicates that the liquid left in the pores of the sand body is retained in the

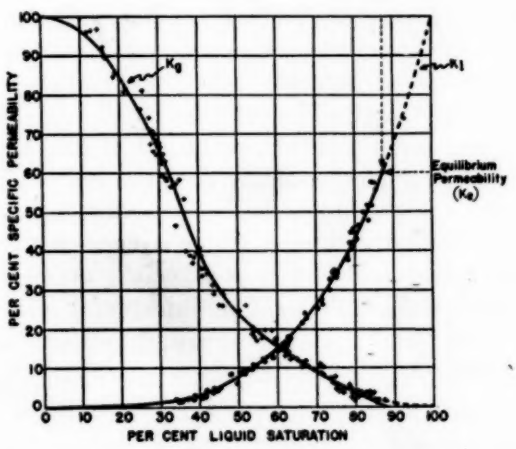


FIG. 6. Permeability-saturation relation for unconsolidated (heterogeneous) sand with specific permeability of 44.3 darcys.

[5] Usual units in American petroleum technology.

sharp angles between the sand grains and that in normal homogeneous-fluid flow this fraction of the pore volume makes an insignificant contribution to the total flow. These sharp angles retaining liquid are thus comparatively dead spaces in which there is never any appreciable amount of flow, consequently their plugging or filling by a solid or incompressible material has a negligible effect on the apparent permeability of the sand. This result would, of course, be anticipated from consideration of well-known principles applicable to any flow channel of similar section. But the experimental evidence shows strikingly that the removal of the last 10 to 15 percent liquid from a liquid-saturated sand body involves practically an evaporation process; the flow comprising essentially a wet gas.

If one were to postulate the simplest conceivable mechanism for the flow of mixtures of two immiscible fluids the $k_g$ and $k_l$ curves as in Fig. 9 would be straight lines intersecting at the 50 percent saturation point so that the total effective permeability of the sand would be constant and equal to the specific permeability ($k_0$) regardless of the liquid saturation of the sand. Such would be the case if in effect each of the component fluids maintained the characteristics of homogeneous fluids and no extraneous energy loss or obstruction of the channel occurred. However, the dotted curve of Fig. 9 which represents the observed total permeability of the sand shows that when the fluid content of the sand body constitutes approximately a 1 : 1

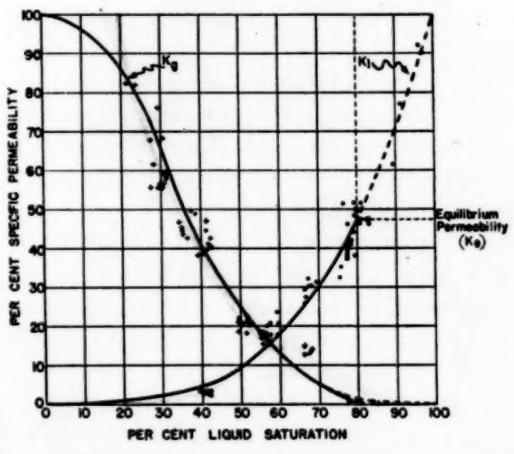


FIG. 7. Permeability-saturation relation for unconsolidated (40–50 mesh) Ottawa sand with specific permeability of 53.6 darcys.

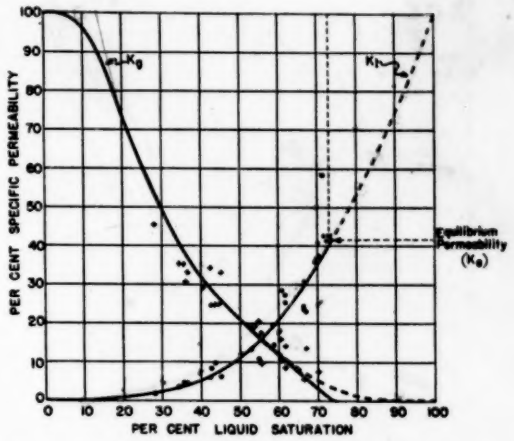


FIG. 8. Permeability-saturation relation for unconsolidated (20–30 mesh) Ottawa sand with specific permeability of 262 darcys.

gas/liquid ratio, the effective permeability reaches a minimum which is only about 1/3 of its normal value.

We have already mentioned the well-known Jamin effect[1] which tends to lock bubbles of the dispersed gas within the pores thus decreasing the effective cross section of the channel. Visual examination of a flowing mixture indicates also the possibility of an extraneous energy loss arising from an apparent pulsation of entrapped gas masses which would induce local eddies in the liquid. In fact it is reasonable to surmise that a large portion of the decrease in permeability might be assignable to such eddy losses. In an attempt to isolate these two factors and obtain at least a qualitative indication of their relative importance the following experiments were performed.

### 4. Flow of two immiscible liquids

If the gas bubbles present in the previous experiments were replaced by noncompressible liquid the pulsations giving rise to local eddies would be minimized. Such experiments were made using oil and water, the sand being initially saturated with water, oil being the dispersed phase; a small sand column was used. The volume of oil in the sand and hence the water saturation was determined from the difference between the volume of oil injected and the volume collected at the outlet. The oil was forced into the sand from a graduated cylinder through a porous disk in order to disperse it as

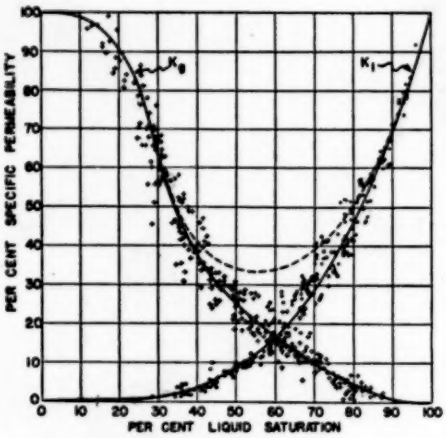


FIG. 9. Composite curves showing permeability-saturation data for all four sands.

finely as possible within the sand column and simultaneously water was flowed through the sand in order that steady state conditions might be attained.

In all these experiments the rate of accumulation of oil in the pores was quite rapid. All the inflowing oil was held within the sand until about 30 percent of the pores were filled. When the oil viscosity was increased by the addition of a heavy refined oil, the percentage of pores filled with oil before any began flushing through was about 40. The resulting saturation-permeability relation for oils in water is shown in Fig. 10. The viscosities of the oils used ranged from 1.5 to 7.2 centipoises. Although the curve resembles that for gas-liquid mixtures quite closely, there is considerably more spread in the data for oil-water mixtures than in those for gas-water mixtures. This is probably due in large part to the difficulty in accurately measuring, with the apparatus used, the volumes of oil input and output from the sand. However, it seems possible to say from the similarity of the curves that the flow of oil-in-water mixtures is similar in its general mechanism to that of gas-water mixtures.

It is of particular interest, however, that replacement of the compressible gas bubbles in the system by incompressible liquid bubbles did not result in a significant change in the extra energy losses as will be evident upon comparing Figs. 9 and 10. Thus it would appear that the saturation-permeability relations of Fig. 9 are due largely to actual plugging of a portion of the pores by the dispersed bubbles and any extraneous energy losses assignable to local eddies must be unimportant in comparison.

A series of experiments was made in which the phases were reversed, water being the dispersed, and oil the dispersing medium. In contrast to the flow of oil in water, the water began flowing out of the sand almost as soon as injection was started. There was no building up of a definite gradient before the water broke through the sand. The saturation of the water in the sand was always comparatively low. Channels of water ("piping") were seen to form almost immediately in the sand (the flow tube was of glass) and to persist throughout the flow. No consistent data were secured, the steady state values depending apparently on what water channels happened to form in the sand at the beginning of the experiment.

Thus is evidenced a pronounced difference between the nature of the flow of oil in water and of water in oil brought about, no doubt, by the relative wetting power of the liquids for the sand used in the experiments. In the case of oil dispersed in water, the sand is initially wet with water and probably remains so. The oil is introduced into the sand in small drops, and due to the inability of the oil to wet the sand, probably remains as dispersed droplets when forced into the small pores. Due to the Jamin effect these drops tend to remain in the pores, thus producing a random and fairly uniformly distributed resistance to flow. Apparently no channels in the sense of "piping" are formed by this mechanism.

When water is dispersed in oil, however, it appears that the preferential wetting of the sand by the water results in the formation of definite channels which are thereafter maintained. These channels may vary from one experiment to another, in number, size, and distribution, in such a way that the resulting permeabilities show no relation to the oil saturation of the sand. This hypothesis is in accord with pressure gradient variations observed during the experiments, for when oil was dispersed in water the pressure gradient for a constant volume input rose rapidly to a comparatively high value and then, as oil broke through the sand column,

settled to a stable steady state value, whereas when water was dispersed in oil there was only an extremely small change in gradient when the water flow began, the steady state value being only slightly above that for the flow of pure oil. This difference in behavior between water injected into an oil sand, and oil injected into a water sand (and in fact, the entire problem of immiscible liquids) has not been studied further by us and is mentioned here merely to call attention to the importance of the surface phenomena involved.

## IV. General Discussion

We believe that the experimental evidence presented is adequate to establish the general applicability of the curves shown in Fig. 9 for the case of gas-liquid mixtures flowing through *unconsolidated* sand. It will be recalled that within the limits of observational accuracy, or inherent repeatability, the same curves apply regardless of the grain size of the sand or its heterogeneity. Furthermore they apply over a wide range of liquid viscosity and some evidence was presented which indicates that they may be valid even for the case of immiscible liquids provided the dispersed phase does not preferentially wet the sand. While it is clear that the detailed mechanism is not understood nor are the quantitative variations due to changes in certain parameters such as interfacial tension, contact angle of films, etc., involving physical properties of the fluids, it seems evident from the experimental results that in comparable systems these variations will have only a minor influence on the behavior. Assuming, therefore, the general applicability of the empirical relations given by Fig. 9, it is of interest to examine their consequences when applied to questions of practical interest.

### 1. Steady state gas/liquid ratio *vs.* liquid-saturation of the sand

On the assumption that the curves of Fig. 9 may be applied to the steady state flow of a gas-liquid mixture through any unconsolidated sand it is clear that the gas/liquid ratio must have a particular value for every value of liquid-saturation of the sand or conversely, for a given liquid-saturation the steady state flow can be maintained only at a particular gas/liquid ratio. By this is meant that if at a given liquid-saturation of the sand the gas/liquid ratio is greater than indicated by the curves, the liquid-saturation of the sand must decrease, or conversely if the ratio is less than that indicated, liquid will *accumulate* within the sand. It is of interest, therefore, to plot the data of Fig. 9 in the form $k_g/k_l$ *vs.* percent liquid saturation (Fig. 11).

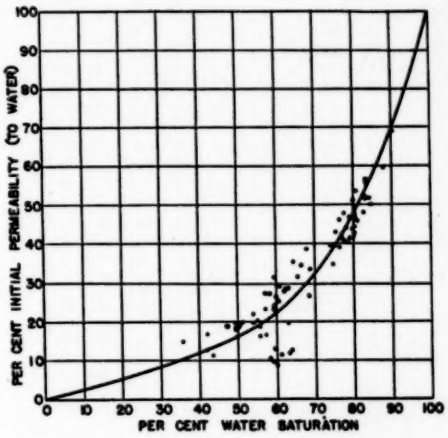


FIG. 10. Permeability-saturation relation for oil-in-water mixtures (oil viscosity varied from 1.5–7.2 centipoises).

Now the rate of flow of the liquid component at any liquid-saturation of the sand is given by

$$v_l+\Delta P k_l/\mu_l, \tag{1}$$

and the gas component by

$$\bar{v}_g=\Delta P k_g/\mu_g, \tag{2}$$

where

$v_l$ = cc/sec. liquid,
$\bar{v}_g$ = cc/sec. gas at mean pressure $(P_1+P_2)/2$,
$\mu_l$ = viscosity of the liquid,
$\mu_g$ = viscosity of the gas,
$\Delta P$ = pressure drop per unit length of sand column.

Thus the gas/liquid ratio will be

$$\bar{v}_g/v_l=k_g\mu_l/k_l\mu_g, \tag{3}$$

and from a knowledge of the fluid viscosities and the curve of $k_g/k_l$ *vs.* liquid-saturation of the sand the steady state gas/liquid ratio is easily computed.

As an example, the steady state flow of an air-water mixture at 20°C through an unconsolidated sand whose liquid saturation is 70 percent

would be, from Eq. (3) and Fig. 9 ($\mu_l = 1.0$ centipoise, $\mu_g = 0.018$ centipoise):

$$\bar{v}_g/v_l = (9.6/30.0) \cdot (1.0/0.018) = 17.8 \text{ cc gas/cc water}$$

and the pressure gradient required to maintain a flow of 0.1 cc of water and 1.78 cc of air/sec. through 1 cm² cross section of sand of $k = 50$ darcys would be, from Eq. (1),

$$\Delta P = 0.1/50 \times 0.30 = 0.0067 \text{ atmos./cm or } 5.06 \text{ mm Hg/cm.}$$

It is of interest to note the very rapid increase in the gas/liquid ratio as the sand is depleted of liquid. Thus to remove 50 percent of the water from a sand by driving with air, the air/water ratio at the final stage would be

$$\bar{v}_g/v_l = (25/9) \cdot (1/0.018) = 154 \text{ cc air/cc water,}$$

and the pressure gradient required to maintain a flow of 0.1 cc of water and 15.4 cc of air per second through the sand as above would be:

$$\Delta P = 0.1/50 \times 0.09 = 0.0222 \text{ atmos./cm} = 16.9 \text{ mm Hg/cm.}$$

This pressure gradient is more than three times that required to maintain the same liquid flow at 70 percent saturation and the volume of air required is 8.6 times greater.

If, instead of air and water, the fluid mixture comprised fluids of other viscosities the appropriate values of $\mu_l$ and $\mu_g$ would be applied. One other precaution should be mentioned. The curves of Fig. 9 apply for cases in which there is sufficient gas in solution in the liquid to permit the evolution of some free gas during passage through the sand. Thus free gas is able to accumulate in the smallest of the pores. If, however, the sand is initially saturated with liquid and the gas-liquid mixture is merely driven through the system the behavior may be slightly modified since the gas in transit may be unable to penetrate some of the smaller pores. However, if only a very small percentage of the total gas traversing the system comprises gas evolved from solution then the system will behave according to the empirical curves.

Some question may arise as to the meaning of steady-state flow as used in this discussion when it is evident that there can be no very

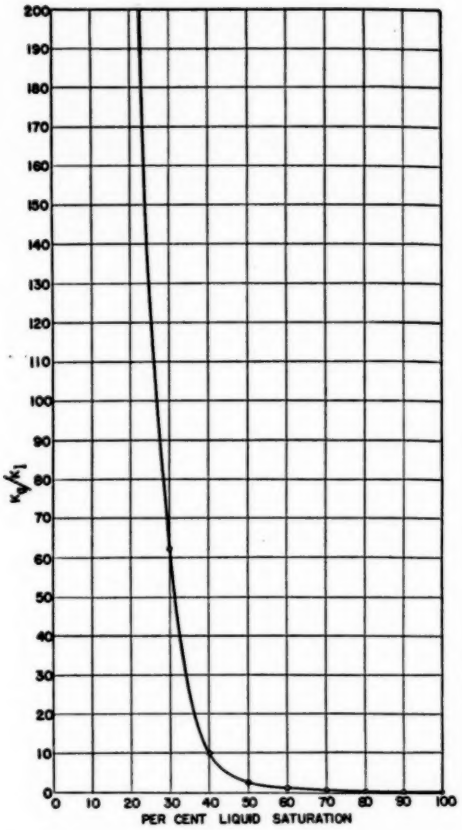


FIG. 11. Relation between gas/liquid ratios and saturation for flow through unconsolidated sands (obtained from the curves of Fig. 9).

sudden transition from one liquid saturation of the sand to another. Attention has been called to the fact that the $k_g$ or $k_l$ value for any saturation (Fig. 9) is the same regardless of whether it is reached by increasing or decreasing the liquid saturation of the sand (accomplished in practice by changing the gas/liquid ratio). It follows from this characteristic that a true steady-state phenomenon is involved but a transition period is required in the change from one state to another during which accumulation or depletion of gas takes place until the appropriate steady state liquid-saturation of the sand exists. It is impossible at this time to describe quantitatively the behavior of the system in these transient periods. However, some experiments intended to clarify this point indicate that the change from one state to another is at first very rapid but the final liquid-saturation is approached asymptotically. The duration of the transient seems

dependent primarily upon the total volume of free gas traversing a given cross section and the lower the liquid-saturation of the sand the greater the total free-gas flow required to make a certain percent change in saturation. The performance is far too complex and the experimental evidence too meager to permit further discussion of details. But it should be clear that the final condition of liquid saturation to be observed at any point in a sand body is dependent upon the gas/liquid ratio of the mixture which last traversed it (subject to the intermediate transient phenomena just mentioned). This fact is of very great importance when considering the behavior of a system comprising a well penetrating an oil and gas saturated sand.

## V. The Concept of an Equilibrium Permeability

In the above discussion nothing was said regarding the saturation-permeability relation for very low gas/liquid ratios. It was stated, however, that the points from which the curves were drawn were obtained under steady state conditions. This is not true for those few points on the curves which are found above the point marked "equilibrium permeability," as it was necessary to obtain these points under *transient conditions*. It was found that for low gas/liquid ratios the steady-state saturation and permeability condition obtained for a given sand was always the same regardless of the gas/liquid ratio, provided only that the ratio was less than a certain value (approximating 1.5 cc/cc). Various experiments were made at widely different liquid velocities and with extremely small gas/liquid ratios, without changing the final steady-state values for permeability and saturation.

At these very low gas/liquid ratios, gas gradually accumulates in the pores until the pressure gradient has built up sufficiently high to flush some of the bubbles out of the pores, a steady state condition finally being obtained in which the bubbles are flushed out as rapidly as they are formed. Since this steady state is a definite characteristic of a given sand and fluid system it has been called "equilibrium permeability," and the liquid saturation of the sand corresponding to the equilibrium permeability has been called the "equilibrium saturation." Experiments were performed in which tap water was flowed through the sand without the addition of any gas other than that naturally dissolved in the water. The minute quantity of gas dissolved in the tap water was sufficient eventually to produce the equilibrium permeability. Other experiments at various pressures and rates of flow showed that final equilibrium permeability ($k_e$) was, within reasonable limits, independent of the velocity of flow provided only that the amount of free gas accompanying the liquid did not exceed a certain critical value. Thus the attainment of a constant pressure gradient represented not only a steady-state flow but a true *equilibrium* value of the permeability.

It is also of interest to observe that if an experiment is performed in which an excessive amount of free gas is flowed along with the gas-saturated liquid so that $k_l$ is forced lower than the equilibrium permeability value ($k_e$) and the volume of free gas is then reduced to any value below the critical limit, the system will automatically flush or dissolve out the excess of accumulated gas and the permeability to liquid will increase until the value $k_e$ is attained.

In some cases involving the flow of mixtures, the high pressure portion of the system will be above saturation pressure, and consequently there will be no free gas present in that part of the system. At the point, along the direction of flow, at which saturation pressure is reached, gas will begin coming out of solution; above this point there will be only liquid and immediately below it, gas bubbles. It is of interest to know how far below this saturation point it is necessary to go before equilibrium permeability is attained, in other words, how extensive is the transition region between the normal homogeneous fluid permeability and equilibrium permeability zones. In one experiment the pressures were such that the first section of the sand column was above saturation pressure, i.e., the low pressure end of the first section of the sand was at saturation pressure. At the end of the experiment when equilibrium was attained, the ratios of equilibrium to normal permeability for the four sections along the glass flow tube were, respectively, 1, 0.593, 0.653, 0.561. Thus the last three sections of the tube were essentially at equilibrium while

the first section maintained its original specific permeability. In other words, the transition region between dead fluid and equilibrium permeability is extremely narrow. This sharpness of the zone separating the regions of normal and equilibrium permeability is, indeed, a necessary requirement if the concept of an equilibrium permeability is correct. Thus it requires that the presence of a mere trace of free gas evolving from the liquid within the system must necessarily result in the *gradual* accumulation of fixed gas masses within the pores, the accumulation in time reaching the volume represented by the equilibrium saturation.

The concept of "equilibrium saturation" as discussed here requires that for a given sand the equilibrium value of saturation must eventually be obtained, if only a minute trace of free gas is formed and flowing, and when this steady state condition is reached, its position in the sand will be at that point at which the liquid containing the dissolved gas reaches its saturation pressure. In the sand, above the saturation pressure "dead" liquid (liquid containing no free gas) will be flowing. At, and immediately below, the saturation pressure, equilibrium saturation will prevail while at lower pressures the saturation at any point in the sand will be appropriate to the gas/liquid ratio at that point as indicated in the curves of Figs. 5–8. The gas permeability under steady-state conditions is indicated in the curves by the solid lines. It must, of course, be zero above equilibrium saturation. The dotted portion of the gas permeability curve is merely that portion of the transient curve which does not coincide with the steady state curve. For points in the sand which will eventually have a low saturation, the transient follows the dotted curve until it merges with the solid portion and then follows that to the final steady state saturation. For points in the sand near that at which saturation pressure prevails, the transient may follow some other path lying between the dotted and solid portions of the gas permeability curve, but every point in the sand will, for steady state conditions, lie on the solid curve.

A question which immediately arises is that concerning the relation between equilibrium permeability and the normal or specific permeability of the sand. The equilibrium permeability (but not equilibrium saturation) was determined for a number of different sands in a glass flow tube. The results are given in Table I.

It will be noted that as the grain size gets smaller and hence the permeability lower, the ratio of equilibrium to specific permeability, $k_e/k$, approaches unity. The range of velocities used in these experiments was about 10–1 on a given sand and the gas/liquid ratio was as high as 1 cc of gas per cc of liquid. The data of Table I are plotted on log−log paper Curve I, Fig. 12, specific permeability ($k$) on one coordinate and equilibrium permeability ($k_e$) on the other.

In order to determine the effect of a change of liquid and gas on the equilibrium permeability a series of experiments was made using kerosene as the liquid with carbon dioxide as the dissolved gas, and another series with kerosene and natural gas. The same sands were used as for the experi-

TABLE I. *Equilibrium permeability for a number of different sands in a glass flow tube.*

| SAND | GRAIN SIZE (mm) | SPECIFIC PERMEABILITY | EQUILIBRIUM PERMEABILITY | EQ. PERM. / SPEC. PERM. |
|---|---|---|---|---|
| Ottawa (20–30 mesh) | 0.701 | 167.3 | 84.6 | 0.506 |
| Ottawa (20–30 mesh) | | 140.1 | 67.68 | 0.483 |
| | | 232 | 97.0 | 0.420 |
| | | 261 | 110 | 0.421 |
| | | 246 | 96 | 0.390 |
| | | 244 | 105 | 0.430 |
| | | 244 | 101.7 | 0.417 |
| 40–45 mesh | 0.351 | 58.7 | 32.9 | 0.560 |
| 50–60 mesh | 0.271 | 24.82 | 16.82 | 0.677 |
| 50–60 mesh | | 20.9 | 14.9 | 0.712 |
| 60–65 mesh | 0.237 | 24.1 | 16.85 | 0.699 |
| 60–65 mesh | | 22.73 | 15.01 | 0.660 |
| 80–100 mesh | 0.150 | 11.17 | 8.62 | 0.771 |

TABLE II. *Equilibrium permeability as affected by a change of liquid and gas.*

| SAND MESH | LIQUID AND GAS | POROSITY | SPECIFIC PERM. | EQUIL. PERM. | EQUIL. PERM. / SPEC. PERM. |
|---|---|---|---|---|---|
| 20–30 | Kerosene $CO_2$ | 30.7 | 175 | 569 | 0.325 |
| 40–45 | Kerosene $CO_2$ | 39.4 | 74.2 | 31.2 | 0.421 |
| 40–45 | Kerosene Natural Gas | 40.6 | 72.2 | 34.7 | 0.481 |
| 60–65 | Kerosene $CO_2$ | 39.6 | 24.6 | 11.9 | 0.483 |
| 60–65 | Kerosene Natural Gas | 39.6 | 24.6 | 12.4 | 0.504 |
| 80–100 | Kerosene $CO_2$ | 40.7 | 12.81 | 7.18 | 0.560 |
| 80–100 | Kerosene Natural Gas | 40.7 | 12.81 | 8.28 | 0.646 |
| Heterogeneous Sand | Kerosene $CO_2$ | 35.1 | 47.5 | 19.52 | 0.411 |
| Heterogeneous Sand | Kerosene Natural Gas | 35.1 | 47.5 | 24.54 | 0.516 |

ments of Table I. The results of these experiments are shown in Table II.

The data from this table are plotted in Fig. 12, Curves II and III. It will be noted that the points fall quite closely on straight lines and that the lines are practically parallel. It is also significant that the data for heterogeneous (30–100 mesh) sand also fall on the curves, indicating that the important parameter is the permeability, $k$, and not the grain size or porosity of the sand. It might be mentioned that the equilibrium permeability relations of Fig. 12 were obtained many months earlier than those shown in Figs. 5–8, and on quite different apparatus, yet the agreement is quite satisfactory.

For unconsolidated sands *within* the range studied and including heterogeneous sands it appears, therefore, that the relation between dead fluid permeability and equilibrium permeability for the above three types of fluid mixtures may be expressed approximately by the following empirical equations obtained from the curves of Fig. 12.

$$k_e = 1.26\ k^{0.8} \text{ (water and } CO_2\text{)}, \quad (4)$$

$$k_e = 1.11\ k^{0.8} \text{ (kerosene and natural gas)}, \quad (5)$$

$$k_e = 0.91\ k^{0.8} \text{ (kerosene and } CO_2\text{)}. \quad (6)$$

Where $k_e$ is the equilibrium permeability and $k$ is the specific permeability. (No attempt has been made in this preliminary work to correlate the numerical coefficients with the viscosity and surface tension parameters. Indeed, we imply no theoretical significance to the above equations since they are merely a convenient representation of the observed data.)

It has been pointed out that even at *very low* gas/liquid ratios gas will gradually accumulate in the pores until an equilibrium permeability or an equilibrium liquid-saturation of the sand is reached. Thus in the region of saturation from 100 percent to the equilibrium value the curves of Figs. 5–8 have no steady-state meaning since a steady state $k_l$ in this region is nonexistent. Therefore, observed points on the complete curves in this region necessarily were obtained during a transient stage. The curves in this transient region, and particularly the gas/liquid ratios defined by the curves, are to be interpreted as limiting values only, for any gas/liquid ratio below the value defined by the curves is

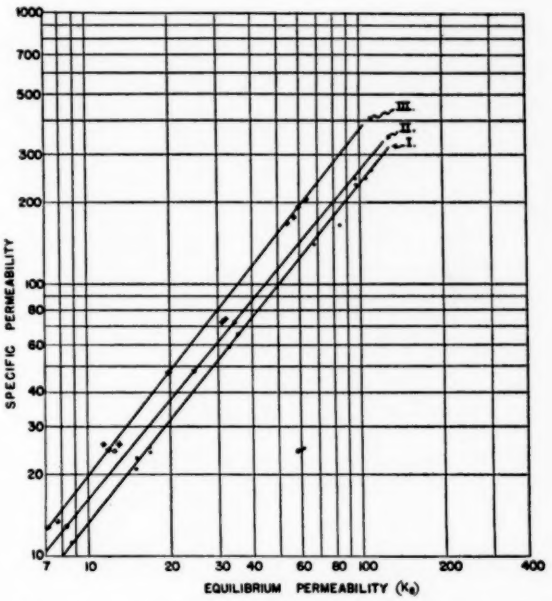


FIG. 12. Relation between equilibrium and specific permeability for various fluids in unconsolidated sands. Curve I, water and carbon dioxide, Curve II, kerosene and natural gas, Curve III, kerosene and carbon dioxide.

possible. Thus, as previously explained, regardless of the gas/liquid ratio prevailing, $k_l$ will continue to decline until the value $k_e$ (defined by curves Fig. 12) has been reached and thereafter $k_e$ will remain constant and steady state flow will obtain until the gas/liquid ratio is increased beyond the limiting value as represented by the curves.

To make clear the anomalous performance in this region let us consider a typical example. Assume a sand whose permeability $k$ is 45 darcys. From Curve I, Fig. 12, the equilibrium liquid permeability ($k_e$) for this sand when flowing a water-$CO_2$ mixture, is 26.5 darcys or 59 percent of its normal value. From the $k_l$ curve of Fig. 6 the liquid-saturation of the sand corresponding to $k_e = 59$–$60$ percent is 87 percent and the normal steady-state gas/water ratio at 20°C is:

$$\bar{v}_g/v_l = (1.5/60)\cdot(1.0/0.015)$$
$$= 1.68 \text{ cc } CO_2\text{/cc water.}$$

Thus if the flow through any section of the sand comprises a mixture of $CO_2$ and water whose ratio is *anything less* than 1.68/1 a steady state flow will eventually be reached wherein the liquid permeability will be $k_e = 26.5$ darcys, the

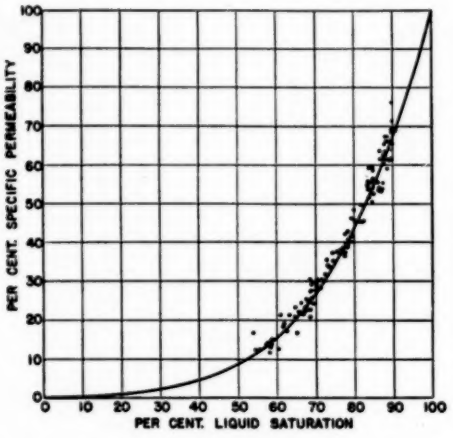


FIG. 13. Permeability-saturation curve for liquids of various viscosities (0.9–3.4 centipoises).

pressure gradient will be appropriate to the rate of flow of water at this value of $k_l$, and the liquid saturation of the sand will be 87 percent. If the gas/liquid ratio is then increased above the value 1.68 as by forcing additional free gas through the system, the liquid-saturation of the sand will be decreased below the equilibrium value and will be maintained at a value defined by the curves of Fig. 6. Thus, as outlined earlier, the equilibrium regime maintains at any gas/liquid ratio below the critical value defined by the curves, but if the critical ratio is exceeded then the normal steady-state conditions apply and the gas/liquid ratio uniquely defines the liquid saturation of the sand.

## VI. Effect of Liquid Characteristics upon Permeability-Saturation Relations

In the discussion thus far no mention has been made of the possible effect of variations in the properties of the liquid upon the permeability-saturation relation. The two liquid properties whose variation would be expected to have the most significance are viscosity and surface tension. While no exhaustive study was made to determine the effect of viscosity variations of the liquid it is significant to note the agreement of the $k_l$ curve of Fig. 13 with that of Fig. 9. The data of Fig. 13 resulted when the viscosity of the water was increased to 3.4 centipoises by the addition of sugar solution (thus not impairing its electrical conductivity). Evidently the more than threefold increase in viscosity of the liquid made no appreciable change in the performance of the system.

The other liquid property which should be of some significance in the flow of gas-liquid mixtures is surface tension. It might be expected that both the permeability-saturation relation, and the equilibrium permeability should be dependent in some degree upon the surface tension of the liquid. Some experiments were made to determine the effect upon these of a change in surface tension. Since the surface tension of water is approximately 72, it was decided to use a liquid with a surface tension of not over 35 dyne cm, the surface tension of many oils being between 25 and 30. It was also desirable that viscosity of the liquid should not be widely different from that of water in order that the significant variable should be that of surface tension. An attempt to use water after lowering its surface tension by the addition of Gardinol, an extremely effective surface tension depressor, was unsuccessful for two reasons. The Gardinol was adsorbed on the sand surfaces, thus raising the surface tension of the effluent liquid, and quite stable rigid emulsions were formed when the pressure was lowered sufficiently to permit the evolution of gas in the sand. These emulsions were sufficiently rigid to plug the sand quite effectively.

The selection of a suitable liquid of low surface tension was greatly limited by the fact that the liquid or solution had to be capable of dissolving an ionizable salt so that it might be electrically conductive. This restriction practically eliminates organic liquids except for certain alcohols. Ethyl alcohol will dissolve certain inorganic salts and has a low surface tension. A few preliminary experiments indicated that a 90 percent solution of ethyl alcohol would dissolve sufficient cupric chloride to be adequately conducting. Its surface tension was found to be 27 dyne cm and its viscosity about twice that of water.

Experiments were made upon two sands: 40–50 mesh and 20–30 mesh Ottawa sand. The experiments were extended through the region of extremely low gas/liquid ratios. The results are shown in Figs. 14 and 15. The equilibrium permeability for water and 40–50 mesh sand, as predicted from the specific permeability and the curve of Fig. 12 was 59.2 percent. It will be

seen that in Fig. 14 there is a distinct break in the curve at this point. According to the idea of equilibrium permeability developed above, the region between equilibrium and specific permeability is a transient region. It seems probable that the break in the curve is the result of not running the experiment sufficiently long to attain equilibrium conditions at these extremely low gas/liquid ratios. The approach to equilibrium seemed to be much slower with the liquid of low surface tension and it is probable that several days of continuous flow might have been required to attain complete equilibrium. Experiments of such length could not be carried out because of the nature of the apparatus and the supply of liquid available. Below equilibrium permeability the curve is in satisfactory agreement with the other curves obtained for water and carbon dioxide.

In Fig. 15 are seen the results for the experiments with 20–30 mesh sand. The equilibrium permeability as predicted from the curves for water was 41.7 percent. The value obtained by experiment was 43 percent. The data for both sands and the alcohol solution checked very satisfactorily the composite curve of Fig. 9, the principal difference being that the curves for alcohol-gas lie slightly above those for water-gas mixtures.

This result seems to indicate that surface tension has a very minor effect upon the permeability-saturation relation. It appears then that the characteristics of the sand alone are of major significance in the flow of gas-liquid mixtures, the fluid properties being of decidedly minor importance.

The gas permeability, when flowing alcohol-gas mixtures, appears to be negligible until the sand saturation reaches the equilibrium value or lower, whereupon the gas permeability rises quite rapidly. This appears to be in some disagreement with data for water-gas mixtures. It does, however, agree with observations on the flow of oil-in-water mixtures. In the flow of these mixtures it was observed as noted above that no oil flowed out of the sand (zero permeability to oil) until an appreciable fraction of the pores were filled with oil. This is a point which will require additional study.

## VII. The Recovery of Gas-Saturated Liquid from Unconsolidated Sands

While the modification of the normal dynamic characteristics of mixture flow caused by the existence of an equilibrium regime is of considerable importance a further and equally significant consequence is evident.

If a gas-saturated liquid under pressure completely fills the pores of a closed sand body the question arises as to the volume of liquid which can be recovered by permitting the pressure to decline to atmospheric through a suitable orifice placed at some part of the sand body. Assuming no super-saturation effects as the pressure is

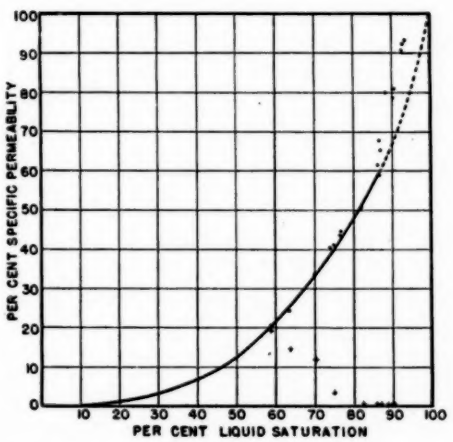


FIG. 14. Permeability-saturation relation for unconsolidated (40–50 mesh) Ottawa sand flowing alcohol-carbon dioxide mixture. Specific permeability 35.4 darcys. Liquid surface tension, 27 dyne cm.

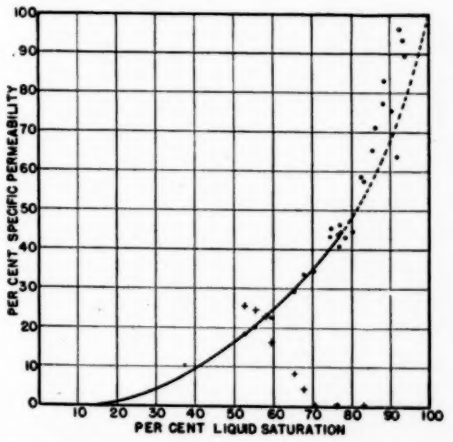


FIG. 15. Permeability-saturation relations for unconsolidated (20–30 mesh) Ottawa sand flowing alcohol-carbon dioxide mixture. Specific permeability 264 darcys. Liquid surface tension, 27 dyne cm.

lowered, evidently there will be an evolution of free gas at every point in the system. By the time the pressure *at any point* has been lowered sufficiently to have resulted in the evolution of enough free gas to permit attainment of the equilibrium condition, the liquid saturation of the sand at that point will have reached the value defined by $k_e$ (Figs. 9 and 12). Thus every unit volume of the sand must be depleted of liquid at least to the extent indicated. In other words, the accumulation of free gas within the system due to the Jamin forces which tend to lock the gas bubbles in the pores, must be accompanied by the displacement from the sand body of an equal volume of liquid. Furthermore the existence of an equilibrium regime requires that the minimum recovery of liquid correspond with the reduction in liquid saturation of the sand indicated by the equilibrium value. Therefore, provided only that the gas content of the liquid be in excess of a certain value (of the order of 10 to 1) the liquid recovery from an unconsolidated sand body upon release of pressure must everywhere reach a certain *minimum* value defined only by the equilibrium saturation and quite independent of the rate of release of pressure or the geometry of the flow system.

To indicate further the importance of this concept assume an unconsolidated sand body of any desired dimensions surrounded by impermeable boundaries and saturated with a liquid under such pressure that it contains a reasonable amount of dissolved gas. If this "reservoir" is then tapped by a well maintained at atmospheric pressure, liquid and gas will be produced. The initial rate of flow will be relatively high with a decline determined by the complex relations involved in the flow of compressible fluids further complicated by the fact that the permeability constant $k$ of the sand is no longer applicable, but must be replaced by a variable permeability factor $k_l$, which is a function of the state of depletion existent at the particular point in the system under consideration. However, quite regardless of the dynamical behavior one can say with certainty that *eventually* the pressure of the reservoir will fall everywhere to a value departing by only a negligible amount from atmospheric pressure. The equilibrium-permeability concept then requires that the recovery of liquid at every point in the reservoir *cannot be less* than the value determined by the equilibrium saturation. Since this equilibrium value may be determined from the empirical curves of the type shown in Figs. 9 and 12 it appears that the *minimum* ultimate recovery of liquid from an unconsolidated sand reservoir is definitely related to the normal permeability of the sand and is independent of the geometry or dynamical behavior of the flow, that is, the rate of flow or the number and distribution of the wells.

Such are the implications which follow from the empirical results which have been described in the foregoing discussion. We wish to emphasize that further study may reveal modifying details which have been overlooked here because of the necessity of averaging results which are not perfectly reproducible. For example the scattering of the observed points shown in Figs. 5–8 may be due to an hysteretic effect in the behavior of the accumulating gas bubbles responsible for the attainment of equilibrium permeability. Thus, whereas we have shown the value of $k_e$ to be apparently independent of the velocity of flow it may not be strictly independent and at *very* low velocities the $k_e$ value may be *lower* than shown by the curves. Indeed, intuitively one would believe such to be the case and certain details in the experiments to be described next give some hint of this. However, quite regardless of the existence of detailed modifications we have here been interested primarily in presenting the over-all behavior with the object of showing the general nature of the phenomena and the type of studies required for further extension of our knowledge concerning them.

Having concluded from consideration of the equilibrium regime that the minimum ultimate liquid recovery from an unconsolidated sand is determined by the permeability of the sand, some experiments were performed to ascertain the reliability of the empirical prediction.

The apparatus used consisted of the eight-section flow tube equipped as described so that the liquid saturation in the several sections could be determined from electrical resistance measurements. The sand column was filled completely with water saturated with $CO_2$ at about 50 lb. gauge pressure. The input end of the

system was closed off and the output valve opened slightly to permit a slow production of fluid. No portion of the system contained space unfilled by sand so that end corrections were entirely eliminated. The tube was horizontal and the fluid was produced over the entire area of the outlet end of the sand column. The volume of liquid and gas produced by permitting the pressure in the system to fall to atmospheric was measured by the usual methods and in addition the electrical resistance measurements permitted an independent determination of the average liquid depletion as well as the variation in depletion along the column. While it would be desirable to have a complete record of the pressure gradient and saturation distribution during the decline, the transient would have required automatic recording equipment which was not available.

Table III shows the results of a series of such production experiments. A very reasonable uniformity in saturation is indicated over the entire length of the column although it will be noted that in all three experiments the final saturation in the end of the tube opposite to the producing end is slightly less than the average saturation, while in general the saturation at the outflow end is somewhat higher than the average: where the velocities are lowest, the final depletion is slightly higher, perhaps lending some support to the assumption previously mentioned, that a somewhat lower value might be obtained for the equilibrium permeability if its determination were made at extremely slow rates of flow. In these production experiments the fluid velocities were many times as high as would be encountered in practice at any considerable distance from a producing well. Consequently it was decided that production experiments should be made on some different sands at flow rates comparable with those encountered at reasonable distances from producing wells.

A shorter (3-foot) flow tube was set up and adjusted to an accurately horizontal position so that no "gas-caps" could be formed which would augment production by displacement effects. Production was obtained from the exact top of the sand column through a needle valve capable of maintaining extremely small rates of flow. Producing rates were so slow that practically the entire pressure drop occurred across the needle valve and gradients through the sand were almost negligible. The results of these experiments on four different sands are given in Table IV.

It is seen that for all four of the sands the production was very close to that predicted from the original equilibrium permeability measurements by means of the curves of Figs. 12 and 5 to 8. Further, the final saturations in the experiments are observed to be slightly lower than the values obtained from the curves, confirming the earlier suggestion that very slow velocities are conducive to lower equilibrium saturation values.

Three experiments were run on the 30–100 mesh sand, at three different saturation pressures, in order to determine, qualitatively, the minimum gas/liquid ratio necessary to obtain the final equilibrium saturation. It appears that this ratio for the sand in question lies between 8 and 12. This ratio is the total volume of gas dissolved in each volume of liquid and should not be confused with the flowing gas/liquid

TABLE III. *Recovery of fluid from unconsolidated sand.*

| Distance from Outflow End (feet) | Final Saturation (percent) | Average Saturation | Deviation from Average % Saturation | Volume Produced (cc) |
|---|---|---|---|---|
| 1 | 73.5 | | +1.8 | |
| 2 | 73.7 | | +2.0 | |
| 3 | 72.7 | | +1.0 | |
| 4 | 69.4 | | −2.3 | |
| 5 | 72.8 | | +0.9 | |
| 6 | 71.7 | | 0.0 | |
| 7 | 69.8 | | −0.9 | |
| 8 | 70.3 | 71.7 | −1.4 | 760 |
| 1 | 71.2 | | −1.1 | |
| 2 | 73.4 | | +1.1 | |
| 3 | 73.8 | | +1.5 | |
| 4 | 71.0 | | −1.3 | |
| 5 | 74.2 | | −1.9 | |
| 6 | 72.3 | | 0.0 | |
| 7 | 71.5 | | −0.8 | |
| 8 | 71.3 | 72.3 | −1.0 | 730 |
| 1 | 71.6 | | −0.2 | |
| 2 | 73.2 | | +1.4 | |
| 3 | 72.5 | | +0.7 | |
| 4 | 70.3 | | −1.5 | |
| 5 | 73.2 | | +1.4 | |
| 6 | 72.4 | | +0.6 | |
| 7 | 70.6 | | −1.2 | |
| 8 | 70.6 | 71.8 | −1.2 | 710 |

TABLE IV. *Fluid production experiments from different sands at flow rates comparable with those encountered at reasonable distances from producing wells.*

| Grain Size | Perm. (darcys) | Volume Liquid Produced | Average Liquid Velocity (cc/cm²/sec.) | Volume Gas Produced (cc) | Gas/ Liquid Ratio (cc/cc) | Final Saturation (Production Experiment) (percent) | Equilibrium Saturation (from Curves) (percent) |
|---|---|---|---|---|---|---|---|
| 20– 30 | 261 | 144 | $9.18\times10^{-5}$ | 3250 | 22.6 | 78.0 | 78 –80 |
| 40– 60 | 59.4 | 119 | $7.04\times10^{-5}$ | 2410 | 20.2 | 87.7 | 84.5–86.2 |
| 70–120 | 16.06 | 87 | $5.6\times10^{-5}$ | 2440 | 28.0 | 89.8 | 90.5 |
| 30–100 | 45.9 | 114 | | 2800 | 24.6 | 84.8 | 85.4–87.2 |
| 30–100 | 45.9 | 117 | | 1400 | 12.0 | 83.9 | 85.4–87.2 |
| 30–100 | 45.9 | 84 | | 700 | 8.3 | 88.8 | 85.4–87.2 |

ratio involved in attaining equilibrium permeability.

The significance of these production experiments is at once apparent. It appears to be quite certain that in the normal process of recovery of liquid from an unconsolidated sand body originally filled with gas-saturated liquid, two distinct phases are involved. On the one hand the equilibrium saturation determines the minimum recovery, predictable from the specific permeability-equilibrium permeability relations and applicable to every element of the sand body provided only that the pressure drop at every point is sufficient to result in the evolution of a total volume of free gas sufficient to build up the equilibrium condition. On the other hand if the free-gas/liquid ratio of the flowing mixture at any point is higher than the equilibrium gas/liquid ratio, the liquid saturation will be lowered in accordance with the $k_g/k_l$ curve Fig. 11 (derived from Fig. 9) and the liquid depletion of the sand will be enhanced at that point.

Thus the normal process of recovery involves an equilibrium phase which calls for uniform recovery throughout the system and is determined primarily by the specific permeability of the sand, and a second or gas-drive phase which induces further depletion depending upon the free-gas/liquid ratio provided it is greater than the critical equilibrium ratio. It is apparent from the relatively small total volume of free gas necessary to obtain equilibrium saturation, that a comparatively small drop in reservoir pressure below saturation pressure should be sufficient to produce equilibrium conditions and hence establish that phase throughout the reservoir.

## VIII. CONCLUSIONS

From the experiments described above, the following general conclusions may be drawn with regard to the flow of gas-liquid mixtures through unconsolidated sands:

1. Under steady state conditions of flow, the liquid saturation of the sand is determined by the gas/liquid ratio, and for a given ratio is not appreciably different for large differences in the sand permeability.

2. For all gas/liquid ratios below a certain critical value the steady state condition for a given sand is always reached at the same saturation and permeability; these have been called "equilibrium" saturation and permeability since they appear to represent a definite characteristic of the sand.

3. The equilibrium permeability and saturation of a sand may be predicted from a measurement of its specific permeability and this equilibrium saturation determines the *minimum* recovery obtainable from the sand. Moderate variations in liquid viscosity and surface tension appear to have negligible effect on the permeability-saturation relation for a sand.

4. Gas/liquid ratios of the order of 20,000 cu. ft. per bbl. are required to obtain a liquid saturation as low as 30 percent—liquid recovery of 70 percent—a factor of major significance of a sand when considering efficiencies of secondary methods of oil recovery or natural recovery methods which depend upon the sweeping action of gas traversing the sand, or the so-called gas drive effects. Moreover, it is evident that high efficiency in natural or in secondary recovery is attainable only by discarding the gas-drive principle wherever possible in favor of the so-called repressuring or expanding gas-cap method. The latter method takes advantage of structural conditions wherein the geometry of the sand body results in natural closed traps or domes in which free gas will tend to collect because of buoyancy. Continued accumulation of gas within such closed domes or the expansion of the gas-cap incident to decline in pressure must result in the displacement of oil down the flanks of the structure where it is recovered via wells penetrating only the flanks.

Clearly the ultimate recovery under such

methods is not limited or controlled by the phenomena discussed in this paper for, considering the entire sand body, under such conditions the expanding gas tends to act as a piston driving oil ahead of it, resulting in continuous replacement of the liquid content of the sand down the flanks as it is depleted by the producing wells. Thus it is evident that in practice the ultimate recovery of oil from a given body of sand may be greatly enhanced by making proper use of the action of gravity—a factor carefully eliminated in the experimental work discussed here and designed to study only the normal gas drive phenomena.

The authors wish to acknowledge the assistance of Mr. M. W. Meres and Mr. D. W. Reed in the experimental work and to thank Dr. M. Muskat and Dr. W. N. Arnquist for valuable assistance and suggestions. They also wish to thank the executives of the Gulf Research & Development Company for permission to publish this paper.

# The Flow of Heterogeneous Fluids Through Porous Media

MORRIS MUSKAT AND MILAN W. MERES, *Gulf Research & Development Company, Pittsburgh, Pa.*

(Received July 22, 1936)

The empirical results established by R. D. Wyckoff and H. G. Botset on the flow of gas-liquid mixtures through unconsolidated sands have been formulated into basic differential equations governing the motion of general heterogeneous fluids through porous media under both steady state and transient conditions. This formulation is based upon a representation of the porous medium as having a macroscopically local structure defined by the liquid saturation, or volume composition of the gas-liquid mixture, this saturation in turn determining the separate permeabilities of the medium to the liquid and gas phases. The steady state solutions of these equations are derived for the cases of linear, radial, and spherical flow, and the distributions of the pressure, permeability, and saturation are given graphically. It is found that the properties of these flow systems change but little from the corresponding ones for homogeneous fluids as long as the pressure exceeds about half the saturation pressure of the gas, except for the fact that the liquid saturation is very approximately equal to the equilibrium value and the liquid permeability has a value very near to its equilibrium value. The drop in liquid permeability and saturation is highly localized about the outflow surfaces and in those regions where the pressure is very much less than the saturation pressure, the increase in the pressure gradients above their normal homogeneous fluid values being also largely confined to these regions. For the study of the early stages of transient types of flow an analytical theory is derived, in the case of the linear system, based upon a representation of the transient as a continuous succession of steady states. For the investigation of the complete history of the linear transient system a numerical method is presented in which is developed a stepwise integration of the simultaneous partial differential equations for the pressure and liquid saturation, after the replacement of the various derivatives by their appropriate differences. The specific problem is treated in which a linear column of sand of unit length filled with liquid saturated with an ideal gas to a pressure of 10 units is suddenly exposed at one terminal to a pressure of 1 unit, which is thereafter permanently maintained at that value while the other end is permanently kept closed. The results of the calculations for this problem are given graphically in the form of sets of curves showing the history of the saturation and pressure distributions within the flow channel, the time variation of the flux from the system, and the time variation of the gas-liquid ratio associated with the liquid efflux. It is found that the liquid saturation at the time of physical depletion of the system, corresponding to an equalization of the pressures to that maintained at the outflow terminal, is quite uniform, being only 5 percent less at the outflow terminal than at the closed terminal of the linear column. The gas-liquid ratio is found to increase monotonically with the time. The bearing of these results on such problems as well spacing and gas recycling in the production of oil from underground reservoirs, and the manner of treatment of other typical heterogeneous fluid systems so as to include both the deviations from the ideal behavior of the free gas phase and the effect of gas segregation are discussed in detail.

## INTRODUCTION

ALTHOUGH the subject of the flow of homogeneous fluids through porous media has been rather thoroughly explored during the last several years, the literature contains not even a satisfactory beginning of a general treatment for the problem of the flow of heterogeneous fluids through porous media. The data at present available in the literature on the flow of gas-liquid mixtures all refer to particular experimental arrangements, the individual effects of which have not been abstracted from the numerical results. Only the most general and broad inferences can, therefore, be drawn from such work, and it is impossible to apply the results quantitatively to systems which are of different geometry or subject to somewhat different physical conditions than those yielding the original data.

In this paper will be given an analytical formulation of the problem of the flow of heterogeneous fluids through porous media, based upon the fundamental experiments of R. D. Wyckoff and H. G. Botset,[1] and several simple examples will be carried through numerically. Both the basic empirical data underlying the analytical formulation and the latter itself have been developed by analogy with, and as a generalization of, the empirical and analytical foundations of the theory of the flow of homogeneous fluids through porous media.

Insofar as the flow of a homogeneous fluid through a porous medium is microscopically viscous or streamline in character, it is, in

[1] Cf. preceding paper.

principle, subject to complete description by the laws of the classical hydrodynamics, as contained in the Stokes-Navier equations. However, the obvious futility of attempting to solve these equations for the multiply connected passages composed of the pores of a porous medium has necessitated a direct empirical solution of the problem. These have led to the beautifully simple result, first obtained by H. Darcy[2] for a liquid flow, and since generalized to gas flow,[3] and now generally known as Darcy's law, that the vector fluid velocity, $\bar{v}$, is directly proportional to the gradient of the pressure, $p$, or

$$\bar{v} = -(k/\mu)\nabla p, \tag{1}$$

where $\mu$ is the viscosity of the fluid and $k$ is the "permeability" of the medium, which is really best defined by Eq. (1) itself. This equation is not, of course, an analytical solution of the Stokes-Navier equations. Rather, it represents only the *macroscopic* equivalent of such solutions, in which $\bar{v}$[4] and $p$ represent statistical averages over a great number of pores. Combining Eq. (1) with the equation of state defining thermodynamically the nature of the fluid and the character of the flow—whether it be isothermal or adiabatic, for example, in the case of gas flow—and the equation of continuity, a complete formulation is obtained for the hydrodynamics of the flow of the homogeneous fluid through a porous medium. Thus, for effectively incompressible liquids, one finds at once in this manner that in homogeneous porous media the pressure must obey Laplace's equation, namely,

$$\nabla^2 p = 0, \tag{2}$$

and the associated analytical problems become potential theory problems.

It is important to note that in Eq. (1) the characteristics defining the nature of the fluid and of the porous medium are explicitly separated. The former is expressed simply by the viscosity of the fluid $\mu$. And the porous medium is uniquely and completely described by its permeability $k$. Of course, the final pressure distribution within the flow system will depend also upon the equation of state of the fluid, whether it be gas or liquid, and on the thermodynamic character of the expansion of the former or on the compressibility of the latter, if appreciable, but the definition of the porous medium itself has been completed once the value of $k$ has been assigned.

When the fluid flowing through the porous medium is heterogeneous, there are, of course, two (at least) fluids whose character must be defined. This, however, is in itself not the significant feature giving rise to the fundamental difference between the problems of the flow of homogeneous and heterogeneous fluids through porous media. Rather it is the variability in the volume composition of the mixture as it progresses along the porous medium that necessitates the difference in treatment from that for a single homogeneous fluid. For it is clear that if the volume composition of the mixture were the same at all points of the medium, it would only be necessary to change the effective permeability and porosity of the medium for either component to reduce the problem to that of the flow of homogeneous fluids, as can indeed be done in the treatment of the steady state flow of two immiscible liquids.

Although this variation in the volume composition of the mixture might be represented from a thermodynamic point of view simply as a variation in the equation of state of the gas-liquid fluid, a more fundamental interpretation suggests that it be associated with changes in the effective dynamical characteristics of the medium itself. Thus expressing the volume composition of the mixture by the liquid saturation of the medium $\rho$—the part of the pore volume instantaneously occupied by the liquid—this same saturation will also determine the effective permeability of the medium for either component of the mixture. That is, the porous medium itself is to be considered as changing from point to point. It can, therefore, no longer be defined by a single invariable permeability. Rather, one must generalize this concept which is based upon the assumption that all of the interconnected pores of the medium are filled by the fluid it is bearing, and assign to the medium a *local* structure,

---

[2] H. Darcy, *Les fontaines publiques de la ville de Dijon* (1856).

[3] M. Muskat and H. G. Botset **1**, 27 (1931).

[4] In fact, $\bar{v}$ is not to be considered as a *physical* velocity, but is simply the volume fluid flux per unit *macroscopic* area of the porous medium.

defined by the liquid[5] saturation, this latter, in turn, uniquely determining the *local* permeabilities for both the gas and liquid phases of the mixture, the permeabilities representing the macroscopic velocities of the two phases per unit pressure gradient. Of course, these local saturations and permeabilities are themselves ultimately determined by the boundary pressures imposed on the system, the character of the fluids, the saturation pressures, and the production history of the system, and furthermore they may vary with the time, but the significant fact is that they represent the fundamental dynamical elements constituting the hydrodynamic mechanism whereby the flow system may be physically described. Indeed, it is the character of the variation of the saturation and permeability together with the fluid pressure in space and time that is the "unknown" to be predicted by the "solution" of a problem in the flow of heterogeneous fluids through porous media.

As the carrier of a heterogeneous fluid, a porous medium is thus characterized by the relation—curves or equations—between its local permeabilities for the liquid and free gas phases and the local saturation. The elements of these relations corresponding to complete or zero liquid saturations will give the special cases representing the homogeneous fluid permeability for either liquids or gases. Just as the latter are to be considered as constants of the medium to be determined empirically rather than by a calculation from the microscopic structure of the medium, so must the relations between the local permeabilities and the saturation be considered as the composite definition of the porous medium, which must be provided by empirical measurements before any particular flow problem can be discussed numerically. A satisfactory calculation of these relations theoretically would obviously be of an even higher order of complexity than that of the homogeneous fluid permeability, which already presents entirely insurmountable analytical difficulties.

[5] The choice of the liquid saturation is, of course, based only upon convenience. The use of its complement, the gas saturation, would evidently be equally definitive from a physical point of view.

It is also to be noted that whereas for a homogeneous fluid system the permeability is the same for both gases and liquids, this is no longer true when the medium carries a mixture of a gas and liquid. For insofar as the permeability refers to the *macroscopic* velocity of each fluid phase in the mixture per unit pressure gradient, it is clear that the permeability for either the gas or liquid phases will increase as the fractional volume of the pores occupied by either increases. Thus when the medium is completely saturated with liquid the gas permeability in the above sense will be zero, since no free gas is actually being transmitted through the medium. And conversely, when there is no liquid phase present, the liquid permeability, from the point of view of heterogeneous fluid flow, will be zero, as no liquid is being produced even though the medium is subjected to a nonvanishing pressure differential. This generalization of the permeability concept based upon the flow of homogeneous fluids is necessary in order to be able to identify and follow the behavior of the individual components of the two phase system.

Finally it is to be observed that although in the calculation of the individual gas and liquid permeabilities the effect of the differences in viscosities between the two fluids is eliminated by reducing them both to unit viscosity—as is always done in calculating homogeneous fluid permeabilities—their sum will still not equal the single homogeneous fluid value, except at the end points of complete and zero liquid saturation. For the continuous creation and destruction of interfaces between the immiscible fluids in the interior of the porous medium will clearly lead to appreciable energy losses in addition to that due to the viscous friction, which alone enters in a homogeneous fluid flow. Indeed, it is clear that, in principle, the interfacial tensions of the fluids should be required as an additional parameter with which to fix uniquely the value of the local permeability for any given local liquid saturation, although the experiments show that the variation with the interfacial tension of the permeability *vs.* saturation curves for unconsolidated sands, at least under steady state conditions, is not large, and may be neglected in a first approximation.

## I. Analytical Formulation of the Problem of the Flow of Heterogeneous Fluids Through Porous Media

With the above considerations in mind, we are ready to construct the analytical formulation of the problem of the flow of heterogeneous fluids through porous media. This will consist of the following elements:

(1) A statement of the viscosities $\mu_g$, $\mu_l$ of the gas and liquid phases.

(2) A statement of the solubility $s$ of the gas in the liquid, and its "equation of state" in the forms:

$$S=sp; \quad \gamma=cp, \tag{3}$$

where $S$ is the mass of gas dissolved in unit volume of the liquid, and $\gamma$ is its density at the pressure $p$, assuming that the gas obeys the ideal gas laws as well as Henry's law.

(3) The "laws of flow" for the gas and liquid phases, as

$$\bar{v}_g=-(k_g/\mu_g)\nabla p; \quad \bar{v}_l=-(k_l/\mu_l)\nabla p, \tag{4}$$

where $\bar{v}_l$, $\bar{v}_g$ are the macroscopic velocities—volume fluxes per unit area of the medium—of the liquid and free gas phases, and $k_l$, $k_g$ are their permeabilities.

(4) The empirical relation between the gas and liquid permeabilities and the liquid saturation, $\rho$, as

$$k_g=k_0F_g(\rho); \quad k_l=k_0F_l(\rho), \tag{5}$$

where $k_0$ is the homogeneous fluid permeability and $\rho$ is here considered as the actual liquid saturation divided by the normal porosity $f$[6] and:

(5) The equations of continuity for both the gas and liquid:

$$\nabla\cdot(\gamma\bar{v}_g)+\nabla\cdot(S\bar{v}_l)=-f(\partial/\partial t)\{Sp+\gamma(1-\rho)\},$$

and

$$\nabla\cdot\bar{v}_l=-f\partial\rho/\partial t. \tag{6}$$

Inserting Eqs. (3) and (4) into Eqs. (6) we obtain at once:

$$(c/\mu_g)\nabla\cdot(k_gp\nabla p)+(s/\mu_l)\nabla\cdot(k_lp\nabla p)=f(\partial/\partial t)p\{sp+c(1-\rho)\}, \tag{7}$$

$$\nabla\cdot(k_l\nabla p)=f\mu_l\partial\rho/\partial t. \tag{8}$$

Eqs. (5), (7), and (8) thus give four equations for the determination of the four unknown variables $k_g$, $k_l$, $\rho$, and $p$. And replacing $k_g$ and $k_l$ by $k_0F_g(\rho)$ and $k_0F_l(\rho)$, the equations are reduced to the two:

$$\frac{c}{\mu_g}\nabla\cdot\{pF_g(\rho)\nabla p\}+\frac{s}{\mu_l}\nabla\cdot\{pF_l(\rho)\nabla p\}=\frac{f}{k_0}\frac{\partial}{\partial t}p\{sp+c(1-\rho)\}, \tag{9}$$

$$\nabla\cdot\{F_l(\rho)\nabla p\}=\frac{f\mu_l}{k_0}\frac{\partial\rho}{\partial t}, \tag{10}$$

in the two variables $\rho$ and $p$.

These represent the fundamental equations which will govern the flow of heterogeneous fluids through porous media. And, as indicated above, the functions $F_g(\rho)$ and $F_l(\rho)$ must be predetermined empirically,[7] and are to be considered as physical data to be provided, together with the constants $c$, $s$, $f$, $\mu_g$, and $\mu_l$, before any numerical analysis of a particular flow problem can be attempted. Unfortunately, however, the nonlinear and complex character of these equations makes it impossible to treat or solve them generally. In the present paper we shall, therefore, content ourselves with a discussion of several simple special cases.

### A. Steady state linear flow

By definition, the steady state condition of flow will be governed by Eqs. (9) and (10) with the right sides set equal to zero. Although the time variable is thus eliminated, the resulting

[6] These definitions of the term $\rho$ and the functions $F$ as $k/k_0$, are used here because it is found empirically (cf. preceding paper) that the curves $F_g$ and $F_l$ will then be practically independent of the nature of the sand (if unconsolidated).

[7] Although these functions $F_g$ and $F_l(\rho)$ are, of course, the products of definite physical factors and of the properties of the sand structure, attempts to calculate them by considerations of the capillary structure of the medium must obviously involve such extreme simplifications as to dispel all confidence in their numerical implications. While it is most helpful to construct a physical picture for qualitatively explaining the variations of the $F_l$ and $F_g$ curves, it is clear that a quantitative treatment of such models of the microscopic flow system is even more remote from any practical applicability than the many fruitless attempts that have been made to calculate the normal homogeneous fluid permeability from grain size distributions. Furthermore, the practical situation with respect to the study of heterogeneous fluid systems, at least in the field of oil production, demands the recognition of the fact that sands do have the properties they are found with, which must therefore be determined by direct measurements, so as to permit an analysis of their macroscopic behavior under practical field conditions, and that even a satisfactory calculation of what the sand properties would have been if they had a certain idealized structure will have at best only an academic interest.

equations still present formidable analytical difficulties in the finding of general solutions. In the cases of linear, radial, and spherical flow, however, the solutions can be reduced so as to involve only single quadratures.

Thus for the problem of linear flow (along the $x$ axis), we have, from Eqs. (9) and (10):

$$\frac{c}{\mu_g}\frac{d}{\partial x}\left\{pF_g(\rho)\frac{dp}{dx}\right\}+\frac{s}{\mu_l}\frac{d}{dx}\left\{pF_l(\rho)\frac{dp}{dx}\right\}=0, \quad (11)$$

$$(d/dx)\{F_l(\rho)(dp/dx)\}=0, \quad (12)$$

which give immediately

$$[(c/\mu_g)F_g(\rho)+(s/\mu_l)F_l(\rho)]pdp/dx = \text{const} = -cQ_g/k_0, \quad (13)^8$$

$$F_l(\rho)dp/dx=\text{const}=-Q_l\mu_l/k_0, \quad (14)$$

where $Q_g$ and $Q_l$ are total volume rates of flow per unit area of the porous medium, as indeed they must be from elementary considerations. $Q_g$ refers, of course, to the gas volume at atmospheric pressure. Introducing now the notation

$$\Psi(\rho)=\frac{F_g(\rho)}{F_l(\rho)}=\frac{k_g(\rho)}{k_l(\rho)}; \quad \frac{Q_g}{Q_l}=R; \quad \frac{s\mu_g}{c\mu_l}=\alpha, \quad (15)$$

so that $R$ represents the gas-liquid volume ratio of the flux, as measured at atmospheric pressure, an elimination of $dp/dx$ gives

$$p=(R\mu_g/\mu_l)/(\Psi(\rho)+\alpha). \quad (16)$$

Differentiating, we have

$$\frac{dp}{dx}=-\frac{Q_l\mu_l}{k_0F_l(\rho)}=-\frac{R(\mu_g/\mu_l)\Psi'(d\rho/dx)}{[\Psi(\rho)+\alpha]^2}, \quad (16a)$$

so that

$$x=-\frac{Rk_0\mu_g}{\mu_l^2Q_l}\int_\rho^{\rho_1}\frac{F_l(\rho)(d\Psi/d\rho)d\rho}{[\Psi(\rho)+\alpha]^2}, \quad (17)$$

where the saturation at $x=0$ is $\rho_1$. To avoid the inaccuracies in finding the values of $d\Psi/d\rho$, Eq. (17) may be integrated by parts, giving

$$x=\frac{k_0}{\mu_lQ_l}\left[p_lF_l(\rho_1)-\frac{R(\mu_g/\mu_l)F_l(\rho)}{\Psi(\rho)+\alpha}-\frac{R\mu_g}{\mu_l}\int_\rho^{\rho_1}\frac{F_l'(\rho)d\rho}{\Psi(\rho)+\alpha}\right], \quad (18)$$

$p_1$ being the pressure at $x=0$.

Although, in principle, Eq. (18) permits the determination of the saturation distribution, and hence pressure and permeability distributions, for any set of boundary pressures and saturations, it has been found empirically, however, that it is impossible to maintain a steady state condition of the flow of a heterogeneous fluid as long as the liquid saturation exceeds a certain critical value, corresponding to the "equilibrium permeability" of the sand (cf. the preceding paper). Thus as long as there is any free gas at all in the sand it will, in effect, accumulate until the liquid saturation does not exceed the critical value, and will even accumulate at points where the pressure has dropped below the saturation pressure only by an infinitesimal amount. Hence the boundary conditions at a point where the system assumes the character of a heterogeneous fluid system are:

$$\begin{aligned} p &= \text{saturation pressure} = p_s; \\ \rho &= \text{critical saturation} = \rho_c. \end{aligned} \quad (19)$$

Furthermore at the equilibrium point the gas permeability (of the steady state) vanishes, so that $\Psi(\rho_c)=0$.

By Eq. (16), the resultant gas-liquid flux ratio is then uniquely determined. Taking this point as that corresponding to $(p_1, \rho_1)$, i.e., $x=0$, Eq. (18) can now be rewritten as

$$x=\frac{\alpha k_0p_s}{\mu_lQ_l}\left[\frac{F_l(\rho_c)}{\alpha}-\frac{F_l(\rho)}{\Psi(\rho)+\alpha}-\int_\rho^{\rho_c}\frac{F_l'(\rho)d\rho}{\Psi(\rho)+\alpha}\right], \quad (20)$$

with $R=(s/c)p_s$.

The other boundary condition may be expressed either by a specification of the terminal saturation $\rho_2(<\rho_c)$, or the terminal pressure $p_2(<p_s)$, at the distance $L$ from the point $x=0$. This will, in turn, determine the value of $Q_l$, by Eq. (20), by simply interchanging $Q_l$ and $x$, and setting $x=L$, $\rho=\rho_2$. From this it is seen that the flux through such a system, for given terminal conditions, is inversely proportional to its length.

[8] The minus sign on the right sides of Eqs. (13) and (14) simply anticipates the choice of $x=0$ as the *inflow* terminal of the system, so that $\partial p/\partial x<0$.

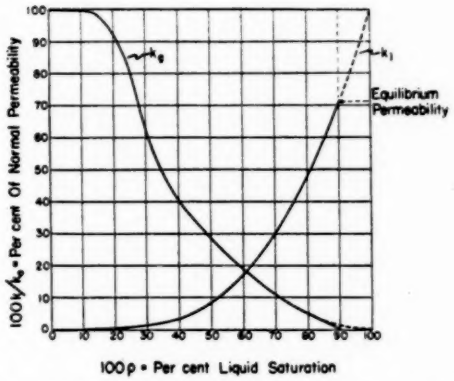


FIG. 1. Liquid ($k_l$) and gas ($k_g$) permeability curves as a function of the liquid saturation, replotted from Fig. 5 of preceding paper, for a 70–120 mesh sand carrying a water-carbon dioxide mixture. Homogeneous fluid permeability = 17.8 darcys. Dotted curves represent transient states of flow.

However, if $L$ is fixed, $Q$ varies with $p_2$, and hence the total pressure differential, in a nonlinear and more complex manner.

The significance of Eq. (20) may be seen most readily by a numerical application. Choosing for the fluid system that of carbon dioxide and water, for which

$$s/c = 0.88 \text{ cc/cc/atmos.}; \quad \mu_l/\mu_g = 59.3; \quad \alpha = 0.0148, \tag{21}$$

and for $F_l(\rho)$ and $\Psi(\rho)$ the functions given in Figs. 1 and 2, which were replotted from the data of the preceding paper, the relation between the bracket in Eq. (20) or: $Q_l\mu_l x/\alpha k_0 p_s$ and $\rho$ is plotted as Curve I in Fig. 3. $\rho_c$ has been taken as 0.90, corresponding to the 70–120 mesh sand, for which $k_0 = 17.8$ darcys. In Curve II the corresponding values of $p/p_s$, as given by Eqs. (16) and (21), are plotted also against $Q_l\mu_l x/\alpha k_0 p_s$. The variations of the relative liquid permeability, $k_l/k_0$, are shown in Curve III.

It will be seen that the saturation remains quite uniform and the pressure closely linear until $xQ_l\mu_l/\alpha k_0 p_s$ exceeds the value 20. In this range, of course, the flow approximates[9] that of a homogeneous fluid. It should be pointed out, however, that the limiting value for the abscissas of Fig. 3, do not imply any physical limitation on the length of the system under consideration.

[9] In a strict sense, however, there must be *some* variation of the permeabilities and saturations along the flow column, as is explicitly required by Eq. (16), as a consequence of the relation between $p$ and $\Psi(\rho)$.

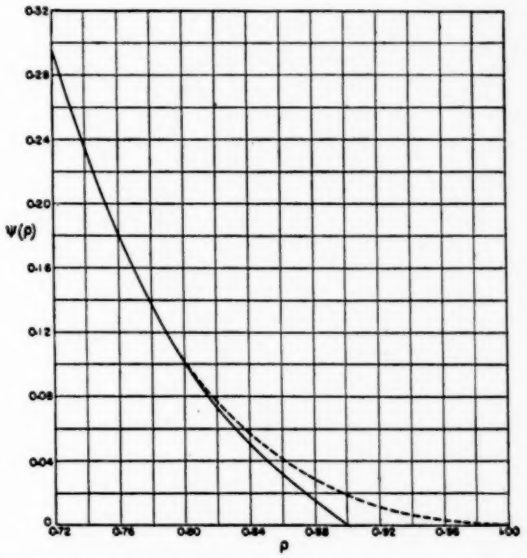


FIG. 2. $\Psi(\rho)(=k_l/k_g)$ *vs.* liquid saturation $\rho$, plotted from curves of Fig. 1.

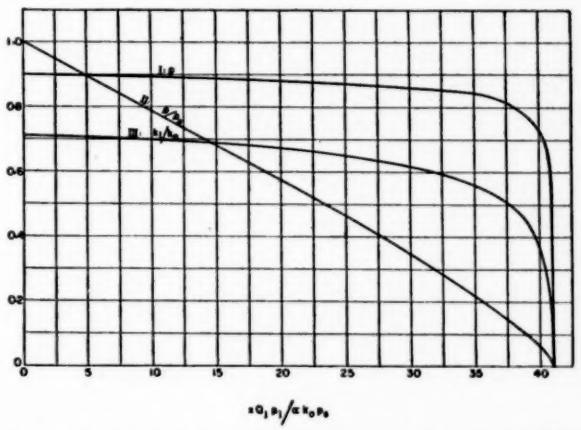


FIG. 3. Saturation (I), pressure (II), and permeability (III) distributions in a linear system carrying a heterogeneous fluid in the steady state. $p_s$ = saturation pressure; $k_0$ = homogeneous fluid permeability; $x$ = distance from inflow end where $p = p_s$. $Q_l$ = liquid flux per unit area; $\alpha = s\mu_g/c\mu_l$; $s$ = gas solubility; $c$ = gas density/atmos. $\mu_l$, $\mu_g$ = viscosity of liquid and gas.

Rather it represents only a limitation on the *product* of the length of the flow channel and the flux $Q_l$. Thus supposing that the pressure at the outflow end is effectively zero, so that $x$ corresponds to the total length $L$, the curves of Fig. 3 show that the maximum value of the liquid flux possible in the system is

$$Q_l = 41.0\alpha k_0 p_s/L\mu_l = 0.61 k_0 p_s/\mu_l L = 10.80 p_s/\mu_l L, \tag{22}$$

using the constants of Eq. (21).

Thus, if the outlet pressure be kept effectively at zero, the flux through a given channel will be directly proportional to the saturation pressure (or gas-liquid ratio), and hence pressure differential. The effective average permeability of the channel will then be (for the physical system chosen above) 61 percent of that of the homogeneous fluid permeability. If, however, the saturation pressure, and hence the gas-liquid ratio, is kept fixed, the variation of the flux through a channel of a given length with the pressure differential $(p_s-p)$ may be obtained from Curve II of Fig. 3 by simply interpreting the abscissas as proportional to $Q_l$ and subtracting the ordinates from 1. The curve so found is plotted in Fig. 4 ,where the quantity $(p_s-p)/p_s$ has been plotted as the effective pressure differential, and $(L\mu_l/\alpha k_0 p_s)Q_l$ as the flux. It will be observed from this curve that here, too, the flux increases almost exactly linearly with the pressure differential until the outflow pressure has fallen to less than half of the saturation pressure, beyond which the decreasing permeability near the outflow end cuts down the flux so that it increases less rapidly than the pressure differential. On the other hand, it should be noted that even in the approximately linear range of the flux *vs.* pressure differential curve the average effective permeability for the liquid, up to $(p_s-p)/p_s=0.5$, will be only 70 percent of the homogeneous fluid permeability.

## B. Steady state radial and spherical flow

When the steady state condition of flow has axial (radial) or spherical symmetry, the analysis will be identical with that given above for linear flow provided one makes the changes of variables as given by:

$$\begin{aligned}&\text{Radial flow:}\quad x=(1/2\pi h)\log r_e/r,\\ &\text{Spherical flow:}\quad x=(1/4\pi)(1/r-1/r_e),\end{aligned}\tag{23}$$

where $r_e$ represents the external (cylindrical or spherical) boundaries corresponding to $x=0$, where $\rho=\rho_c$, and $h$ is the sand thickness in the case of radial flow. From these definitions it follows that the saturation distributions for radial and spherical flow will be given by the equations:

Radial flow:

$$\log\frac{r_e}{r}=\frac{2\pi hk_0\alpha p_s}{Q_l\mu_l}\left[\frac{F_l(\rho_c)}{\alpha}-\frac{F_l(\rho)}{\Psi(\rho)+\alpha}-\int_\rho^{\rho_c}\frac{F_l'(\rho)d\rho}{\Psi(\rho)+\alpha}\right],\tag{24}$$

Spherical flow:

$$\frac{1}{r}-\frac{1}{r_e}=\frac{4\pi k_0\alpha p_s}{Q_l\mu_l}\left[\frac{F_l(\rho_c)}{\alpha}-\frac{F_l(\rho)}{\Psi(\rho)+\alpha}-\int_\rho^{\rho_c}\frac{F_l'(\rho)d\rho}{\Psi(\rho)+\alpha}\right].\tag{25}$$

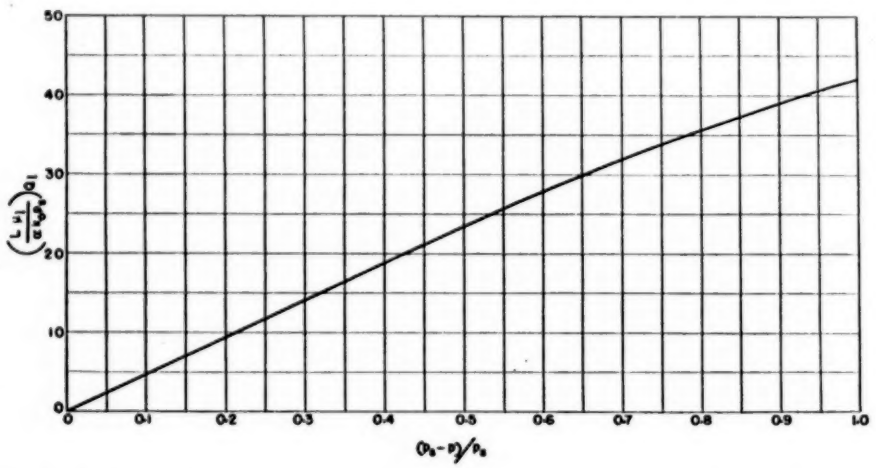


FIG. 4. Variation of the liquid flux $Q_l$ with the pressure differential $p_s-p_l$ across a length $L$ of a linear channel carrying a heterogeneous fluid. Notation same as in Fig. 3.

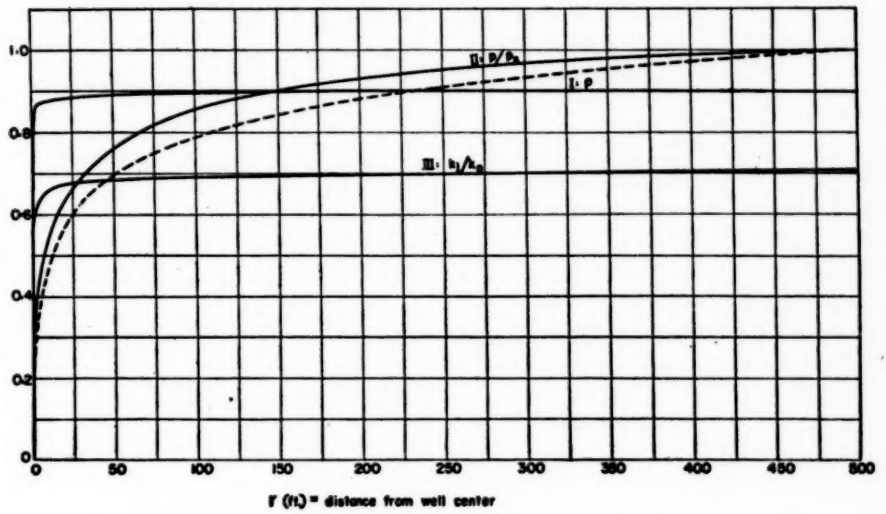


FIG. 5. Saturation (I), pressure (II), and permeability (III) distributions in a radial system carrying a heterogeneous fluid in the steady state. Dotted curve gives the pressure distribution in the equivalent homogeneous liquid radial system. Well radius = $\frac{1}{4}'$, external boundary radius = 500′. Notation same as in Fig. 3.

Assuming that $hk_0\alpha/Q_l\mu_l = 0.0295$, so as to make the limiting value of $x$, as given by Fig. 3, correspond to $r_e/r_w = 2000$, or a well radius, $r_w = 1/4'$, and an external boundary radius, $r_e = 500'$, the saturation, permeability, and pressure distributions for this radial system are shown in Fig. 5. The extreme localizations about the well center of the drops in the saturation and permeability below their equilibrium values are to be noted. However, although the highly localized saturation variation means only an extremely small change in the total liquid volume content of the sand from that in a uniformly saturated (to equilibrium value) sand, the drop in the permeability near the well does result in an appreciable increase in the concentration of the pressure gradients about the well center. This will be obvious on comparing the heterogeneous fluid pressure distribution as computed in the same manner as that for the case of linear flow, shown in Curve II, with that for a homogeneous fluid, given by the dotted curve.

The variation of the flux in radial and spherical systems with the pressure differential will be identical with that shown in Fig. 4 for the linear system, provided only that one interprets the ordinates of Fig. 4 to be

$$\frac{\mu_1 \log r_e/r_w}{2\pi h k_0 \alpha p_s} Q_l$$

for the case of radial flow and

$$\frac{\mu_l(1/r_w - 1/r_e)}{4\pi k_0 \alpha p_s} Q_l$$

for the case of spherical flow. Thus for a fixed pressure differential $((p_s - p)/p_s)$, the flux $Q_l$ will vary with the geometrical dimensions $h$, $r_e$, $r_w$ of these heterogeneous fluid systems in exactly the same manner as does that in the corresponding homogeneous fluid system.

With regard to the saturation and permeability distributions in a spherical flow system, it is clear that the appreciable deviations from the equilibrium values will be even more localized about the center of convergence of the flow than in the case of radial flow. And as in the latter case, the pressure gradients near the outflow surface will nevertheless show appreciable increases as compared to those in the corresponding homogeneous fluid system.

As to the numerical values plotted in Figs. 3, 4, and 5, it should be specifically understood that they refer only to the particular sand described by Fig. 1 and for the fluid constants defined by Eq. (21). Furthermore, it has been assumed that

the inflow terminal of the linear channel was in all cases maintained at the saturation pressure. The results are therefore quantitatively applicable only to these specific cases. However, the significant qualitative features displayed by the curves of Figs. 3–5 should persist even when the detailed numerical constants of the flow system are varied over a considerable range. For, as shown in the preceding paper, the curves $F_g(\rho)$ and $F_l(\rho)$ are changed but slightly even for large variations in the nature of the sand, as long as it is unconsolidated. And while the relation between the equilibrium permeability and the normal homogeneous fluid permeability, as shown in Fig. 12 of the preceding paper, may be appreciably changed when passing into the domain of consolidated sands, it is not unlikely that the relation between the heterogeneous fluid permeabilities and the saturation will still retain the general form of the curves of Fig. 1.

With regard to the terminal condition that the inflow pressure be the saturation pressure $p_s$, it is to be noted that the curves of Figs. 3 and 5 will also apply for any inlet pressure less than $p_s$ provided only the origin be shifted to the point where the pressure on the curves marked II has the appropriate value chosen for the inflow pressure. And if the inflow pressure exceeds $p_s$, one need only add the linear distribution for the homogeneous fluid flow until the pressure falls to the value $p_s$, the gradient being so adjusted that the same liquid flow will pass through the homogeneous and heterogeneous parts of the composite system.

## II. The Flow of Heterogeneous Fluids in the Nonsteady State

It will be recalled that Eqs. (9) and (10) are the basic differential equations governing the flow of a heterogeneous fluid through a porous medium. For the nonsteady state condition of flow, when the right sides of these equations are nonvanishing, they are evidently partial differential equations even for such cases as linear and radial flow. And as they are nonlinear, their solution presents a most formidable task. We are therefore forced to resort to approximation methods, which we shall now outline.

### A. "Continuous successions of steady states"

Although the basis for the discussion to be given here of the general problem of transient states of flow of heterogeneous fluids will be a numerical solution of the fundamental Eqs. (9) and (10), it is of interest to note that at least for the very early life of such transient systems the introduction of a physical approximation will permit the derivation of closed analytic expressions for the significant physical properties. This physical approximation method is simply that of representing the nonsteady state or transient history of the flow system as a continuous succession of steady states, each corresponding to instantaneous values of the boundary conditions, the variation of the latter being so chosen as to satisfy the physical conditions imposed on the system, such as a preassigned variation of the flux, or a closure of the system at one of the boundaries, etc. This method has been found useful in the study of the nonsteady state flow of gases in gas reservoirs, where the governing partial differential equation is also nonlinear.[10] While such a procedure has as yet no direct analytical justification, its implications in the case of gas flow have all been physically reasonable. Furthermore, a closer study of a similar problem of the flow of a compressible liquid through a sand, where the analysis could be carried through rigorously, indeed resolved itself, from a physical point of view, into a representation of the transient behavior of the system that was equivalent to a continuous succession of steady states of the type just described.[11]

This method of the continuous succession of steady states may be most easily illustrated by actually carrying through the appropriate analysis. Thus supposing that the outflow pressure (at $x=0$) of a linear system of length $L$, which is initially saturated everywhere with gas to the pressure $p_i$, is reduced at the initial instant and is maintained thereafter at the pressure $p_w(<p_i)$, it will be assumed that the resulting efflux of fluid will be given by the steady state values corresponding to the gas-liquid ratio of solution, namely: $R=(sp_i/c)(\Psi(\rho)=0$ in Eq. (16)). The

[10] M. Muskat and H. G. Botset, Physics **1**, 27 (1931), and M. Muskat, Physics **5**, 71 (1934).

[11] Cf. last reference, in particular section II, D.

length of this region of steady-state flow will be taken to grow (increasing "radius of drainage") at such a rate that the corresponding loss of fluid content of the system will just balance the flux. Specifically, then, if $x(t)$ is the length at the time $t$ of the region of steady state flow, we shall have that the associated liquid flux will be, by Eq. (17)

$$Q_l(t)=\frac{Rk_0\mu_g}{\mu_l^2 x(t)}\int_{\rho_c}^{\rho_w}\frac{F_l(\rho)(d\Psi/d\rho)d\rho}{(\Psi(\rho)+\alpha)^2}, \quad (26)$$

where $\rho_w$ is given by:

$$R\mu_g/\mu_l=p_w\{\Psi(\rho_w)+\alpha\}=\alpha p_i, \quad (27)$$

and the pressure at $x(t)$ is taken to be the initial saturation pressure $p_i$, at which the saturation has already fallen to the critical equilibrium value $\rho_c$. Furthermore, as the flux $Q_l$ is being supplied by the spread of the "radius of drainage" $x(t)$, we must have

$$\begin{aligned}Q_l(t)&=f\frac{\partial}{\partial t}\int_0^{x(t)}\{1-\rho(x)\}dx\\&=f\frac{\partial}{\partial t}\int_{\rho_w}^{\rho_c}\frac{(1-\rho)d\rho}{(d\rho/dx)}\\&=\frac{-Rk_0f\mu_g}{\mu_l^2}\frac{\partial}{\partial t}\int_{\rho_w}^{\rho_c}\frac{(1-\rho)F_l(\rho)d\Psi/d\rho}{Q_l(t)\{\Psi(\rho)+\alpha\}^2}d\rho, \quad (28)\end{aligned}$$

by Eq. (16a). Hence

$$Q_l(t)=A(\partial/\partial t)(1/Q_l);$$

$$A=\frac{-Rk_0f\mu_g}{\mu_l^2}\int_{\rho_w}^{\rho_c}\frac{(1-\rho)F_l(\rho)(d\Psi/d\rho)d\rho}{\{\Psi(\rho)+\alpha\}^2}, \quad (29)$$

with the solution

$$Q_l=(A/2t)^{\frac{1}{2}}. \quad (30)$$

The recession of the "radius of drainage" $x(t)$ is, therefore, given by

$$x(t)=Ct^{\frac{1}{2}};$$

$$C=\frac{\left(\frac{2Rk_0\mu_g}{f\mu_l^2}\right)^{\frac{1}{2}}\int_{\rho_c}^{\rho_w}\frac{F_l(\rho)(d\Psi/d\rho)d\rho}{\{\Psi(\rho)+\alpha\}^2}}{\left[-\int_{\rho_w}^{1}\frac{(1-\rho)F_l(\rho)(d\Psi/d\rho)}{\{\Psi(\rho)+\alpha\}^2}\right]^{\frac{1}{2}}}. \quad (31)$$

Thus the flux during the initial transient has the same simple time variation as the heat flux from an infinitely long rod whose end is suddenly lowered in temperature below its initial uniform temperature.

### B. Numerical method of solution

Although the case of the radial flow system can be treated in a similar manner, the analysis in both cases becomes considerably more complicated after the passing of the "initial transient" and the recession of the "radius of drainage," ($x(t)$ of Eqs. (26)–(31)) to the external boundary of the system. We shall, therefore, proceed now directly to the numerical solutions of Eqs. (9) and (10) for the problem of linear flow, defined by:

$$\begin{gathered}x=0:p=1;\quad x=L:\partial p/\partial x=0,\\ t=0:p=10;\quad \rho=1.0.\end{gathered} \quad (32)$$

Physically, Eq. (32) represents a linear column of length $L$, initially filled with a liquid which is saturated to a pressure of 10 units, and which is subsequently exposed to the terminal conditions of zero flux or closure at $x=L$, and a pressure of 1 unit at $x=0$. The problem is to determine the behavior of the pressure and saturation distributions after the initial instant, together with the associated fluxes.

To eliminate the absolute numerical values of some of the physical constants of the system, the dimensionless variables $\bar{x}$, $\bar{t}$ were introduced, where

$$\bar{x}=x/L;\quad \bar{t}=k_0t/f\mu_lL^2. \quad (32a)^{12}$$

Eqs. (9) and (10) then reduce, for the linear system, to:

$$\frac{\partial\rho}{\partial\bar{t}}=F_l\frac{\partial^2p}{\partial\bar{x}^2}+\frac{\partial F_l}{\partial\bar{x}}\frac{\partial p}{\partial\bar{x}},$$

$$\left\{\frac{c}{s}+\left(1-\frac{c}{s}\right)\rho\right\}\frac{\partial\rho}{\partial\bar{t}}=p\left\{\frac{c}{s}\frac{\partial\rho}{\partial\bar{t}}+\frac{F_g}{\alpha}\frac{\partial^2p}{\partial\bar{x}^2}+\frac{1}{\alpha}\frac{\partial F_g}{\partial\bar{x}}\frac{\partial p}{\partial\bar{x}}\right\}+\left(\frac{F_g}{\alpha}+F_l\right)\left(\frac{\partial p}{\partial\bar{x}}\right)^2, \quad (33)$$

where $\alpha$ is defined by Eq. (15). In order to sim-

[12] It is also assumed that the pressure $p$ is measured relative to some unit pressure, which is to be considered as multiplied into the right side of the equation for $\bar{t}$.

plify the calculations the special case was chosen in which: $c/s=1$, and $\alpha=1/100$.

The numerical work was then carried out in the following manner.

The partial derivatives were replaced by the difference expressions:

$$\frac{\partial G(q)}{\partial q}\sim\frac{G(q+h)-G(q-h)}{2h};$$

$$\frac{\partial^2 G(q)}{\partial q^2}\sim\frac{G(q+h)-2G(q)+G(q-h)}{h^2};\qquad(34)$$

$$G(\bar{t}+\Delta\bar{t})=G(\bar{t})+(\partial G/\partial\bar{t})\Delta\bar{t}.$$

The length of the system, that is, from $\bar{x}=0$ to $\bar{x}=1$, was then divided into segments spaced by 0.05 unit up to $\bar{x}=0.3$ and by 0.1 unit to $\bar{x}=1$. In the first part the differences given by Eqs. (34) were taken with $h=0.05$, and in the second $h$ was taken equal to 0.1. Beginning then with the initial condition in which the saturation $\rho$ was uniform over the whole range $\bar{x}=0$ to 1.0, and the pressure $p$ had the value 10 at all points except at $\bar{x}=0$, where it was set equal to 1, both the quantities $\partial\rho/\partial t$ and $\partial p/\partial\bar{t}$ were calculated by Eqs. (33), these values corresponding to the initial instant $\bar{t}=0$. The values of $F_l$ and $F_g$ were taken from Fig. 1. By means of the last of Eqs. (34) the values of $\rho$ and $p$ were then calculated at the time $\Delta\bar{t}$ which was chosen as $10^{-5}$. With these new values of $\rho$ and $p$ for the various values of $\bar{x}$ new values of $\partial\rho/\partial\bar{t}$ and $\partial p/\partial\bar{t}$ were computed by Eq. (33), thus giving the rates of change of these fundamental dependent variables at the time $\Delta\bar{t}$. The application of the last of Eqs. (34) was then repeated with a new increment $\Delta\bar{t}$, new values of $\rho(\bar{x})$ and $p(\bar{x})$ were obtained, and Eq. (33) once more applied, etc. The boundary condition in which the pressure was to be maintained at the value 1 at $\bar{x}=0$, was introduced by deliberately setting $p=1$ at $\bar{x}=0$ at each step, in spite of the fact that $\partial p/\partial\bar{t}$ at $\bar{x}=0$ always came out to have a positive value, except at the late stages of the calculations. In order to make possible the calculation of $\partial p/\partial\bar{t}$ as well as $\partial\rho/\partial\bar{t}$ at $\bar{x}=0$, values of $\partial p/\partial\bar{x}$ and $\partial^2 p/\partial\bar{x}^2$ were necessary. This required an effective extension of the range of $\bar{x}$ to the point $\bar{x}=-0.05$; and instead of extrapolating $p(\bar{x})$ linearly across $\bar{x}=0$ to $\bar{x}=-0.05$, as is usually done in such calculations, the value $p(-0.05)$ was so chosen that $\partial^2 p/\partial\bar{x}^2$ was equal at $\bar{x}=0$ and 0.05, as it is clear from the first of Eqs. (33) that a linear extrapolation at $\bar{x}=0$ would have given a positive value to $\partial\rho/\partial\bar{t}$ at $\bar{x}=0$, which would, of course, be physically inadmissible. While this mode of extrapolation is also arbitrary, it was found rather satisfactory until the later stages of the calculation, where obvious discrepancies necessitated the change to the requirement that the value of $\partial^2 p/\partial\bar{x}^2$ at $\bar{x}=0.05$ was $\frac{2}{3}$ of that at $\bar{x}=0$. $\rho(\bar{x})$, however, was extrapolated linearly at $\bar{x}=0$.

Although the effect of the imposition of the boundary condition $p=1$ at $\bar{x}=0$ was transmitted towards $\bar{x}=1$ only stepwise with each stage of the calculation, the boundary condition at $\bar{x}=1$ was introduced ultimately by the requirement of symmetry both in $p$ and $\rho$ at $\bar{x}=1$. That is, the range of $\bar{x}$ was extrapolated to $\bar{x}=1.1$, and the values there were taken equal to those at $\bar{x}=0.9$, so as to make both $\partial p/\partial\bar{x}$ and $\partial F/\partial\bar{x}$ vanish at $\bar{x}=1$.

While the procedure thus outlined appears to be completely numerical, it was found that the actual values obtained for $p$ as a function of $\bar{x}$ gave rather irregular values for $\partial^2 p/\partial\bar{x}^2$ which, when used directly in Eq. (33), ultimately led to a marked lack of smoothness in the values of the $\rho$ and $p$ themselves. It was, therefore, necessary to graphically smooth out the curves of $\rho$ and $p$ at each stage of the calculation and use the values from the curves in each subsequent stage according to Eqs. (33).

As the calculations proceeded and the values of $\partial\rho/\partial\bar{t}$ and $\partial p/\partial\bar{t}$ began declining from their maximal values the time interval $\Delta\bar{t}$ were gradually increased, those in the latter half of the decline exceeding the value 0.001.

It should be mentioned that the values for $F_g$ and $F_l$ used in these calculations for high saturations were those given by the dotted curves of Fig. 1. Since the detailed empirical study of the transient types of flow has not yet led to an unambiguous identification of the exact paths the $F_g(\rho)$ curves will take between the steady state curve and the upper dotted curve until the latter merges with the former, as the volume of available gas or its velocity is varied, we have

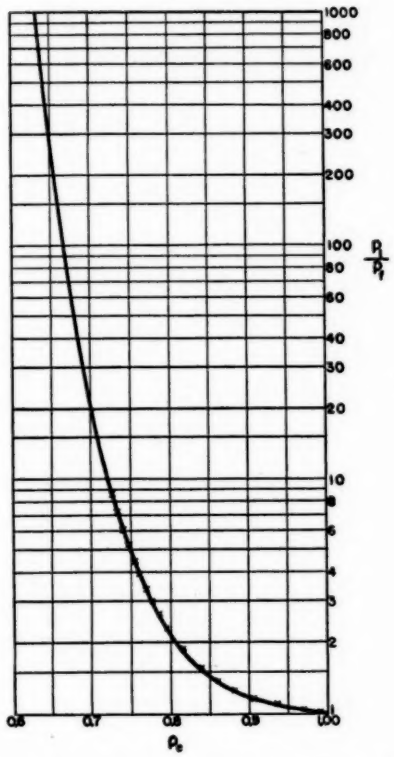


FIG. 6. Pressure drop *vs.* saturation $\rho_e$ at the closed boundary of a heterogeneous fluid system as given by Eq. (37). $p_i/p_f$ = (initial pressure)/(pressure when saturation has fallen to $\rho_e$). Crosses are values found in calculations of the production from a linear system. In both $c/s=1$, $\alpha=0.01$.

used what appears to be the envelope of the various possible $F_y(\rho)$ curves, namely, the dotted one. While this fact leads to some uncertainty as to the uniqueness of the exact numerical results of the calculations, it is very unlikely that any of the general features will be thereby affected.

### C. Tests of the calculations

In addition to the general physical requirements that both the pressure and saturation must monotonically decrease with the time, and that they must increase with $x$, a further check on the calculations was obtained by means of a relation that was derived[13] rigorously from the original differential equations between the saturation and pressure at the closed boundary. This relation, which is valid for a closed system of general[14] geometry, may be derived as follows. Thus since at such closed boundaries $\nabla p=0$, it is readily found by dividing Eqs. (9) and (10) that

$$(\Psi(\rho)+\alpha)p\partial\rho/\partial t = \alpha(\partial/\partial t)p\{\rho+(c/s)(1-\rho)\}, \quad (35)$$

where all the terms refer to a point on the closed boundary. Making the substitution

$$\alpha g(\rho)=\int\frac{(\Psi+\alpha c/s)d\rho}{c/s+\rho(1-c/s)}, \quad (36)$$

it is readily found that

$$g(\rho_i)-g(\rho)=\log p_i/p, \quad (37)$$

where $\rho_i$ and $p_i$ are the initial saturations and pressures at the closed boundaries, and $\rho$ and $p$ are those at the time $t$. For the present case, where $c/s$ was taken as 1 and $\alpha$ as 0.01, and with $\Psi(\rho)$ given by Fig. 2, the resulting plot of $\rho$ as a function of the pressure is given in Fig. 6 where $p_f$ and $\rho_e$ correspond to $p$ and $\rho$ of Eq. (37). As the calculation of this curve involved only the quadrature required by Eq. (36), it may be considered as a rigorous analytical implication of the differential Eqs. (9) and (10). And while the calculation of $\rho_e$ and $p_f$ by the numerical method here described is also essentially equivalent to the analytical integration involved in Eqs. (35) to (37), the actual values of $\rho_e$ and $p_f$ as used in the calculations were dependent on the smoothing out of the $\rho(\bar{x})$ and $p(\bar{x})$ curves as well as on the replacement of the differential quantities by their differences. The agreement of these values with those given by Eq. (37), as shown by the crosses in Fig. 6, may, therefore, be considered as at least a partial check upon the calculations as a whole.

A further check of an integrated character on the accuracy of the calculations may be obtained by comparing the total integrated liquid outflow from the system with the loss of liquid saturation in the interior, that is, by a test of the equality of the two sides of the equation

$$\int_0^{\bar{t}}\left\{F_l(\rho,\bar{t})\frac{\partial p(x,\bar{t})}{\partial\bar{x}}\right\}_{\bar{x}=0}d\bar{t}=\int_0^1(1-\rho(\bar{x},\bar{t}))d\bar{x}. \quad (38)$$

[13] Because of the lack of automatic recording equipment it was unfortunately impossible to obtain the detailed transient history of this type of flow system empirically with which to check the calculations directly.

[14] There is the limitation, however, that the closed boundary must also be an equi-pressure surface, as the result either of its natural geometrical symmetry, as in strictly radial or spherical flow systems, or of a dynamical symmetry induced by the surrounding and neighboring flow systems.

The discrepancy between the two sides of this equation is clearly a measure of the cumulative errors that might be developed by the time $\bar{t}$ in the calculation of either the pressure distribution $p(\bar{x})$ or the saturation distribution $\rho(\bar{x})$, or both. It was found by carrying out the indicated integrations that the right-hand side exceeded the left at the stage of complete ($\bar{t}=0.15$) depletion by 5.4 percent, and this may be considered as the overall error of the calculations as a whole. In view of the sensitivity of the left part of Eq. (38) to the extrapolation of $p(\bar{x})$ across $\bar{x}=0$, which had to be effected on the basis of the arbitrary assumption mentioned above, and the great number of graphical adjustments of the $\rho(\bar{x})$ and $p(\bar{x})$ curves at each stage of the calculation, the agreement within 5 percent of the two sides of Eq. (38) is felt to be quite satisfactory.

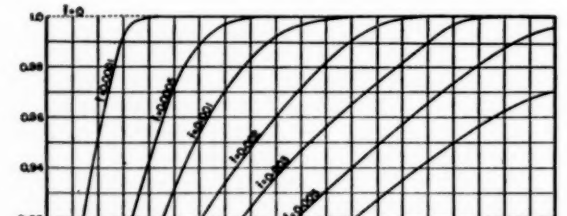

FIG. 7. History of the decline in liquid content of a linear channel with one terminal closed and the other opened to production. $(1-\rho)$ = fractional depletion. $\bar{x}$, $\bar{t}$ are dimensionless length and time defined by Eq. (32a).

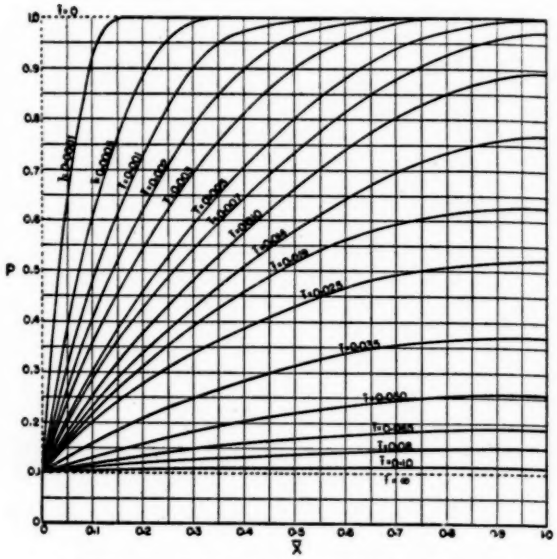

FIG. 8. History of the pressure decline in a linear channel with one terminal closed and the other opened to production. Notation same as in Fig. 7.

## D. Results

The essential results of these calculations are:

1. The history of the saturation and pressure distributions within the flow channel, and the final distribution of the former.
2. The variation of the flux from the system with the time, and the cumulative ultimate efflux.
3. The time variation of the gas-liquid ratio from the system.

The first set of results is simply given by the group of saturation and pressure distributions obtained at the various stages of the calculations. Typical ones of these are shown in Figs. 7 and 8.[15] While the general character of these curves could have been anticipated from elementary physical considerations, that of the ultimate saturation distribution is of particular interest, for it gives what is perhaps the first quantitative theoretical evidence with respect to the much debated question of the so-called "radius of drainage," that is, the extent of the zone of appreciable liquid depletion. Thus it is clear from this curve that except for the localized excess of depletion about the outflow surface, the ultimate saturation is for all practical purposes quite uniform over the whole flow system.

[15] In the whole range of $\bar{t}(0<\bar{t}\leq 0.15)$ there were 65 intervals of $\Delta\bar{t}$, for each of which complete $\rho(\bar{x})$ and $p(\bar{x})$ curves were calculated.

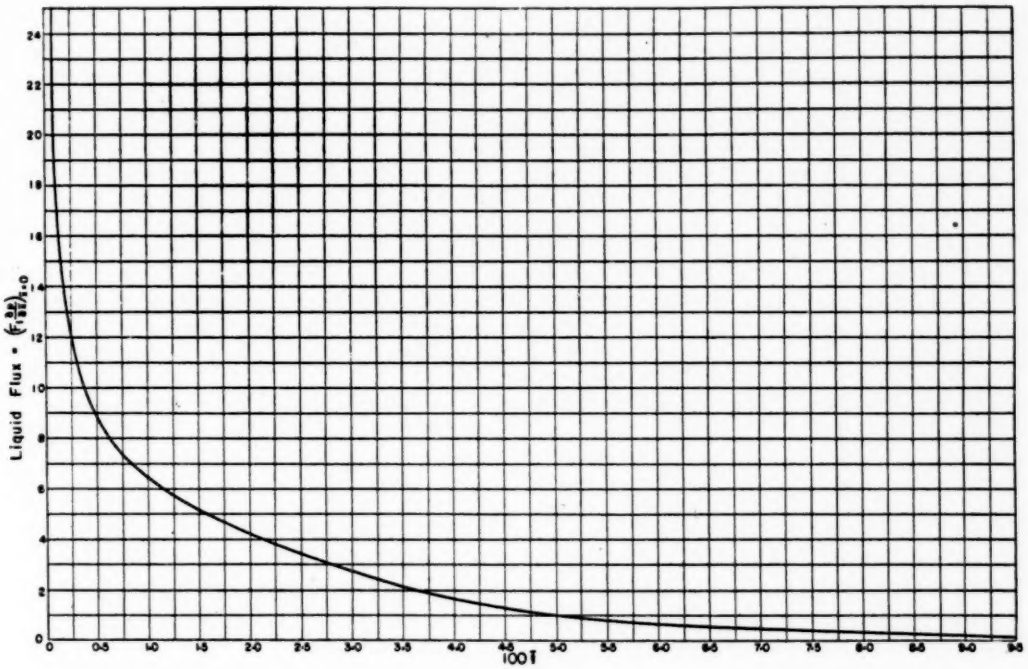


FIG. 9. Decline in flux from a linear channel which is originally saturated to a pressure of 10 units and is exposed at one end to a unit pressure at the outflow end. Real flux in cc/sec. per unit area of sand column is $k_0/\mu L$ times ordinates.

Or conversely, the ultimate depletion at the closed external boundary, as given by Fig. 6, is practically as great as that of the rest of the system except only in the immediate vicinity of the outflow surface, this depletion being determined only by the ratio of the original saturation pressure to the pressure representing the state of physical depletion. While the saturation at the outflow face as shown by the last curve of Fig. 7 is 5.2 percent lower than that at the closed external boundary, it is not unlikely that at least part of this excess depletion is only apparent and due to the errors inherent in the calculation, in view of the above-mentioned discrepancy in the two sides of Eq. (38).[16] One may, therefore, conclude that from a practical point of view, and insofar as the empirical bases of the whole analysis used here will retain their validity in consolidated sand systems, there is no "radius of drainage" which delimits and separates the part of the flow system in which there will be a large depletion as compared to that in which the depletion may be negligible. The immediate implication of this result is, of course, that the depletion or ultimate recovery will be essentially independent of the well spacing unless the latter be made so small as to become prohibitively expensive in the extreme. Of course, the time that would be required to obtain the physical ultimate recovery as given by the last curve of Fig. 7 will obviously increase with the effective length of the flow system, that is, the well spacing, and indeed it will be directly proportional to the square of this spacing as follows from Eq. (32a). But the extent to which the saturation will ultimately fall will be determined essentially by the ratio of the original reservoir pressure to the final ultimate pressure.

It is also to be emphasized that the result just discussed explicitly assumes an extended homogeneous sand. When the latter is lenticular it is clear that the spacing must be made sufficiently small as to insure a high probability that each individual lens is penetrated by at least one well. Beyond that, however, the whole question of well spacing appears to reduce largely to one of economics in which must be balanced the value

[16] That the actual variation in ultimate saturation is even less than shown in Fig. 7 is also indicated by the direct production experiment described in the preceding paper. (Cf. Table III.)

of a quick recovery of oil against the cost of additional wells and the associated additional investment, with the understanding that when the pressure within the sand has been reduced to any definite value the total recovery by that time will be essentially the same regardless of the number of wells involved. Furthermore, the same conclusion should apply in a physical sense when the sands are "tight," except insofar as the associated retardation in the depletion of the pressure at distant points may accentuate the economic problem of decreased rates of recovery and an increase in the period required for the return of the investment.

On the other hand, it is not to be concluded that the ultimate recovery of the liquid will also be independent of the *manner* of production. For the present calculations refer only to the single case where the outflow pressure has been immediately lowered to its ultimate minimum, thus corresponding to a "wide open" flow. While the recovery at the closed boundaries appears to be determined only by the actual resultant depletion of the fluid pressure, regardless of the mode of depletion of that pressure, as required by Eq. (37), that nearer the outflow surfaces will undoubtedly vary at least to some extent with the character of the pressure variation which is imposed at the outflow surfaces.

The rate of decline of the flux is shown in Fig. 9. Its general form is, of course, what might have been *a priori* anticipated, and no further comments are necessary. The integrated area under this curve, or the cumulative recovery until $\bar{t}=0.15$, is 27.7 percent, when averaged with the equivalent area above the curve $\bar{t}=0.15$ of Fig. 7. Since, at $\bar{t}=0.15$, the saturation at $\bar{x}=1$ has already fallen to 0.724, whereas the limiting value, by Fig. 6, is 0.722, it is clear that the recovery at $\bar{t}=0.15$ should be no more than a few percent below the physical ultimate, at which the pressure has fallen everywhere to the value 1.

The variation of the gas-liquid ratio given by Eq. (16), which, for the present case, becomes

$$R(\bar{t})=1+100\Psi(\rho_0,\bar{t}), \qquad (39)$$

where $\rho_0$ is the saturation at $\bar{x}=0$, is shown in Fig. 10.[17] The rise in the gas-liquid ratio and its asymptotic behavior at its last stages of depletion are to be noted. And incidentally it may be observed that we have here a general conclusion with regard to what has been again a much debated question, namely, the continuous rise in gas-liquid ratio with the depletion of the producing sand. For as is clear from physical considerations, the saturation at an outflow surface which is maintained at a pressure lower than that of the original saturation pressure must necessarily decrease monotonically with the time. By Eq. (16) and Fig. 2 it then follows at once that the gas-liquid ratio must, therefore, necessarily increase monotonically with the time.

Again, however, it should be clearly understood that this last result refers only to the heterogeneous fluid phase of the production of oil and gas from producing reservoirs. For it may be shown that if there are distinct free gas zones which are also exposed to the producing well, they will give contributions to the resultant gas-oil ratio which *decrease* with the life of the system. Hence, depending upon the relative importance of the contributions of gas which come from free gas zones and from the oil bearing sand body, the resultant gas-oil ratio may show a wide variety of characteristic histories during the decline of the oil production.

Likewise, the fundamental observation that the gas-liquid ratio is very sensitive to and is largely determined by the liquid saturation in the immediate vicinity of the outflow surface seems to provide a physical mechanism for ex-

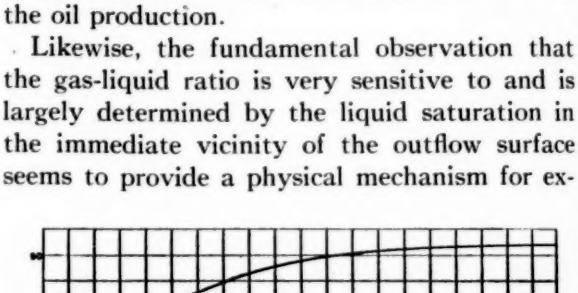

FIG. 10. History of the gas-liquid ratio (gas vol. at atmos. pres.)/(liquid vol.) in the production from a linear channel closed at one terminal. Normal gas-liquid ratio of solution = 10.0.

[17] The average of $R$ as weighted with respect to the liquid flux, i.e., $R=(\int RdQ_l)/Q_l=31.94$ to $\bar{t}=0.15$ gives an added check on the calculations, since the fractional recovery, $P$, till the average pressure has fallen to $\bar{p}$, which should be given by: $P=R_i(p_i-\bar{p})/p_i\bar{R}$, thus has the value 0.279, lying just between the values 0.269 and 0.284 given by the left and right sides of Eq. (38).

plaining the fact that many wells under actual producing conditions show gas-oil ratios which not only vary with the production rate but which moreover yield a minimum gas-oil ratio at a definite production rate. Here, too, the contribution to the gas-oil ratio due to free gas zones will in general decrease as the production rate increases, excepting only when the reservoir pressure in the free gas zone is less than that of the oil zone, when a maximal gas-oil ratio might result at a certain rate of production. For, as follows from Eq. (16), the gas-oil ratio is proportional to the well pressure and to the function $\Psi(\rho_w)$, where $\rho_w$ is the liquid saturation at the well face. Now although an increase in production rate necessarily means a decrease in the well pressure, it also seems almost certain that the lower pressure and greater gas evolution will result in a decrease in the liquid saturation at the well face. Hence, due to the very rapid rise in $\Psi(\rho)$ with decreasing $\rho$, when the latter is less than about 0.75, it is very probable that the product $p_w(\alpha+\Psi(\rho_w))$ may definitely increase even though $p_w$ be decreased, thus giving rise to a gas-oil ratio which grows with the production rate. When this effect is combined with the behavior of the free gas zone which will contribute a gas-oil ratio which decreases with increasing production rate, it is clear that the result may well lead to a gas-oil ratio *vs.* production rate curve which shows a minimum at a certain production rate. While these general considerations are still very distant from the answer to the question as to the gas-oil ratio to be expected in any specific case, it is felt that they represent the physical basis upon which such answers are to be ultimately developed.

In interpreting the numerical significance of the quantitative results obtained here, one must, of course, translate the dimensionless lengths $\bar{x}$, and time $\bar{t}$, into their normal equivalents by means of Eqs. (32a). Thus, for example, a 300 ft. column of sand of porosity 20 percent and permeability of 0.1 darcy carrying a liquid of viscosity 10 centipoises, would, if the pressure units be taken as atmospheres, give: $t=19{,}360\bar{t}$ days. Hence, by Fig. 7, it will take 290 days for the depletion at the end of the column to fall to half of its ultimate depletion, and 512 days for the pressure at the closed end to fall to half of its original pressure of 10 atmospheres. For the terminal depletion to reach $\frac{3}{4}$ of its ultimate value it would take 628 days, and for the pressure to fall to 2.5 atmospheres 1240 days would be required. Likewise the values of the fluxes of Fig. 9 must be multiplied by $k_0/\mu L$ to get the flux in cc/sec. per unit area of sand column. Thus for the above case, $Q_l=1$ corresponds to a flux of $1.093\cdot10^{-6}$ cc/sec. per cm$^2$ of sand column, or $5.52\cdot10^{-4}$ bbl./day per sq. ft. of sand.

Returning now to Fig. 6, one may draw the following implication of considerable practical interest. It is that in view of the rapid rise of the values of $p_i/p_f$ with $\rho_e$, the ultimate recovery of sands will increase but very slowly with their original reservoir pressures. And conversely, the application of vacuum to a sand, which would increase the ultimate values of $p_i/p_f$ attainable for the sand, will again increase the ultimate recoveries but very slightly even if one should neglect the associated increases in liquid viscosity which may quite possibly compensate for most of the gain. Thus in the system discussed numerically above, in which the ultimate $p_i/p_f$ was 10, and hence $\rho_e$ was 0.722, the application of a vacuum so as to reduce the final average pressure over the sand to $\frac{1}{2}$ would decrease $\rho_e$ by only 2 percent, that is, to 0.702.

A somewhat similar interpretation follows from Fig. 2 with regard to the effectiveness of gas recycling. For since $\rho$ increases but slowly with increasing values of $\Psi(\rho)$, which is essentially proportional to the gas-liquid ratio, it is clear that the latter will soon become extraordinarily large if small values of the saturation $\rho$ are to be attained. Hence the method of gas recycling must be expected to involve very high gas-liquid ratios[18] if appreciable secondary recoveries and hence decreases of the average liquid saturation are to be attained beyond those given by the methods of natural recovery.

In view of the practical importance of the conclusions drawn above from the analysis of the problem of the linear flow of a mixture through a sand, recognition must be taken of the fact that they have been derived from a very idealized and simple special case. On the other hand, it is

[18] When the gas-liquid ratios become excessive the additional factor of the evaporation of the liquid into the gas phase will enter the problem.

felt that in the large these conclusions will be modified only with respect to their quantitative implications. Thus the assumption that the system is linear rather than radial or of a more general character, as it will usually be in a practical situation, will probably be of no great significance, since, for example, the fundamental curve of Fig. 6 is independent of the geometry as long as the system is closed. Moreover, this closure need not necessarily be that arising from a physical closure of the physical system such as a pinching out of the sand. Rather an artificially created closure, as might be caused by neighboring wells which give rise to effective boundaries where the pressure gradients vanish, will suffice.[19] In such latter cases these boundaries may not be permanently fixed with respect to time and will indeed move in a manner determined by the production from and behavior of the surrounding wells. However, it is clear that such effects again will not alter the predominant features of the solution. Likewise, the deviation of the gas from the ideal gas laws and from Henry's law will cause some modification, but should not seriously affect the major conclusions. Indeed, insofar as the solution of the problem is inherently numerical such deviations can be readily included in the analysis by simply making the parameters $c$ and $s$ variable with the pressure, and appropriately modifying Eq. (9) so that the $c$ and $s$ will be left in front of the differential operators. Similarly the variation of the viscosity of the liquid with its dissolved gas content, and hence the pressure, can be readily taken into account in the numerical treatment, as could be variations in the original homogeneous fluid permeability of the porous medium, by simply putting in the appropriate numerical values for these parameters at each stage of the calculation. Such refinements will only lengthen the numerical analysis but will not require any changes in the principles of the method. However, it is doubtful if they would result in sufficient changes in the ultimate conclusions to be worth taking into account at the present time.

On the other hand, there is one factor which may well be of very material importance and which has not been taken into account in the present calculations. It is that which may be termed the "gas segregation," and which refers to the natural tendency of the gas to rise to the higher parts of the producing sand with the associated tendency of the liquid to settle to the lower parts, thus creating a vertical variation in the fluid permeabilities. In particular, this would give rise to a region of higher gas permeability at the upper parts of the producing sand in which the gas may be considered to be "channeling." This will lead to higher gas-liquid ratios for the same average liquid saturation than is given by the two-dimensional theory, in which vertical motions are taken as negligible, and consequently the recoveries would be correspondingly lower. Again, the physical treatment of this situation is quite clear, and the problem could be discussed quantitatively by extending the calculations so as to include in the expressions for the velocities along the vertical coordinate a driving force acting upon the fluid phases which is equivalent to the hydrostatic gravitational potential, as must be done in the treatment of homogeneous liquid systems in which an appreciable component of the flow lies in the vertical plane. However, because of the necessary closure of such systems along the upper and lower planes defining the thickness of the producing stratum, the numerical work would become considerably more elaborate and lengthy. Nevertheless, it is important to note that the physical principles describing the problem are available, and its quantitative solution is simply a matter of doing the necessary work. The practical significance of this question of segregation will, of course, increase with the sand thickness, or perhaps more accurately with the ratio of the sand thickness to the lateral extent of the sand. It will also be proportional to the ratio between the vertical drive gradients due to the gravity differences between the gas and liquid phases and the horizontal pressure gradients inducing the horizontal flow, that is, to the ratio between the vertical and horizontal velocities. Hence it will be greatest at the distant parts of the fluid system as compared to those near the outflow surfaces. In this respect it may lead to some degree of accentuation in the difference in recovery between the parts of the flow system distant from the outflow surface and those near it, and, thus may tend to give some-

[19] Cognizance must, however, be taken of the limitation mentioned in footnote 14.

what more meaning to the concept of the "radius of drainage" than would be allowed by a two-dimensional or linear treatment as developed here.

It should also be noted that the problem of the depletion of an originally saturated reservoir is not the only one amenable to the method of treatment given here. On the contrary, every problem of flow of a heterogeneous fluid system can in principle be treated by the basic differential Eqs. (9) and (10), or their modification which takes into account deviations from the ideal gas laws and from Henry's law and possible viscosity variations, provided only that the initial conditions and boundary conditions be appropriately stated. Thus the problem of gas injection into a depleted sand would simply be defined by the statement that the initial pressure and saturation distributions are those left by the natural recovery process at the time the injection is begun, together with the boundary condition that the liquid flux into the external boundary of the producing sand is zero,[20] while the gas flux is that introduced by the compressors, or that the pressure is that maintained by the compressors, and that at the output wells or outflow surfaces the pressures are those that are actually maintained there. Such a formulation together with the geometrical description of the flow system defines the problem of gas drives. In fact the fundamental curves of Figs. 1 and 2, that is, the curves giving both the gas and liquid permeability as functions of liquid saturation, or one of them and a curve giving their ratio, together with the differential Eqs. (9) and (10) contain the whole of the empirical basis necessary for the discussion of any heterogeneous fluid system both in the steady states and transient conditions of flow, although the latter will be subject to a range of uncertainty caused by the ambiguity in the detailed shape of the permeability curves for liquid saturations above the equilibrium value. Of course the details of these curves will be somewhat different for different sands and may be appreciably different for consolidated sands. However, that is physically only a matter of detail, which can be taken care of by an empirical study of the particular sand system of interest by such a method as described in the preceding paper. The basic laws therein established are, however, believed to be fundamentally and physically sufficient for the complete description of heterogeneous fluid systems.

The writer is greatly indebted to Mr. R. D. Wyckoff, Mr. H. G. Botset, and Dr. W. N. Arnquist for many helpful discussions of the questions treated here and for the privilege of using their empirically established data before publication, to Dr. Hervey Hicks of the Carnegie Institute of Technology for discussions concerning the numerical analysis, and to Dr. Paul D. Foote, Executive Vice President of the Gulf Research & Development Company, for the permission to publish this paper.

[20] The analytical expression of this condition is that the saturation is such that the liquid permeability is zero. Whether this is to mean that the saturation is actually zero at the boundary where the gas is injected or that it is still of the order of 20 percent, as is indicated by the experimental data, cannot be settled until more accurate experiments are performed in the region of very low liquid saturations. In any case it may be anticipated that either choice will give essentially the same results, and that when the very low saturations are attained throughout the main sand body, it will be necessary to take into account the evaporation of the liquid into the gas phase, as can be readily done by a slight modification of the fundamental Eqs. (9) and (10).

# A Hydrodynamical Theory of Piston Ring Lubrication

R. A. CASTLEMAN, JR., *East Falls Church, Virginia*

(Received June 24, 1936)

It is shown that, making the assumption that *oils as used in engine lubrication cannot stand absolute tension*, and taking into account the observed tendency of the bearing faces of piston rings to wear into an uneven shape with the "high" point near the middle and a very gentle slope to each edge, Reynolds' theory of bearing lubrication can be extended to ring lubrication. A practical application of this extension is outlined and illustrated. Results of calculations, based on this extension, of ring clearance and wear under average working conditions are in substantial agreement with a number of observations.

## INTRODUCTION

WHILE a satisfactory theory of bearing lubrication was outlined some 50 years ago by Osborne Reynolds,[1] and has since been considerably extended and applied with gratifying results both to the explanation of the lubrication of known forms of bearing, and to the prediction of the performance of new types, by Sommerfeld, Kingsbury, Michell and others, much haziness persists as to the lubrication of the so-called "packing rings" which reciprocate with the pistons of engines. Much of this haziness is probably due to the fact that it is widely assumed that an element of the outer face of the ring remains perfectly straight, and works completely parallel to an element of the cylinder wall throughout the life of the ring.

It must be remembered that the ring is an absolutely necessary link in the chain of functioning of any piston heat engine. Because of thermal expansion the piston must be made a "loose fit" in the cylinder bore, so that slotted rings, which are pressed by their own elasticity close against the cylinder wall, are necessary to prevent the escape of the high pressure gases past the piston without doing useful work on the latter. Another important duty of these rings, which has instigated much inventive application, is scraping the oil from the cylinder wall back into the crankcase. A third duty of the rings in internal combustion engines, which is not always clearly recognized but was vividly brought out by heat-flow measurements made by Salzmann,[2] is the passing to the cylinder wall of most of the heat which traverses the piston. Indeed Mahle,[3] pointing to a piston ruined by allowing the rings to stick in their grooves, so that their elasticity could not act to press them against the cylinder wall, makes the appropriate remark that " . . . this is analogous to closing the outlet tube of a vessel in which the inlet tube still remains wide open."

## PREVIOUS WORK

To the author's knowledge, but two theories applicable to piston ring lubrication have so far been advanced. (1) T. E. Stanton[4] has made the flat statement that ". . . in general engineering practice the lubrication of all machine details in which the relative motion is of a reciprocating character may be taken as boundary lubrication." (2) Salzmann,[5] slightly extending Gümbel's theory of the lubrication of parallel surfaces, has deduced results that are in qualitative agreement with his experimental data. The fact, however, that C. G. Williams[6] has observed a change with use in the rate of wear of piston rings, and therefore a change in the conditions of their lubrication, indicates that Salzmann's theory is not a complete explanation of the general case.

## PRESENT WORK

In the original treatment of this subject the author assumed a simplified form of a rather complicated profile for the outer face of the ring, the only necessary conditions being that: (1) this becomes curved in use; (2) it is higher in the

[1] O. Reynolds, Phil. Trans. Roy. Soc., p. 157 (1886).
[2] Salzmann, Forsch. a.d. Geb. d. Ing. **4**, 193 (1933).
[3] Mahle, Automobiltech. Zeits. **37**, 316 (1934), Fig. 12.
[4] Stanton, The Engineer **135**, 378 (1925).
[5] Salzmann, Diss. Eidg. T. H. Zurich (1933).
[6] Williams, Automobile Engineer **24**, 367 (1934), Fig. 4.

middle than at the edges; and (3) the slope toward each edge is very gentle. Since this theory was outlined at the January 1936 meeting of the American Physical Society,[7] the profiles of the outer faces of six worn piston rings, which, while ground in use to a mirror-like smoothness, could not, on superficial inspection, be suspected of anything but perfect flatness, were submitted to critical examination by the Gage Section of the Bureau of Standards. Each ring was measured at three points separated by 90°—one point opposite the gap, and two points each at 90° therefrom. Of the *18* points thus measured *all showed wear of the general form assumed*, though of various degrees. The unexpected results were: (1) an element of each section of the worn face is sensibly straight, not curved; (2) the angle between an element of the worn face above the bulge or large diameter and an element of the worn face below the large diameter is much smaller than expected—of the order of thirty minutes of arc; (3) the point of intersection of these two elements averages around 72 percent of the distance below the "top" of the ring.

While these findings were in perfect qualitative agreement with the present theory, it seemed desirable to use them as the starting-point for a recalculation. This was submitted at the May 1936 meeting of the American Physical Society.[8]

In this treatment it is assumed that: (1) the rings can completely disappear in their grooves, so that they do not have to support any of the piston's side-thrust; (2) the supply of lubricant is at all times sufficient to fill the gap between the face of the ring and cylinder wall.

Fig. 1 shows (above) the general profile of the outer face of a worn ring, and (below) the pressure distribution under the ring face shown above. Each ordinate in the lower part of the figure represents the pressure (or tension) developed, under an average condition of engine operation, between that part of the cylinder wall and that of the ring face shown just above. The point of closest approach is here taken to be at the geometrical center of this face. In calculating pressures the slope of each end section, with respect to the horizontal, was taken as five parts

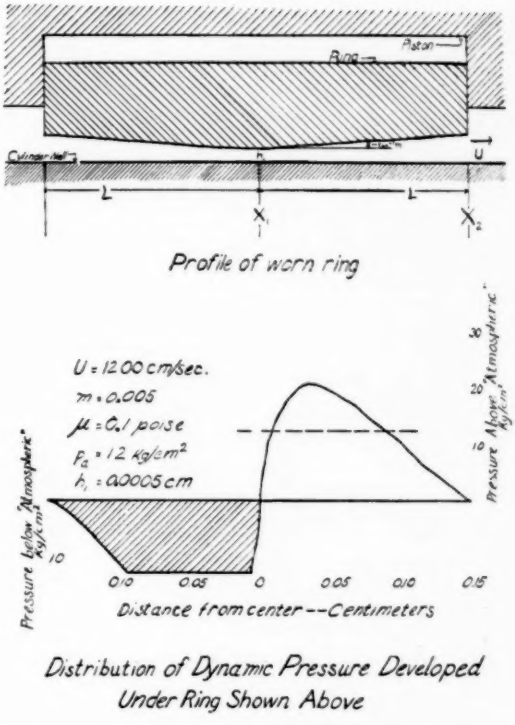


FIG. 1. Profile and pressure distribution for worn ring.

in a thousand, corresponding to a half-angle of about 15 minutes.

Each end surface of this form of bearing immediately reminds us of a block in a thrust bearing. It works at a disadvantage compared to the latter in that its "length"[9] is small and that it cannot be pivoted; but it has the advantage of virtually endless width,[10] so that the pressure which would be developed is not appreciably diminished by "side-flow" of the lubricant.

Now Reynolds[11] has deduced expressions for the pressure distribution and the total pressure developed between a limited flat inclined surface of the form of either end section of the ring of Fig. 1, and a surface of unlimited width. Michell,[12] however, gives these expressions in a form which is both simpler and better adapted to our needs. In the notation of Fig. 1 these become

[7] Castleman, Phys. Rev. **49**, 410 (1936).
[8] Castleman, Phys. Rev. **49**, 886 (1936).

[9] The length of a bearing is here taken as the dimension in the direction of motion, the width as the dimension in the direction perpendicular thereto; regardless of which is the greater.
[10] It should be noted that this is one of the very few cases in practical lubrication where this is true.
[11] Reference 1, Eqs. (33) and (34).
[12] Michell, *The Mechanical Properties of Fluids* (1924 Ed.), Chap. III, Eqs. (30) and (31).

$$p=\frac{6\mu U}{m^2}\left[\frac{1}{x}-\frac{x_1x_2}{x_1+x_2}\cdot\frac{1}{x^2}-\frac{1}{x_1+x_2}\right] \quad (1)$$

for the pressure at any point $x$; and for the total pressure from $x_1$ to $x_2$, per unit width,

$$P=\frac{6\mu U}{m^2}\left[\log_e\left(1+\frac{mL}{h_1}\right)-\frac{2mL}{mL+2h_1}\right]. \quad (2)$$

We now assume that *oils as used in engine lubrication cannot stand absolute tension*, so that there will be cavitation as soon as the pressure falls to absolute zero. This proposition is admittedly difficult to prove or disprove. Indeed the value of *direct* test may be doubted. We remember the minute air bubbles caught up and carried along by the circulating oil, and that engine vibrations would tend to break up any condition of instability that might be formed.

If this assumption is granted, it is seen that a tension will be developed under the trailing edge of the ring, whose distribution is the mirror-image of the pressure developed under the leading edge, and whose local intensity is limited to that of the prevailing "atmospheric" pressure under which the bearing face of the ring works. This tension area (cross-hatched area at left) will cancel an equal area under the *pressure* distribution curve which applies to the leading edge.

We must now consider *static* pressure, since this may be very intense under cetain conditions. Robertson and Ford[13] have shown experimentally that the static pressure back of the top ring (in the groove) is very approximately equal to the cylinder pressure (which for the top ring may be assumed to be the "atmospheric" pressure under which the bearing face of the ring works); so that the static pressures before and behind this ring will cancel, and we need only consider the *dynamic* pressure *developed and permitted* in the motion of the ring. The experimental apparatus used by these investigators was insufficient for specific determination of this relation for the other rings; but their further measurements indicate that this is also probably qualitatively true for all the rings.

It is thus evident that the net pressure effective in supporting the ring against its elasticity is given by the area under the *dynamic* pressure curve and above the broken line in the lower right of the figure, where the absolute pressure is *twice* the absolute "atmospheric" pressure. Just as evidently this net effective pressure is independent of the direction of motion.

An example for average engine working conditions is shown in the lower part of the figure. Piston speed and cylinder pressure assumed roughly correspond to normal full-load conditions in a typical carburetor engine turning over at 2400 r.p.m., when the crank is 40° past dead-center. The viscosity of the lubricating oil is taken as 0.1 poise, corresponding (roughly) to a "medium" oil diluted six percent and raised to 85°C.

We find that in this case the net effective pressure will equal the outward elastic pressure of the ring, the mean of values found by Ebihara,[14] at a minimum ring clearance of about 0.0005 cm, corresponding, in this case, to a *mean* clearance of about 0.0009 cm. This distance, while quite small, is of the order of several thousand times the molecular size, so that the separating film will be "thick" and boundary conditions need not be considered. This result is in substantial agreement with observations of Salzmann,[15] deduced from heat-flow measurements on a Sulzer four-stroke Diesel, when allowance is made for differences in piston speed and in cylinder pressure.

## Remarks

Many of the dimensions shown in the upper part of Fig. 1 are, for the sake of clearness, enormously exaggerated. In particular, if the slope $m$ were made equal to that actually found, the cross section of the bearing face of the ring would appear straight over its entire length.

In Fig. 1 the point of nearest approach is, for convenience, taken at the geometrical center of this face, while the Bureau of Standards measurements showed that it is really much closer to one

[13] Robertson and Ford, Diesel Power **12**, 548 (1934).

[14] Ebihara, Inst. of Phys. Chem. Research (Tokyo)—Sci. Paper No. 182 (1929).

[15] See note 2 above. (The fact that Salzmann's experiments were made at a very low piston speed seems to make little difference in the comparative applicability of his results; for rough calculation of Reynolds' criterion indicates that, even at the high piston speeds used in modern automotive engines, the flow over the bearing face of the ring will be safely streamline.)

edge. This would mean a slight difference in ring clearance with direction of piston motion—also observed by Salzmann.[2]

Williams' observation mentioned above is also in line with the present theory. He found that the ring wear was as great in the first *10* hours of engine operation as in the next *80*. Assuming that the whole outer face of the ring is initially plane and works completely parallel to the cylinder wall, wear will be heavy at first. As, however, this face is ground down to some such shape as that shown in the figure, a protective film would be formed when the ring moved, and the rate of wear would decrease.

A report by Sparrow and Scherger[16] on cylinder wear is of interest in this connection, and vividly illustrates certain main points of the present theory. These investigators mapped the wear along the cylinder wall, after extensive runs under various engine conditions. The outstanding feature of the report is the excessive wear found, in almost all runs, at the position occupied by the top ring at upper dead-center. We remember that the cylinder pressure, and therefore, as brought out above, the "atmospheric" working pressure of the top ring, is greatest at this point, so that the dynamic tension to be deducted (cross-hatched area at left in lower part of figure) is greatest here; also, piston speed being lowest at this point, the dynamic *pressure* developed under the leading edge is lowest here. The net result is that the ring clearance would be expected to be least and cylinder wear greatest at just this point—a result also in agreement with Salzmann's[2] measurements of ring clearance during the stroke.

The object of this treatment is to show that, by making the simple physical assumption that *oils as used in engine lubrication cannot stand absolute tension*, we may extend Reynolds' theory to give a hydrodynamical explanation of the lubrication of piston rings,—not rings of special preliminary design, but rings as they are shaped and used by the engine.

[16] Sparrow and Scherger, J. S. A. E. April, p. 117 (1936).

# Mechanism of Division of Metabolizing Systems

JOHN M. REINER, *University of Chicago, Chicago, Illinois*

(Received May 6, 1936)

In an extension of the work of N. Rashevsky, the problem is treated of the determination of the distribution of concentrations and consequent distribution of osmotic forces in a metabolizing liquid sphere subject to a general infinitesimal deformation. The principle of virtual displacements in the form of an inequality is applied as a criterion of the instability (tendency to divide) of the system. This gives an algebraic equation determining the critical radius at which the system becomes unstable, and the equation is analyzed in detail with reference to the influence of the physical parameters of the system. In particular, it is found that, for a certain range of size of the system, this critical value is practically independent of the surface tension. Finally, the diffusion equations are integrated for a system where the rate of reaction is not constant, but a linear function of the concentration, and a procedure similar to the above is outlined.

## I

THE first systematic treatment of the mathematical physics of spontaneous division in metabolizing liquid systems (i.e., systems which are the seat of physicochemical reactions) was given by N. Rashevsky in two articles in *Physics*,[1, 2] following a number of more abstract preliminary studies.

Rashevsky's results show that when certain inequalities between various parameters characterizing a metabolizing system are satisfied, the system becomes mechanically unstable above a critical size for a particular type of infinitesimal deformation. However, it has not been shown that such an instability will occur for other types of infinitesimal deformations. The purpose of the present paper is to generalize the treatment to a wider range of deformations. The problem, as before, resolves itself into two steps: first, the integration of the diffusion equations for an arbitrary infinitesimal deformation, and second, the subsequent calculation of the forces due to concentration gradients arising in such a system. So far as the first step is concerned, Rashevsky's method can easily be generalized for any arbitrary deformation leaving the system a figure of revolution, the equation of the meridian curve being:

$$r=r_0+\Delta_0\sum_1^\infty{}_n\alpha_nP_n(\theta)=r_0+\Delta, \qquad (1)$$

where $r_0$ is the radius of the sphere, a constant, $\Delta_0$ is an infinitesimal whose higher powers may be neglected, the $P_n$ being the customary zonal surface harmonics or Legendre polynomials, and the $\alpha_n$ being arbitrary constant coefficients which are supposed known.

A very important limitation imposed on the deformations studied is that the meridian curve should be sufficiently simple to justify substitution of $dc/dr$ for $\partial c/\partial n$ in the boundary conditions. Rashevsky has shown this to be justified for the case of the special deformation which he has treated by demonstrating that these two quantities differ only by terms of the order of $\Delta_0^2$, which we have agreed to neglect. It is easy to demonstrate, however, that this holds generally for any infinitesimal deformation of the form (1) or more generally

$$r=r_0+\Delta_0f(\theta). \qquad (1A)$$

For we have in general

$$\partial c/\partial n=(\partial c/\partial r)\cos(rn). \qquad (2)$$

But

$$tg(rn)=dr/rd\theta=(1/r)(dr/d\theta)=(\Delta_0/r)(df/d\theta) \qquad (3)$$

and

$$\cos^2(rn)=1/[1+tg^2(rn)]$$
$$=1/[1+(\Delta_0^2/r^2)(df/d\theta)^2]. \qquad (4)$$

Therefore

$$\cos(rn)=1/(1+(\Delta_0^2/r^2)(df/d\theta)^2)^{\frac{1}{2}}$$
$$=1/[1+(\Delta_0^2/2r^2)(df/d\theta)^2] \qquad (5)$$
$$=1-(\Delta_0^2/2r^2)(df/d\theta)^2.$$

Thus we see that the substitution of the radial for the normal derivative is justified for the case of any $f(\theta)$, continuous and differentiable in the given domain, subject only to the limitation that $df/d\theta$ should not be infinite, in other words,

[1] N. Rashevsky, Physics **2**, 303 (1932).
[2] N. Rashevsky, Physics **5**, 374 (1934).

that the radius vector is nowhere perpendicular to the normal.

As before, we begin by considering a spherical system in which the phenomena of chemical reaction and diffusion are governed by the differential equations

$$D_i\Delta^2 c_i' + q = 0, \quad \Delta^2 c_e' = 0, \tag{6}$$

and the boundary conditions

$$D_i dc_i'/dr = D_e dc_e'/dr = h(c_e' - c_i') \quad \text{for } r = r_0, \tag{7}$$

where $D_i$ and $D_e$ are the diffusion coefficients for the internal and external media, respectively, $q$ is the constant rate of chemical reaction, taken to be positive for the case of production of a substance in the system, and $h$ is the permeability of the membrane. The solution[2] is then given by

$$\begin{aligned} c_i' &= c_0 + qr_0/3h + qr_0^2/3D_e + (q/6D_i)(r_0^2 - r^2), \\ c_e' &= c_0 + (qr_0^3/3D_e)(1/r). \end{aligned} \tag{8}$$

The next step is to deal with the distribution of concentrations in a nonspherical system. An infinitesimal deformation of the sphere will again be considered, the finite case being far too complex mathematically to be approached at the present time. However, instead of the previously discussed special deformation, a simple elongation in the direction of the polar axis, we shall this time consider any general infinitesimal deformation which leaves the cell a figure of revolution (Eq. (1)). The differential equations being linear, it is again possible to represent the distribution of concentrations in the deformed figure by the sum of the spherical solution, $c'$, and a correction term which we shall denote by $c^*$. $c^*$ is determined by the differential equations

$$\Delta^2 c_i^* = 0, \quad \Delta^2 c_e^* = 0 \tag{9}$$

and the boundary conditions[2]

$$\begin{aligned} &D_i dc_i^*/dr - h(c_e^* - c_i^*) = [(D_i + hr_0)/3D_i - hr_0/3D_e] \times q\Delta_0 \sum_1^\infty {}_n\alpha_n P_n(\theta) = A\Delta_0 \sum_1^\infty {}_n\alpha_n P_n(\theta), \\ &D_e dc_e^*/dr - h(c_e^* - c_i^*) = [(hr_0 - 2D_i)/3D_i - hr_0/3D_e] \times q\Delta_0 \sum_1^\infty {}_n\alpha_n P_n(\theta) = B\Delta_0 \sum_1^\infty {}_n\alpha_n P_n(\theta) \\ &\qquad\qquad \text{at} \quad r = r_0 + \Delta_0 \sum_1^\infty {}_n\alpha_n P_n(\theta). \end{aligned} \tag{10}$$

Eqs. (9) are satisfied by

$$c_i^* = \sum_1^\infty {}_n\beta_n r^n P_n(\theta), \quad c_e^* = \sum_1^\infty {}_n\delta_n r^{-n-1} P_n(\theta), \tag{11}$$

where $\beta_n$ and $\delta_n$ are the constants of integration. Combining (10) and (11) we obtain

$$\sum_1^\infty {}_nS_nP_n = A\Delta_0 \sum_1^\infty {}_n\alpha_n P_n, \quad \sum_1^\infty {}_nQ_nP_n = B\Delta_0 \sum_1^\infty {}_n\alpha_n P_n, \tag{12}$$

where $$S_n = (D_i n r_0^{-n-1} + hr_0^n)\beta_n - hr_0^{-n-1}\delta_n, \quad Q_n = hr_0^n\beta_n - [D_e(n+1)r_0^{-n-2} + hr_0^{-n-1}]\delta_n. \tag{13}$$

Simple comparison of coefficients now gives

$$S_n = A\Delta_0\alpha_n, \quad Q_n = B\Delta_0\alpha_n, \tag{14}$$

and by combining (12) and (14) and some elementary algebraic manipulations, we obtain for the constants of integration

$$\beta_n = \frac{A\alpha_n\Delta_0 + hr_0^{-n-1}\delta_n}{(D_i n r_0^{-n-1} + hr_0^n)}, \quad \delta_n = \frac{B(D_i n r_0^{-n-1} + hr_0^n) - Ahr_0^n}{h^2 r_0^{-1} - (D_i n r_0^{-n-1} + hr_0^n)[D_e(n+1)r_0^{-n-2} + hr_0^{-n-1}]}\alpha_n\Delta_0. \tag{15}$$

In taking now $c_i = c_i' + c_i^*$ we have to take $c_i'$, given by (8), at the deformed surface, which gives[2]

$$[c_i']_{r_0+\Delta} = c_0 + qr_0/3h + qr_0^2/3D_e - (qr_0/3D_i)\sum_1^\infty \Delta_0 \alpha_n P_n. \tag{8'}$$

Similarly for $c_e'$ at the surface we find

$$[c_e']_{r_0+\Delta} = c_0 + qr_0^2/3D_e - (qr_0/3D_e)\sum_1^\infty \Delta_0 \alpha_n P_n. \tag{8'}$$

In calculating the relative order of magnitude of the coefficients $\beta_n$ and $\delta_n$, we find that $\beta_n$ may be neglected to a very good approximation with respect to $qr_0\Delta/3D_i$, but $\delta_n$ cannot be neglected with respect to $qr_0\Delta/3D_e$. In this calculation we use for the physical constants the following values, suggested by biological considerations:[2]

$$c_0 = 10^{-4}\ \text{g cm}^{-3},\quad h = 10^{-4}\ \text{cm min.}^{-1},\quad r_0 = 10^{-3}\ \text{cm},\quad q = 10^{-4}\ \text{g cm}^{-3}\ \text{min.}^{-1},$$
$$D_i = 10^{-6}\ \text{cm}^2\ \text{min.}^{-1},\quad D_e = 2\times 10^{-6}\ \text{cm}^2\ \text{min.}^{-1}. \tag{16}$$

This calculation gives $\delta_n r_0^{-n-1} \sim r_0$, and $\beta_n r_0^n \sim r_0^{2n+2}$, the latter being clearly a negligible quantity.

The next step of our investigation is to study the distribution of forces in the deformed system, and to set up a new criterion of division of the system, necessarily more general than that employed by Rashevsky, but strictly analogous in that it must express the condition that the altered distribution of forces due to the infinitesimal general deformation shall tend to increase that deformation.

A general criterion of instability of a system in any field of forces is that the work done by those forces for any virtual deformation of the system should be positive. When a metabolizing spherical drop is deformed according to Eq. (1), two types of forces are operating in the system: the forces due to the surface tension or capillary pressure, and the forces due to the gradients of concentration. Of the latter we shall here confine ourselves for the sake of simplicity to the osmotic forces, leaving out the terms in $\Gamma$ due to intermolecular attractions.[2] No limitation in principle is introduced by this, since the additional forces would merely augment the coefficients of the forces by constant terms of the same order of magnitude or slightly less.

The work done by any volume forces, when the system is deformed, is equal to

$$W_{si} = \int \eta \operatorname{grad} \psi_i d\tau, \tag{17}$$

where $\eta$ is the vector of deformation at any part of the system, and $\psi_i$ the potential of the forces inside the system. But by the generalized Gaussian theorem[3] this is equal to

$$W_{si} = -\int \psi_i \operatorname{div} \eta d\tau - \int \psi_i \eta_n do, \tag{18}$$

where $\eta_n$ is the value of $\eta$ at the surface. In other words

$$\eta_n = \Delta. \tag{19}$$

Since the deformation (1) leaves the volume unchanged, and the external liquid is incompressible also, we have

$$\operatorname{div} \eta = 0 \tag{20}$$

and therefore $W_{si} = -\int \psi_i \Delta do.$ (21)

Remembering that we have two volumes, external and internal, we find finally

$$W_s = W_{si} - W_{se} = -\int (\psi_i - \psi_e)\Delta do. \tag{22}$$

This holds when $\psi_i$ and $\psi_e$ are independent of the deformation. If, as in our case, they are functions of $\Delta$, we find by a similar line of argument:

$$W_s = -\int do \int_0^\Delta (\psi_i - \psi_e) d\Delta, \tag{23}$$

which reduces to (22) when $\psi_i - \psi_e = \text{const.}$

The work done by the capillary forces, when a sphere undergoes a deformation (1), has been

[3] Geiger-Scheel *Handbuch der Physik*, Vol. 7, p. 5.

calculated by Rayleigh,[4] and is given in our notation by:

$$P_s = -2\pi\gamma\Delta_0^2\sum_1^\infty{}_n(2n+1)^{-1}(n-1)(n+2)\alpha_n^2 \quad (24)$$

up to higher powers of $\Delta_0$. The lowest power of $\Delta_0$ in $P_s$ is the second, and must be retained, the higher powers being omitted. We have

$$\psi_i = RTc_i/M, \quad \psi_e = RTc_e/M, \quad (25)$$

where the $c$ are, as stated above, the sum of (8) and (11) evaluated at the deformed surface. We shall omit $c_i^*$ on order of magnitude considerations (see paragraph following (15)). But (8′) is a linear function of the normal displacement $\Delta$ by (1), likewise the coefficient $\delta_n$, which may be written in factored form as $d_n\Delta$. Thus the surface divergence of potential is a linear function of $\Delta$

$$\psi_i - \psi_e = C + a\Delta, \quad (26)$$

where $C$ is the difference of the constant terms of (8′) (difference for the sphere, $\Delta = 0$), and

$$a = (RT/M)(qr_0/3D_e - qr_0/3D_i - d_n r_0^{-n-1}). \quad (27)$$

The work done at a point of the surface by these forces is

$$-\int_0^\Delta (\psi_i - \psi_e)d\Delta = -(C\Delta + a\Delta^2/2). \quad (28)$$

We must now integrate (28) over the entire surface, as in (23), to obtain the corresponding total work. But, remembering that $\Delta$ is proportional to $P_n$, and using the theorem[5]

$$\int_{-1}^{+1} x^\kappa P_n(x)dx = 0 \qquad (\kappa = 0, 1, \cdots, n-1) \quad (29)$$

we have

$$-C\int \Delta do = 0, \quad (30)$$

which is also nothing else but the expression of the constancy of volume of the system, and all that remains of (23) is

$$W_s = -\tfrac{1}{2}a\int \Delta^2 do = \Delta_0^2\sum{}_n 2\pi(2n+1)^{-1}(RT/M)$$
$$\times(qr_0^3/3D_e - qr_0^3/3D_i - d_n r_0^{-n-1})\alpha_n^2. \quad (31)$$

The lowest power of $\Delta_0$ is, as in $P$, the second, higher powers being omitted.

We have the whole work

$$W_s + P_s > 0. \quad (32)$$

Since this inequality must hold for any arbitrary set of coefficients $\alpha_n$, it must hold for each of them separately. We thus have

$$(RT/M)(qr_0/3D_e - qr_0/3D_i - d_n r_0^{-n-1}) - \gamma(n-1)(n+2)r_0^{-2} > 0. \quad (33)$$

In other words, there is a special equation of stability for each partial of the deformation. The actual critical radius at which the whole system becomes unstable is given by the lowest root obtained from those equations and as can be readily seen corresponds to the lowest harmonic of the deformation.

In order to make use of this formula, it is necessary to introduce an approximation for $d_n$. An estimate of the order of magnitude of the terms in (15) shows that all terms save one in both numerator and denominator of $d_n$ are wholly negligible, so that we may write to a very good approximation

$$d_n = -(Br_0^{n+2})/(n+1)D_e, \quad (34)$$

and therefore

$$d_n r_0^{-n-1} = -Br_0/(n+1)D_e = 2qr_0/3(n+1)D_e + (1/D_i - 1/D_e) \times [hqr_0^2/3(n+1)D_e]. \quad (34A)$$

Substituting (34A) in (33) gives

$$(RT/M)q/3[1/D_e - 1/D_i - 1/(n+1)D_e]r_0 + (RT/M)(1/D_i - 1/D_e)[hq/3(n+1)D_e]r_0^2 - \gamma(n-1)(n+2)r_0^{-2} > 0 \quad (35)$$

as the final form of the criterion of spontaneous division of the system. This is an algebraic equation in $r_0$, which determines the critical radius $r^*$ at which division commences if we replace the inequality sign by an equality sign.

The cases $n = 0$ and $n = 1$ are trivial, the first corresponding to a uniform dilatation of the sphere and the second to a simple translation. For $n = 2$ (simple elongation) $r^*$ is of the same order of magnitude as found by Rashevsky, of the order of $10^{-3}$ cm (with the values (16), and $\gamma = 1$).

[4] Wien-Harms *Handbuch der Experimentalphysik*, Vol. 6, pp. 184, 185.

[5] Hobson, *Spherical Harmonics*, p. 36.

The roles of the physical constants in this equation are extremely interesting. First of all we notice that the numerical relationship of the diffusion coefficients is significant. For $D_e > D_i$, and $q > 0$, the linear term of (35) is always negative and the quadratic term always positive; i.e., inequality (35) is satisfied *above* a critical radius. A reversal of this relationship produces a corresponding reversal of sign. A reversal of sign (neglecting the capillary term, a consideration to which we shall return in a moment) would give a real and positive root of the equation, but the equation would be satisfied only *below* that root, so that we should be describing a system which would be unstable below rather than above a certain critical size, i.e., a system which presumably could not spontaneously be formed through gradual coalescence of smaller systems. The opposite holds for $q < 0$.

The effect of varying the constant rate of reaction $q$ is what might be expected. If $q$ is increased, all terms except the capillary term increase, being multiplied by the same factor. Thus increasing $q$ decreases the significance of the capillary term in the equation, and may thus decrease the critical radius. For $q < 0$ (inward diffusion and consumption), all terms save the capillary term change sign. It is again in agreement with our physical expectations in this problem that the stability or instability of the system depends upon the "direction" of the metabolic activity. Another interesting relationship is as follows: For $q = 0$, (35) can never be satisfied, since the surviving third term is always negative. As $q$ increases in absolute value, the equation still depends upon $q$. But if $q$ increases to such an extent that the third term becomes negligible, it is now a factor common to both remaining terms, and may be dropped. The critical radius thus decreases with increasing $q$, but tends asymptotically to a limiting value which is independent of $q$.

Particularly illuminating is the situation with regard to the permeability $h$. The inclusion of the $d_n$ in this equation of stability brings out a very natural relationship which was not found in Rashevsky's analysis due to the omission of the corresponding correction term. Inspection of the equation shows that it is the increase of the quadratic term which causes the function to pass from negative to positive values. But the quadratic term is the only one containing $h$. Therefore, increasing $h$ markedly lowers the critical radius, a circumstance which is in excellent agreement with the observed empirical relationship between high permeability and instability of biological systems.

Eq. (35) gives an accurate picture of the influence of surface tension. The numerical coefficient increases, as we should expect, with the order of the harmonic; for the order of the harmonic is the same as the number of its zeroes, therefore a measure of the "waviness" of the surface, and consequently, a measure of the increase of specific surface, implying an increase of the influence of capillary forces (which are always restoring forces).

On the other hand, an increase of the order of the harmonic (and consequent departure from smooth deformations) manifests itself also in the decrease of the quadratic term, since $n$ appears in the denominator, which would again correspond to a lower critical radius for small $n$ and a higher critical radius for increasing $n$.

Most significant of all in certain respects is the observation that the surface tension $\gamma$ does not play so vital a part in the phenomena of the division of such liquid systems as concern us here as has been previously supposed. For we note that, all parameters being fixed, the capillary term becomes insignificant above a certain value of $r_0$. Now, for positive $q$, and $D_e > D_i$, the linear term is negative and the quadratic term positive; and it is possible to omit the inverse square term altogether and still get a real and positive solution of the equation, of the correct order of magnitude. The result is very suggestive in that it opens up the possibility that a metabolizing system under most circumstances contains in addition to capillary forces both "dividing" and "restoring" forces, sometimes in equilibrium and sometimes in disequilibrium, such that their relationship is the decisive factor in determining whether or not the system will be unstable, except for such small drops that the specific surface is unusually large, and the capillary forces consequently of prime importance (the others at such a stage being practically negligible).

Finally, it is interesting to stress the remarkable agreement in form and in content with the

equation of condition studied by Rashevsky,[2] the case $n=2$ in (35) corresponding to the simple elongation. The primary departure lies in the fact that the correction terms to the concentration due to the infinitesimal deformation play a prominent role in our criterion (being wholly responsible especially for the results with respect to permeability and surface tension). This difference is quite important, and may be said to result directly from the better perspective afforded by the study of a rather general type of deformation.

## II

Similar results may be obtained for the case of a system in which the rate of reaction is not constant, but is a linear function of the concentration.[6] The difference lies in the first step of the problem, that is, the integration of the diffusion equations for an infinitesimally deformed sphere. The rest of the procedure remains the same as before. For future reference we are outlining this integration here.

In this case the diffusion equations take the form

$$\Delta^2 c_i = p c_i / D_i, \quad \Delta^2 c_e = 0, \tag{36}$$

where $p$ is a constant. The boundary conditions are

$$D_i dc_i/dr = D_e dc_e/dr = h(c_e - c_i) \quad \text{at } r = r_0, \tag{37}$$

$h$ being the permeability coefficient, $D$ the diffusion coefficient, and $r_0$ the radius of the system.

The solution will have two forms, one for positive and one for negative $p$, so that it shall always be real. A general solution is

$$c_i = (Ae^{ar} + A'e^{-ar})(1/r), \quad c_e = E + B/r, \tag{38}$$

where $a = (|p|/D_i)^{\frac{1}{2}}$.

It proves possible immediately to determine two of the constants of integration from physical considerations. $c_i$ must remain finite at the center of the cell, for $r = r_0$, therefore $A' = -A$. At sufficient distance from the cell $c_e$ must approach the original constant value $c_0$, therefore $E = c_0$. For $p<0$, the case which we shall treat, we get $c_i = A \sin ar/r$. Now applying the boundary conditions we get for $p<0$

$$\begin{aligned} AD_i(ar_0 \cos ar_0 - \sin ar_0) &= h(c_0 r_0^2 + Br_0 \\ &\quad - Ar_0 \sin ar_0) - BD_e = h(c_0 r_0^2 + Br_0 \\ &\quad - Ar_0 \sin ar_0), \quad \text{and similarly for } p>0. \end{aligned} \tag{39}$$

Solving for $A$ and $B$, we get the solution of our differential equations

$$\begin{aligned} c_i &= -\frac{1}{r} \frac{D_e h c_0 r_0^2 \sin ar}{D_i(hr_0 + D_e)(ar_0 \cos ar_0 - \sin ar_0) + D_e h r_0 \sin ar_0}, \\ c_e &= -\frac{1}{r} \frac{D_i h c_0 r_0^2 (\sin ar_0 - ar_0 \cos ar_0)}{D_i(hr_0 + D_e)(ar_0 \cos ar_0 - \sin ar_0) + D_e h r_0 \sin ar_0} + c_0, \end{aligned} \tag{40}$$

and similarly, using sinh and cosh, for $p>0$.

Now suppose the cell to undergo an infinitesimal deformation which leaves it a figure of rotation, the equation of whose meridian section is

$$r = r_0 + \sum a_n P_n(\theta). \tag{41}$$

Neglecting quantities in the higher powers of the infinitesimal $a_n$, and using $\Delta$ as an abbreviation for $\sum a_n P_n$, we insert this new value in the boundary conditions (37)

$$\begin{aligned} [D_i dc_i/dr - h(c_e - c_i)]_{r_0 + \Delta} &= [AD_i(ar_0 \cos ar_0 - \sin ar_0) - h(c_0 r_0^2 + Br_0 - Ar_0 \sin ar_0)]/r_0^2 \\ &\quad + \{AD_i[2(\sin ar_0 - ar_0 \cos ar_0)/r_0 - a^2 r_0 \sin ar_0] - h[A(\sin ar_0 - ar_0 \cos ar_0) - B]\}\Delta/r_0^2, \\ [D_e dc_e/dr - h(c_e - c_i)]_{r_0 + \Delta} &= [-D_e B - h(c_0 r_0^2 + Br_0 - Ar_0 \sin ar_0)]/r_0^2 \\ &\quad + \{2D_e B/r_0 - h[2c_0 r_0 + B - A(\sin ar_0 + ar_0 \cos ar_0)]\}\Delta/r_0^2. \end{aligned} \tag{42}$$

But by (39) the terms not containing $\Delta$ are identically zero, so that we can write the right-hand sides of (42) in abbreviated form as $-X\Delta$ and $-Y\Delta$. Thus it is clear that the solutions (40) satisfy the

[6] N. Rashevsky, Protoplasma **14**, 99 (1931).

space equations after the deformation (41), but no longer satisfy the boundary conditions as long as $a_n$ is infinitesimal but not identically zero. But since all the operators in the space equations and boundary conditions are linear and distributive we can satisfy them by the functions $c_i = c_i' + c_i^*$, $c_e = c_e' + c_e^*$, where $c_i'$ and $c_e'$ are the solutions (40), and $c_i^*$ and $c_e^*$ satisfy the equations

$$\Delta^2 c_i^* = pc_i^*/D_i, \quad \Delta_e^2 c_e^* = 0, \quad \text{and similarly for } p>0, \tag{43}$$

and the boundary conditions

$$D_i dc_i^*/dr - h(c_e^* - c_i^*) = X\Delta, \quad D_e dc_e/dr - h(c_e^* - c_i^*) = Y\Delta, \quad \text{at } r = r_0 + \Delta, \tag{44}$$

where $dc/dr$ can still be used for $\partial c/\partial n$ (*vide supra*). We now write the Laplacian in polar coordinates, take $c_e^*$ the same as in the paper of footnote 2, and assume for $c_i^*$ a solution of the form $R(r)\cdot T(\theta)$. Substituting in (43) we have instead of a partial differential equation two ordinary differential equations of the same order

$$\frac{(r^2R')' - pr^2R/D_i}{R} = -\frac{r^2}{T\sin\theta}\frac{\partial}{\partial\theta}\left(\frac{\partial T}{\partial\theta}\sin\theta\right) = \text{const.} \tag{45}$$

The constant must be so chosen that $T(\theta)$ is continuous over the entire surface. Taking the constant therefore equal to $n(n+1)$, we obtain $T_n(\theta) = P_n(\cos\theta)$, the $n$th zonal harmonics. Now, taking $p<0$, and accordingly writing $(p/D_i) = -a^2$, we have, with the substitutions $R = y/r^{\frac{1}{2}}$, $r = x/a$, the solution $R_n = T_n(ar) = J_{n+\frac{1}{2}}(ar)/r^{\frac{1}{2}}$, where $J_{n+\frac{1}{2}}$ is the $n$th Bessel function of half-integral order. (For $p>0$, $J_{n+\frac{1}{2}}$ is replaced by $I_{n+\frac{1}{2}}$, where $I_n(x) = e^{-\frac{1}{2}in\pi}J_n(ix)$ which is real for all real values of the argument.[7]) Then (43) is satisfied by

$$c^* = \sum_0^\infty \alpha_n P_n(\theta)\cdot T_n(ar), \quad c_*^* = \sum_0^\infty \beta_n P_n(\theta) r^{-n-1}. \tag{46}$$

Substituting in (44), separating terms in $P_n$, and writing $T'$ for $dT(ar)/dr$

$$\begin{aligned} \sum_0^\infty{}_n[D_i T_n'(ar_0 + a\Delta)\alpha_n - h(\beta_n r_0^{-n-1} - \alpha_n T_n)]P_n &= X\sum_0^\infty{}_n a_n P_n, \\ \sum_0^\infty{}_n[(-n-1)D_e r_0^{-n-2}\beta_n - h(\beta_n r_0^{-n-1} - \alpha_n T_n)]P_n &= Y\sum_0^\infty{}_n a_n P_n. \end{aligned} \tag{47}$$

Then we have by comparison of coefficients

$$S_n = Xa_n, \quad Q_n = Ya_n, \tag{48}$$

and by combining (47) and (48) we can obtain the coefficients $\alpha_n$ and $\beta_n$ as functions of $a_n$, and thus determine the altered distribution of concentrations in the system, in terms of which the forces are to be calculated, and the critical radius determined precisely as in (I).

Thanks are due the Rockefeller Foundation for aid in these investigations through a grant to the University of Chicago.

[7] Watson, *Treatise on the Theory of Bessel Functions*, p. 77.